DANISH
TECHNOLOGICAL
INSTITUTE

Guideline for execution of steel fibre reinforced SCC

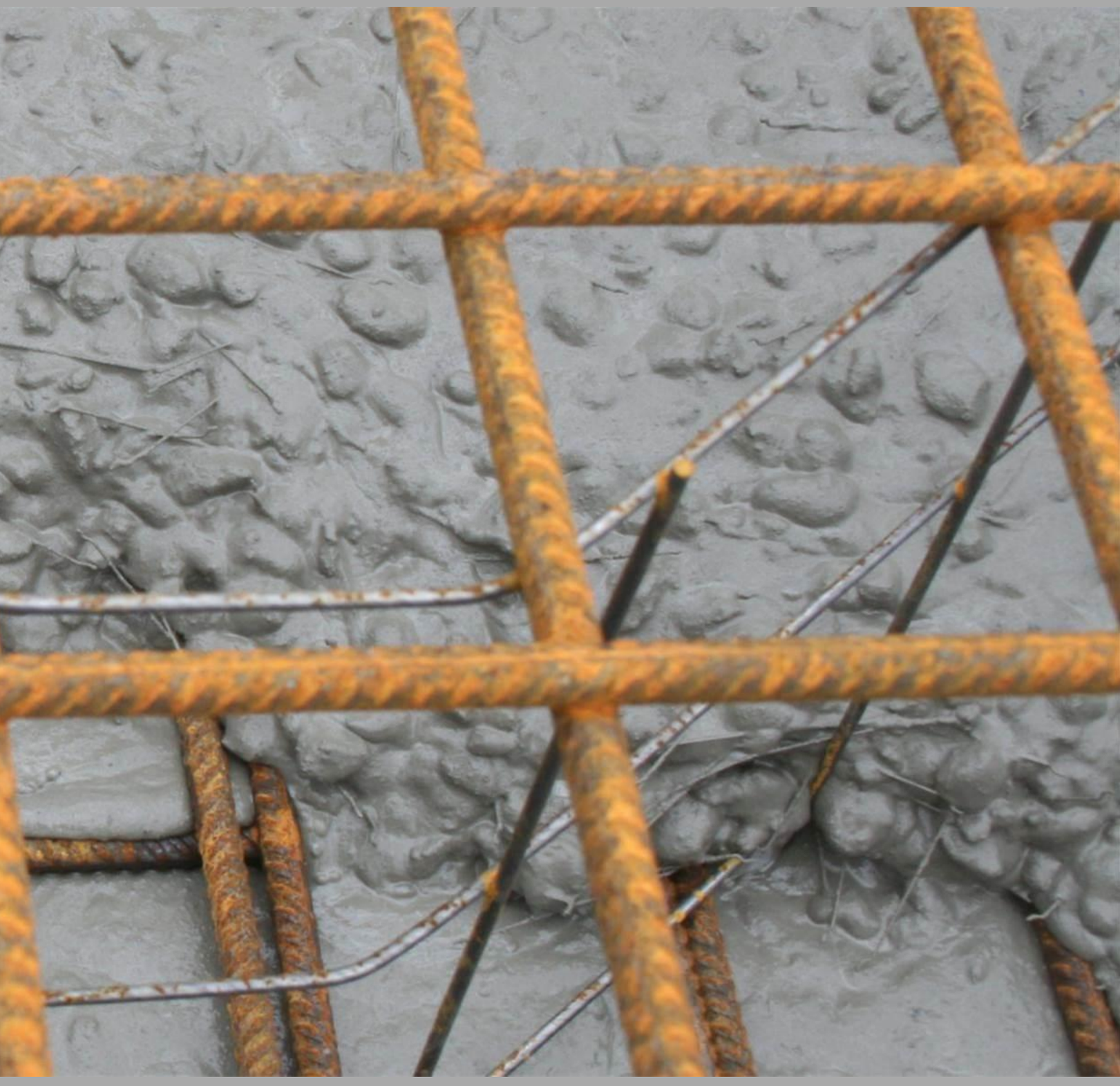

SFRC-Consortium

Table of contents

Guideline for execution of steel fibre reinforced SCC, September 2013

Publisher: *Danish Technological Institute, Concrete Centre*
Gregersensvej, DK-2630 Taastrup
+ 45 7220 2226 - concrete.centre@teknologisk.dk

Printing: *Paritas A/S*
Edition: *1st*
ISBN: *978-87-996246-1-4*

Authors: *Lars Nyholm Thrane*
Oldrich Svec
Michael Strøm
Thomas Kasper

Layout: *Thomas Juul Andersen*

Front cover photo shows steel fibre reinforced self-compacting concrete flowing in a reinforced formwork.

Back cover photo shows steel fibre reinforced concrete after mechanical testing of the load bearing capacity.

Preface

The content of this guideline is based upon the scientific and technical work carried out in the Danish innovation consortium “Sustainable concrete structures with steel fibres” running from 2010 to 2013. The project was funded by the participating partners and by the Danish Agency for Science, Technology and Innovation.

The output of the project is, among others, guidelines on design and execution of steel fibre reinforced concrete (SFRC). In particular, the project has focused on steel fibre reinforced self-compacting concrete (SFRSCC), which is also the focus of this guideline.

SCC is known to improve the working environment and productivity. SFRC is known to improve the ductile behaviour of concrete, which can be taken into account to reduce and simplify the layout of conventional reinforcement. SFRSCC combines advantages of the two types of concrete, making the concrete an attractive building material. On the other hand, SFRSCC brings several new challenges. Steel fibres immersed in SFRSCC quickly orientate following the flow pattern of the concrete. This can lead to a significant anisotropy in the mechanical behaviour of the concrete, which can be viewed as a strength and weakness of the material. Such anisotropy can be unacceptable if the associated variation in strength is not taken into account in the design process.

This guideline is meant as a tool to assist designers and contractors in choosing fibre orientation factors for different types of applications. Furthermore, this guideline gives recommendations for the practical handling of SFRSCC on the job site e.g. what to be aware of compared to ordinary SCC.

This guideline builds upon the ”Guideline for execution of SCC” published in 2008 as a part of the SCC-Consortium running from 2003 to 2007. Therefore, a general understanding of the properties of SCC is assumed.

The SFRC Consortium, September 2013

SCC (Self-Compacting Concrete) is defined as concrete that flows, fills the formwork and embeds reinforcement solely due to its own weight without any need of vibration or other type of agitation.

SFRC (Steel Fibre Reinforced Concrete) is the common term for all types of concrete containing steel fibres.

SFRSCC (Steel Fibre Reinforced Self-Compacting Concrete) is a suspension of steel fibres in self-compacting concrete.

The core partners in the SFRC Consortium were:

- Danish Technological Institute
- Technical University of Denmark
- COWI A/S
- MT Højgaard A/S
- Unicon A/S
- Aalborg Portland A/S
- Bekaert A/S
- Hi-Con A/S
- CRH Concrete A/S
- Convi ApS
- The Danish Precast Association

The associated partners in the SFRC Consortium were:

- Rail Net Denmark
- Femern A/S
- Confederation of Danish Industry
- Danish Road Directorate

1. Introduction

1.1 STEEL FIBRE REINFORCED CONCRETE (SFRC)

Conventional unreinforced concrete is weak and brittle when loaded in tension. Therefore, conventional concrete is often reinforced. In many industrial applications, steel fibre reinforced concrete can be used to reduce or simplify the conventional reinforcement. Contrary to the large continuous unidirectional reinforcement bars, the homogeneously dispersed steel fibres reinforce the concrete evenly. Thus, steel fibres help to reduce and control any micro-cracks arising in the concrete matrix.

In the design guideline, it is allowed to account for the tensile strength of steel fibre concrete in calculations of e.g. the bending capacity, shear capacity, and crack widths. The tensile strength of steel fibre concrete is determined from three point bending tests and depends among other things on the quality, amount and orientation of the steel fibres.

From a construction point of view, handling of conventional reinforcement is a major task and is often associated with heavy lifts and unhealthy working positions. Reducing or simplifying the conventional reinforcement will help to improve the working environment for the concrete workers at the job site. Furthermore, a reduction of the conventional reinforcement may reduce the total costs at the job site. Whether this is possible depends on the extra costs of the concrete due to the addition of the steel fibres.

1.2 SELF-COMPACTING CONCRETE (SCC)

Conventional, vibrated concrete is stiff in the fresh state and thus does not flow. To compact and level the concrete, the casting process is commonly accompanied by extensive vibration. The vibration process of the concrete is a very labour and time intensive process which has negative impacts on the human body and on the working environment in general. SCC flows due to its own weight and no vibration is needed to compact the concrete. Therefore, SCC allows for a fast and simple casting of the material, effectively improving the working environment and productivity.

Figure 1.1: Top: Casting of conventional vibrated concrete. Bottom: Cracked section of steel fibre reinforced concrete.

Figure 1.2: Top: Slump of traditional concrete. Bottom: Slump flow of self-compacting concrete.

1.3 STEEL FIBRE REINFORCED SELF-COMPACTING CONCRETE (SFRSCC)

Steel fibre reinforced self-compacting concrete is a combination of steel fibres and SCC.

It has been observed by many authors that steel fibres orientate and distribute according to the flow of the concrete. As an example, Figure 1.3 shows the casting of a slab with SFRSCC. Figure 1.4 presents the layout of the slab and top views of the fibres within two beam specimens cut from the slab. Knowledge of the position and orientation of the fibres within the beam specimens was obtained experimentally by means of X-ray computed tomography (CT). Ellipses in Figure 1.4 represent the average fibre orientation in the individual regions of the beam specimens and helps to better understand the fibre orientation pattern.

The various fibre orientations presented in Figure 1.4 is a product of the casting process and results in a non-homogeneous and non-isotropic mechanical response of the beam specimens (Figure 1.5). This significantly complicates the design process and without a deeper understanding of the mechanisms responsible for the fibre orientation limits the use of the material.

Figure 1.3: Casting of a slab with SFRSCC.

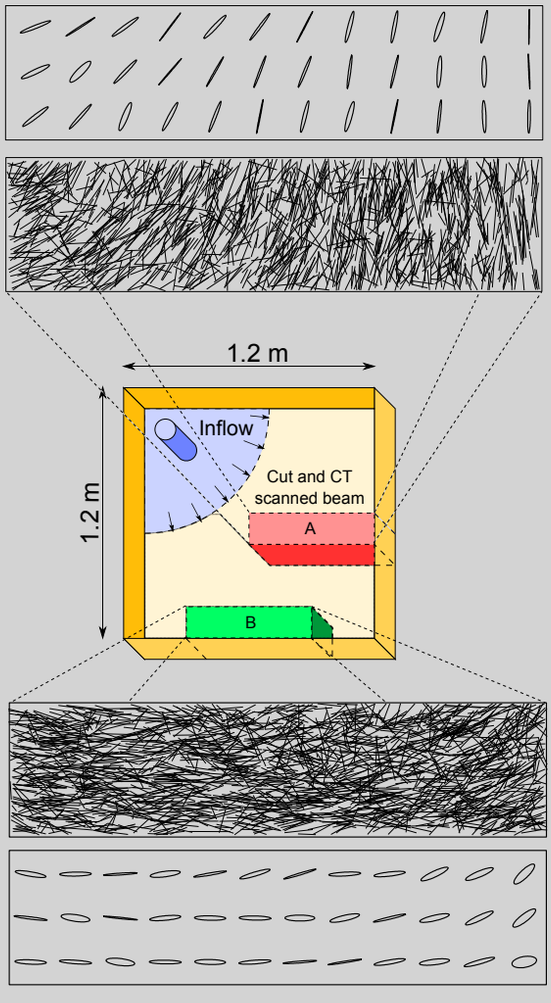

Figure 1.4: Layout of the slab casting. The blue cylinder represents the inlet. Two beam specimens (red and green) were cut from the slab, CT scanned and tested by four point bending test. The fibres within the beam specimens are shown both as lines and orientation ellipses.

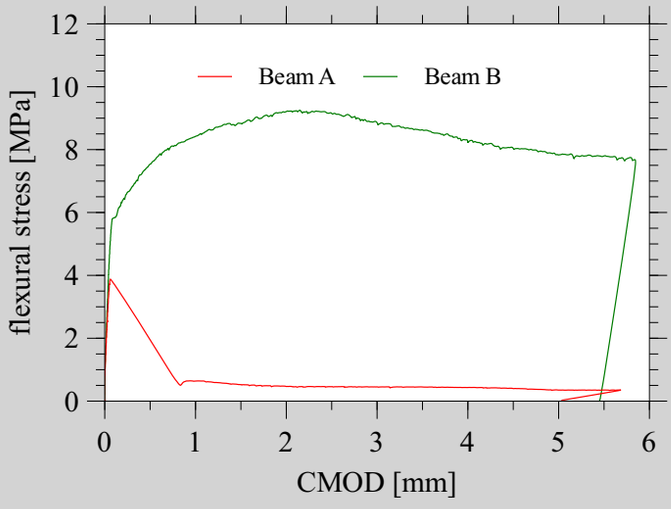

Figure 1.5: Flexural mechanical response of the two beam specimens cut from the slab. Beam A indicates a significantly lower strength compared to Beam B. CMOD = Crack Mouth Opening Displacement.

2. Steel fibres

Steel fibres come in various shapes and qualities. Like with any other reinforcement, it is important to provide the required amount of fibres in a given section. However, it is not only the fibre dosage that governs the mechanical response of SFRC. Other factors that influence the mechanical response are:

- fibre length
  typically from 30 mm to 60 mm
- fibre diameter
  typically from 0.3 mm to a maximum of 1.3 mm
- fibre shape
  straight, hooked, undulated, crimped, twisted, coned
- fibre tensile strength
  depends on material quality and ranges approximately from 800 MPa to 2500 MPa

Figure 2.1: Example of hooked-end steel fibres in SFRSCC.

Figure 2.2: Examples of different types of steel fibres.

2.1 EFFECT OF STEEL FIBRES

Workability of SFRC is characterized by the slump value. Rheology of SCC is characterized by the yield stress and plastic viscosity. Rheology of SFRSCC is characterized in the same way as SCC. However special issues need to be considered related to the risk of blocking and segregation.

2.1.1 Rheology

Steel fibres added to concrete have a direct impact on both plastic viscosity and yield stress of the material. Plastic viscosity and yield stress both increase with the fibre dosage i.e. the slump flow decreases and the concrete flows more slowly. However, the rheological properties are not only dependent on the fibre dosage. For instance, at the same fibre dosage and fibre length, a more slender fibre results in more fibres and thus a stiffer concrete. The fibre slenderness is expressed by the so-called aspect ratio, which is the ratio between the fibre length and the fibre diameter.

2.1.2 Blocking

Blocking occurs if the steel fibres are not able to pass the reinforcement. Blocking can result in honeycombing, poor distribution of fibres and poor surface quality. Based on experiments, a general rule of thumb is that the clear spacing perpendicular to the flow direction should be 2x higher than the length of the fibre. However, in some cases a lower ratio may be applied (see section 8.1.3).

2.1.3 Segregation

Segregation occurs when the fluid phase is not able to carry the particles (coarse aggregates and steel fibres). If the fluidity of the fluid phase increases, the risk of segregation increases. Assuming the mortar phase represents the fluid phase and the basic SCC is stable, then adding steel fibres to the SCC results in a more stiff concrete. To compensate, additional superplasticizer may be added to the concrete, which results in a more fluid mortar phase. As a consequence, the risk of segregation is higher for the SFRSCC compared to the basic SCC.

2.1.4 Form filling ability

Form filling ability of SFRSCC i.e. the ability to fill the formwork depends mainly on the yield stress (slump flow) as is the case for ordinary SCC.

Plastic viscosity governs the rate of flow and the stickiness of the concrete. A high plastic viscosity results in a slow flowing and sticky concrete.

Yield stress governs how far the concrete is able to flow. Yield stress is inversely proportional to the slump flow. A high yield stress results in a low slump flow and vice versa.

The slump value is used as a measure of the workability of conventional slump concrete. Compared to conventional slump concrete, SFRC is more difficult to vibrate. Therefore, it is recommended to specify a higher slump value for SFRC than would normally be specified for a conventional slump concrete. As a rule of thumb, the slump value should be increased with 10 mm for every 10 kg of steel fibres added to the concrete.

Figure 2.3: Example of fibre blocking on top of a reinforcement mesh.

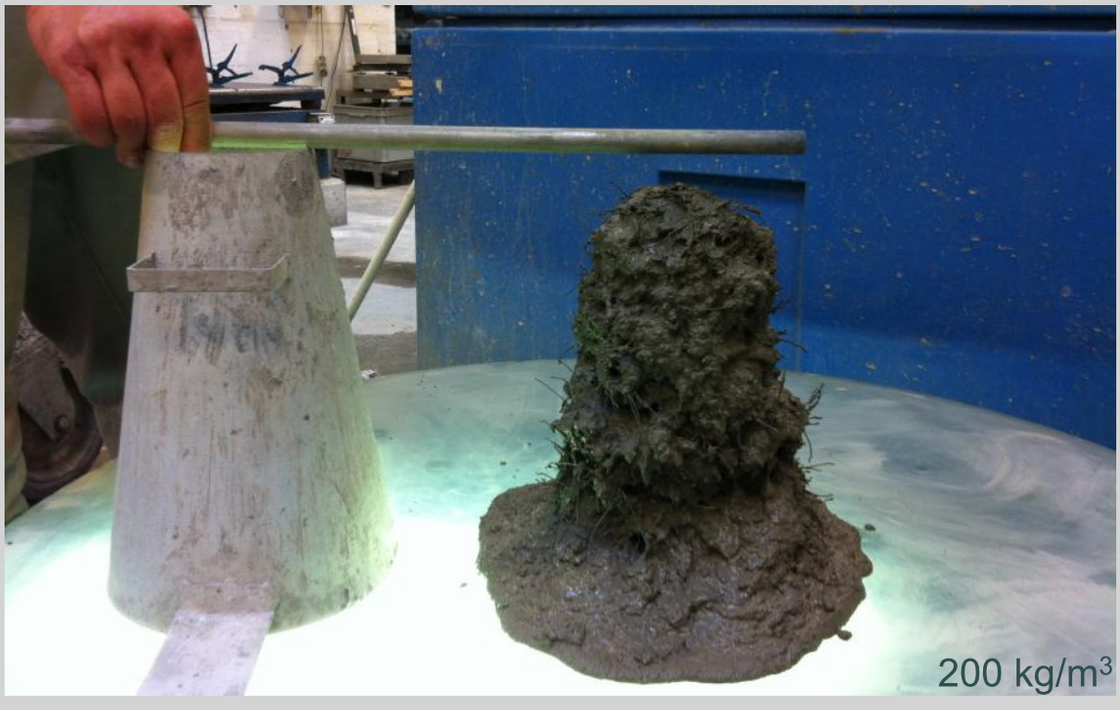

Figure 2.4: SFRSCC. Flow properties with varying fibre dosage. Top: 45 kg of steel fibres per m³. Bottom: 200 kg steel fibres per m³. Hooked end fibres. Length = 60 mm. Aspect ratio = 80. Measurements with the 4C-Rheometer.

Rheological properties

To measure the yield stress and plastic viscosity of SFRSCC, it is recommended to use a rheometer e.g. the 4C-Rheometer.

Workability

As for SCC, it is recommended to use the slump flow SF and the t_{500} value to measure the workability of SFRSCC. It is not recommended to use the V-Funnel due to the risk of blocking.

Blocking

It is recommended to assess blocking as part of a trial casting. The L-box may be applied if the reinforcement is representative of the reinforcement in the actual application.

3. Mechanical response of steel fibre reinforced concrete

The complex mechanical response of SFRC can be approximated by taking into account two main phenomena:

- number of fibres crossing the fracture plane
- pull-out response of individual fibres.

The former is primarily influenced by the fibre dosage, fibre orientation and fibre aspect ratio. The latter is primarily influenced by the concrete type, fibre type, fibre inclination at the fracture plane etc.

3.1 FIBRE TYPE

3.1.1 Fibre length and diameter

Performance of the steel fibre is influenced by the fibre length and diameter (Figure 3.1). Increasing the fibre length or decreasing the fibre diameter results in a better performance when the fibre volume concentration is fixed. The two quantities can be combined into one: Fibre aspect ratio = length / diameter. Increasing the fibre aspect ratio increases the fibre performance and vice versa.

3.1.2 Fibre shape

Fibre shape has a strong influence on the pull-out response of the fibre. Friction is governing the pull-out mechanism of straight fibres (Figure 3.2 top). Friction is significantly enhanced when pulling out deformed fibres compared to straight fibres (Figure 3.2 bottom).

3.1.3 Fibre tensile strength

Correct fibre tensile strength and bond to the concrete matrix are important to obtain a proper pull-out response. Steel fibres usually have hooked ends or other means to transmit stresses from the matrix to the fibre. The anchorage of the fibre must be good enough to attract enough stress to give a high performance while not so high that it results in fibre rupture. In an ideal situation the fibre is slowly deformed and pulled-out from the concrete matrix (Figure 3.3). Fibre rupture often occurs when the fibre stiffness is too high and when the fibre tensile strength is too low (Figure 3.4).

The probability of fibre rupture also increases with an increasing concrete strength. The fibre rupture must be avoided to obtain beneficial post crack response of the SFRC.

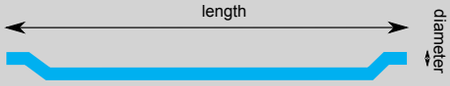

Figure 3.1: Illustration of the fibre length and diameter.

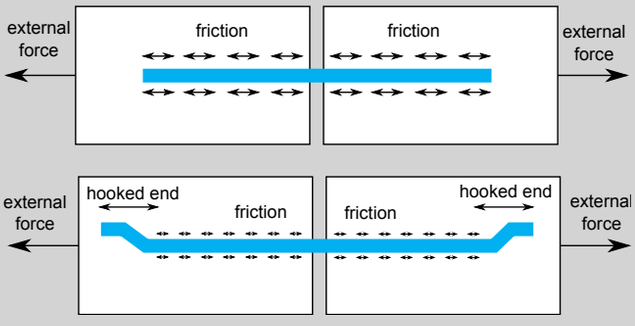

Figure 3.2: Illustration of the various internal and external forces acting on straight and hooked end steel fibres.

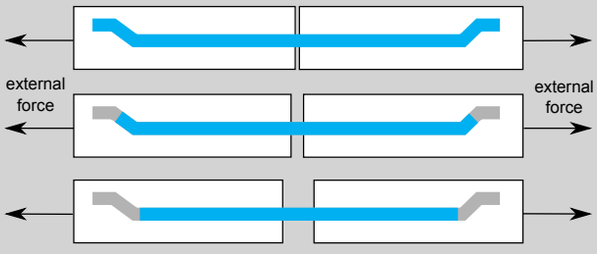

Figure 3.3: Illustration of pull-out steps of one steel fibre - without fibre rupture.

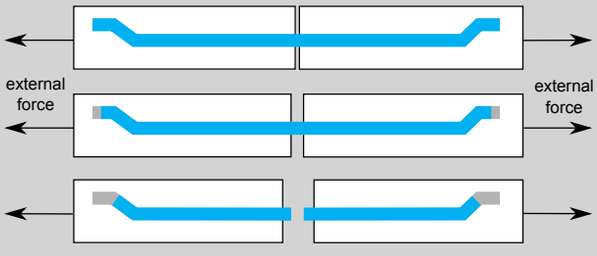

Figure 3.4: Ilustration of pull-out steps of one steel fibre - with fibre rupture.

3.2 FIBRE ORIENTATION

Fibre orientation can have a significant impact on the mechanical properties of SFRSCC.

Figure 3.5 shows an example of four different fracture planes, which are rotated at four different angles relative to the fibres. The fibres are all orientated in one direction. The sketch illustrates how fibre orientation significantly affects the number of fibres and the inclination of the fibres crossing the fracture plane.

Experimental results have shown that the mechanical properties of steel fibre reinforced concrete is primarily dominated by the number of fibres crossing the fracture plane.

3.3 FIBRE DOSAGE

Similar to fibre orientation, fibre dosage has a direct influence on the number of fibres crossing a given fracture plane. The higher the fibre dosage, the more fibres cross the fracture plane and the higher the mechanical performance (Figure 3.6).

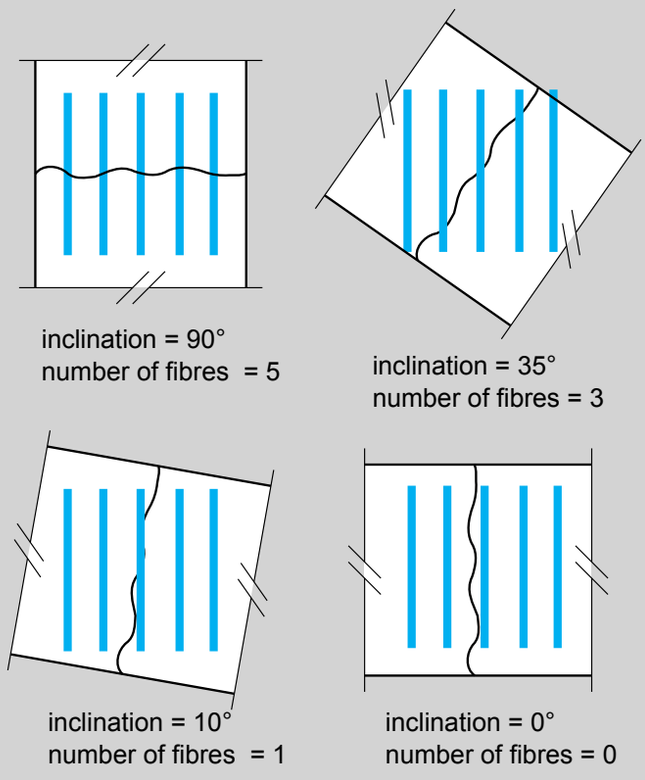

Figure 3.5: Illustration of five fibres crossing four differently oriented fracture planes and their respective number of fibres crossing the fracture plane.

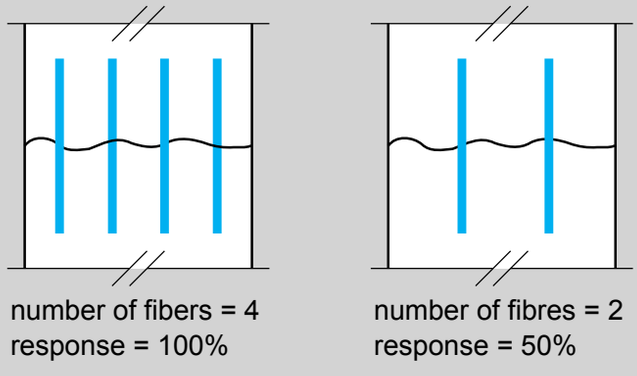

Figure 3.6: Illustration of two different fibre dosages together with their respective relative pull-out responses.

4. Mechanical testing of steel fibre reinforced concrete

Standard beams refer to those beams used to determine the performance classes of steel fibre reinforced concrete according to EN-14651: Test Method For Metallic Fibered Concrete – Measuring The Flexural Tensile Strength. The standard beam dimensions are 550 x 150 x 150 mm.

4.1 CASTING OF STANDARD BEAMS

4.1.1 Standard approach

EN-14651 prescribes the casting procedure for conventional SFRC (Figure 4.1). The concrete is poured into the mould at three different positions. Subsequently, vibration is applied to compact the concrete. This standard procedure induces a reference fibre orientation for conventional SFRC. A 3D random fibre orientation is normally assumed in the bulk region of conventional SFRC, which corresponds to a fibre orientation factor α_0 of 0.50 (see Section 5.3 about fibre orientation factors). However, due to the wall effect, more fibers will be orientated in the beam direction. It has been shown that a fibre orientation factor α_0 of 0.60 may be expected in the fracture plane of standard beams cast with conventional SFRC.

4.1.2 SFRSCC

The standard casting procedure described in Section 4.1.1 is not applicable for SFRSCC. SFRSCC flows on its own. Therefore, there is no reason to place the concrete in three different positions or to vibrate it. To limit operator dependency, improve reproduceability and repeatability and to reduce scatter, a new casting procedure has been proposed and verified (Figure 4.2 and Figure 4.3). At first, the concrete is poured into a funnel placed on top of the formwork at the end of the beam. The gate at the bottom of the funnel is opened and the concrete flows into the mould. Results obtained from experimental testing and from numerical simulations show an average fibre orientation factor α_0 of 0.78 in the fracture plane of standard beams cast with SFRSCC.

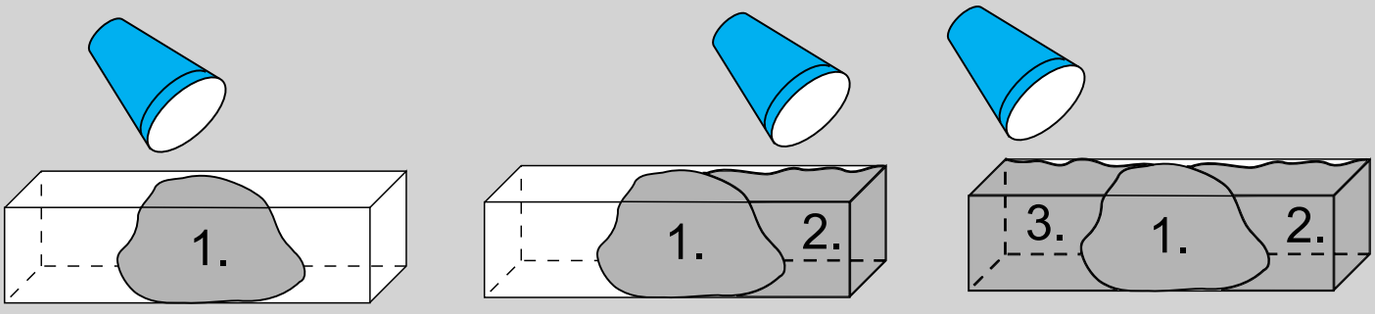

Figure 4.1: Casting of standard beams according to EN-14651: Test method for metallic fibered concrete - measuring the flexural tensile strength. Vibration is applied.

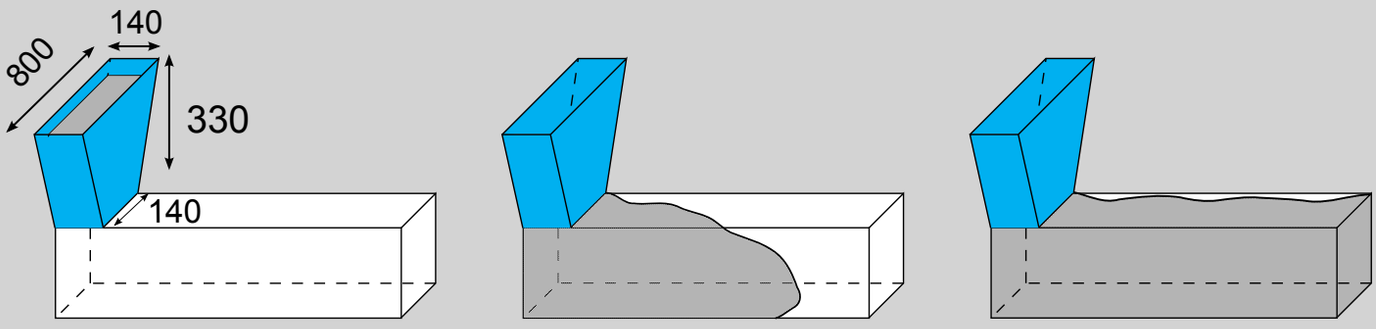

Figure 4.2: New procedure proposed for casting of SFRSCC into standard beams. Vibration is not applied.

Sampling from the wheel barrow.

Filling the funnel.

Filling the funnel.

Pulling the gate. Concrete flows.

Concrete at stoppage. SFRSCC is not self-levelling.

Careful manual finishing to level the surface.

Figure 4.3: Set of photographs showing the procedure proposed for casting of standard beams with SFRSCC.

4.2 DETERMINATION OF THE RESIDUAL TENSILE STRENGTH

For each series, a minimum of six beams are produced and tested in three point bending. The residual flexural tensile strength is measured at different crack mouth opening displacements (CMOD). Based on statistics, performance classes L1 and L2 are determined, which refer to the flexural tensile strength at CMOD of 0.5 mm and 3.5 mm, respectively.

In the accompanying design guide, a concept for determining the performance class of SFRSCC has been introduced. The aim of the concept is to link the performance classes of SFRSCC to a reference fibre orientation, which is comparable to that of conventional SFRC. The performance of the actual structure is then obtained by rescaling the reference performance using the actual fibre orientation in the structure. The rescaling fibre orientation factor is referred to as κ_f^f.

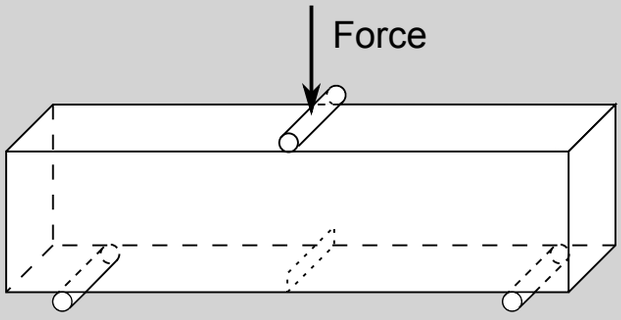

Figure 4.4: Layout of the three point bending test.

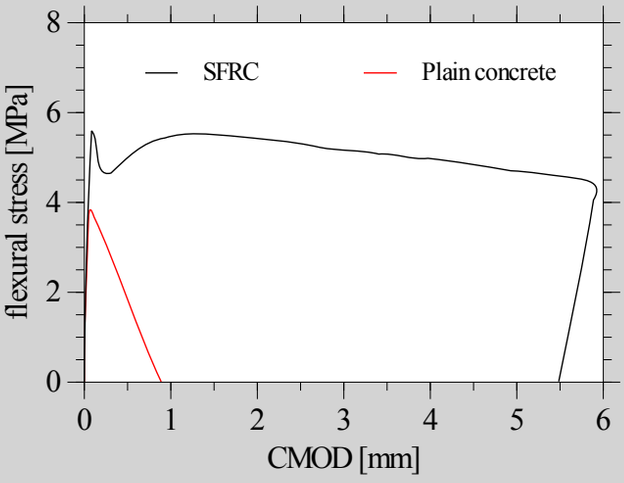

Figure 4.5: Illustrative comparison of the mechanical response of plain concrete and of SFRC. CMOD = Crack Mouth Opening Displacement.

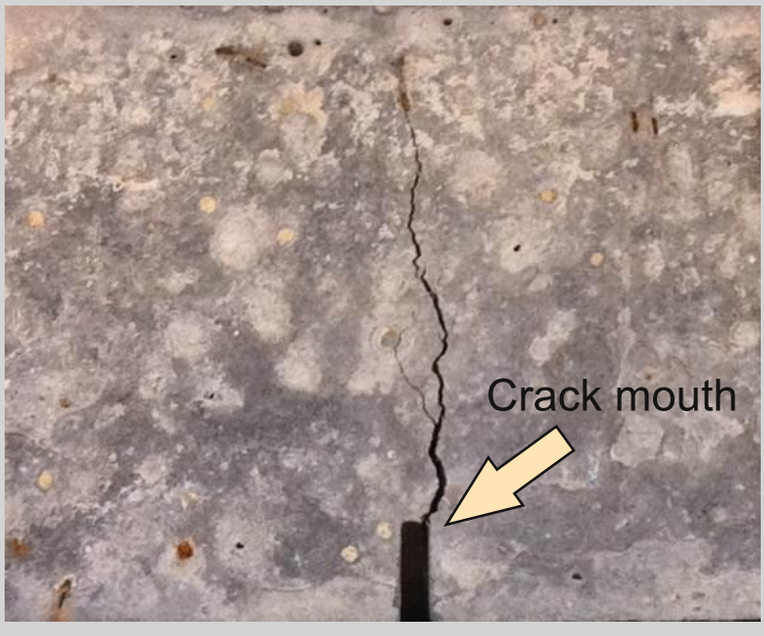

Figure 4.6: Resulting crack pattern after the three point bending test.

Figure 4.7: Photograph of the three point bending test.

5. Fibre orientation - introduction

5.1 ORIGIN OF FIBRE ORIENTATION

Orientation of individual steel fibres immersed in SFRSCC origins from a combination of several basic phenomena of which the most important ones are the so-called wall effect, shear induced orientation and extensional stresses induced orientation.

5.1.1 Wall effect

The wall effect is caused by the interaction of the immersed steel fibres with the surrounding rigid obstacles such as the formwork. It is geometrically impossible to have a rigid fibre located normal to the formwork at a distance less than half-length of the fibre (red rectangle in Figure 5.1). Hence, the rigid fibre tends to orientate according to the surrounding flow with a restriction imposed by the wall (fibre marked as blue rectangle).

5.1.2 Shear induced orientation

Shear induced orientation of steel fibres orientates fibres almost parallel to the shear flow direction. The fibres then remain in that position (Figure 5.2). Shear induced orientation takes approximately 0.5 up to 5 seconds depending on material properties. Compared to the duration of the casting process, it can be assumed that the shear induced orientation is instantaneous.

5.1.3 Extensional stresses induced orientation

Extensional stresses induced orientation orientates the fibres normal to the flow direction. As an example, a plate is cast from a circular inlet (brown circle in Figure 5.3) positioned at one corner of the plate. SFRSCC spreads from the inlet in a circular shape (dashed lines). Figure 5.3 presents three different time steps of the concrete flow. At the initial state, the fibre is almost parallel to the flow direction (red stroke bar). As the fibre moves away from the inlet, the fibre orientates normal to the flow direction (blue bar).

Red, orange and blue dashed curves represent the same material at the three time steps. As the distance from the inlet increases, the length of these curves also increases. With the increasing length, the velocity of the concrete parallel to the flow direction decreases (thickness of the dashed curves). Therefore, at the initial state, the velocity of point "a" is higher than the velocity of point "b". The difference between the two velocities forces the fibre to orientate normal to the flow direction. When point "a" and "b" reach the same circular curve, the fibre remains in that orientation state.

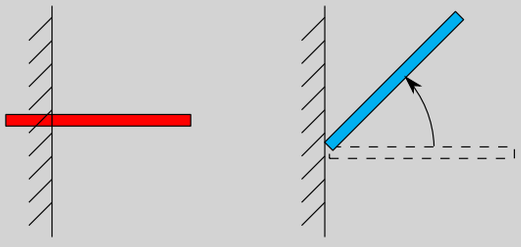

Figure 5.1: Wall effect: Blue and red bars represent the possible and impossible orientation of the rigid fibre.

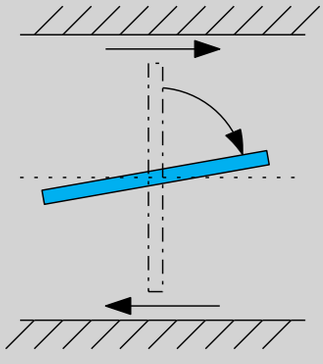

Figure 5.2: Shear induced orientation: Horizontal arrows represent the shear direction. The dot-dashed bar represents the initial fibre position. The blue bar represents the final fibre position.

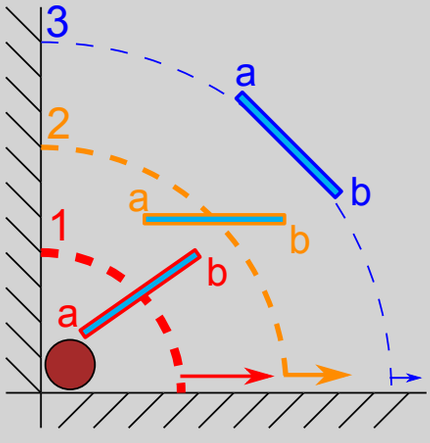

Figure 5.3: Extensional stresses induced orientation: Top view illustration of a plate casting.

5.2 FACTORS INFLUENCING FIBRE ORIENTATION

The resulting fibre orientation is governed by the aforementioned physical phenomena. Thus, fibre orientation is dependent on the flow pattern of SFRSCC, which is influenced by factors such as the:

- Formwork geometry and surface
- Reinforcement layout
- Casting process
- Concrete rheology
- Fibre type and volume fraction

Some basic relations and observations:

- Formwork surface
  - Rough formwork surface results in a more random fibre orientation in the vicinity of the formwork
  - Smooth formwork surface results in less random fibre orientation in the vicinity of the formwork
- Plastic viscosity
  - Based on experience, variations in plastic viscosity in the range of 25 - 100 Pa·s do not have any profound impact on the resulting fibre orientation.
- Yield stress
  - Based on experience, variations in yield stress in the range of 20 - 100 Pa do not have any profound impact on the resulting fibre orientation. This corresponds to slump flows from approximately 520 - 720 mm.

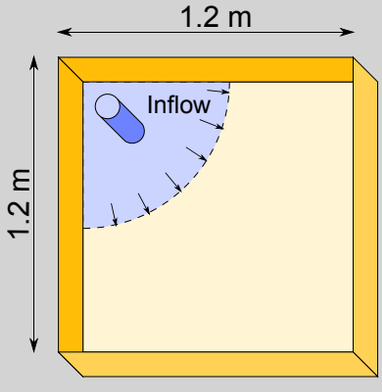

Figure 5.4: Layout of the slab casting. The casting was performed into the formwork made of oiled glue-laminated plywood and ordinary plywood.

Example:

As an example, Figure 5.4 and Figure 5.5 present the effect of formwork surface on the fibre orientation close to the formwork. The first slab was cast into a formwork consisting of smooth oiled glue-laminated plywood. The second slab was cast into a formwork consisting of ordinary rough plywood. The casting into the glue-laminated plywood formwork resulted in a less random fibre orientation compared to the casting into the ordinary plywood formwork.

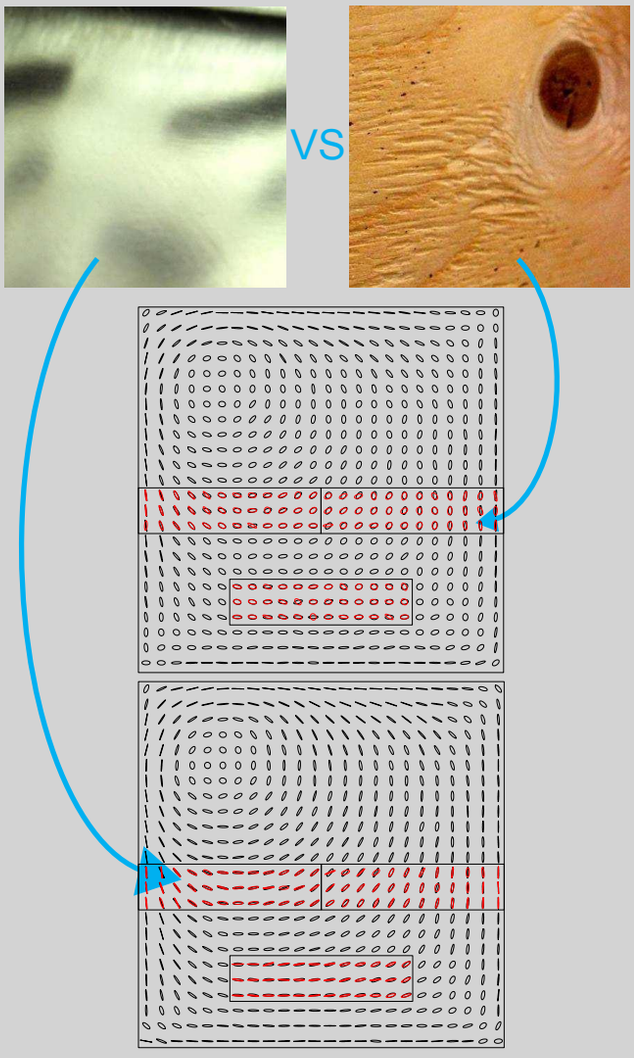

Figure 5.5: Slab castings - effect of formwork surface on fibre orientation close to the formwork (left: glue-laminated plywood, right: ordinary plywood). Bottom: Top view of the slabs - respective orientation ellipses (black = simulation, red = experiment).

5.3 REPRESENTATION OF FIBRE ORIENTATION

The most complete information about the fibre orientation and distribution is achieved when position and orientation of every single fibre is tracked. The main drawback of such a representation is the lack of experimental and analytical tools capable of acquiring and processing that complex information. X-ray computed tomography together with emerging numerical simulations of flow are currently the only techniques that can provide 3D position and orientation of all the individual steel fibres.

5.3.1 Fibre orientation factor (α_o)

Results have shown that the mechanical response of SFRC is primarily influenced by the number of fibres in the fracture plane, N_f. Therefore, It can be advantageous to represent the local fibre orientation in terms of the number of fibres crossing a given plane. According to Krenchel [1975], the fibre orientation factor α_o is defined as $\alpha_o = N_f A_f / (V_f A_c)$ where A_f, V_f and A_c represents the fibre cross-sectional area, fibre volume fraction and the concrete area, respectively. The fibre orientation factor represents fibre orientation in the direction perpendicular to the specific plane of interest. For instance, the fibre orientation factor is equal to 1.00 if the fibre orientation is unidirectional in a certain direction (1D), 0.64 for all in-plane directions when the fibres are randomly oriented in that plane (2D), and 0.50 in all directions when the fibres are randomly oriented in space (3D).

It should be noted that the orientation factor describes fibre orientation in a given plane only. To fully describe fibre orientation in a certain point in space, knowledge of the orientation factor in infinitely many differently inclined planes is required.

5.3.2 Fibre orientation factor (κ_f^f)

In the accompanying design guide, the fibre orientation factor κ_f^f is used to scale the residual tensile strength from the standard beam testing to the actual structure. If $\kappa_f^f = 1$, the fibre orientation in the actual structure is the same as the fibre orientation in the standard beams. If the orientation factor α_o in the actual structure is higher than the fibre orientation in the standard beams, then $\kappa_f^f > 1$ and vice versa. See example below with a reference fibre orientation factor α_o of 0.60.

5.3.3 Fibre orientation ellipses

Fibre orientation ellipsoids in 3D or ellipses in 2D provide spatial information of local fibre orientation (Figure 5.6 right). When the orientation ellipse becomes a circle, the local fibre orientation is random. There is a prevailing fibre orientation in a certain direction when the orientation ellipse becomes elongated in that direction. Currently, fibre orientation ellipses can be obtained only from numerical simulations or from CT scanning of real specimens. Fibre orientation ellipses provide an alternative for visualisation of the fibre orientation in a certain point in space.

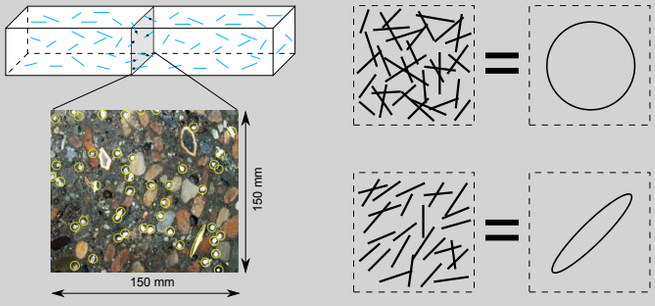

Figure 5.6: Left: Detection of fibres in a cracked plane. Number of fibres = 180. Right: Illustration of fibres and orientation ellipses.

Example:

- number of fibres (N_f) = 180
- concrete area (A_c) = 150*150 = 22500 mm^2
- fibre length (L_f) = 60 mm
- fibre aspect ratio (Ψ) = 80
- fibre density (ρ_f) = 7800 kg/m^3
- fibre dosage (M_f) = 40 kg/m^3
- fibre volume fraction (V_f) = $M_f / \rho_f \approx 0.5\%$
- fibre radius (r_f) = $L_f / \Psi / 2$ = 0.375 mm
- fibre area (A_f) = πr_f^2 = 0.44 mm^2

Fibre orientation factor $\alpha_o = N_f A_f / (V_f A_c)$ = **0.70**

Fibre orientation factor $\kappa_f^f = \alpha_o / 0.60$ = **1.17**

5.4 DETERMINATION OF FIBRE ORIENTATION

5.4.1 Manual counting

Manual counting is a simple destructive experimental method, which is used to determine the number of fibres crossing a given plane. The number of fibres is used to determine the fibre orientation factor α_o assuming the fibre volume concentration and the fibre cross sectional area are known.

The method does not require any special equipment or skills but it is relatively time consuming. If the local fibre volume concentration varies, the method does not provide enough information to properly distinguish between the effect of fibre orientation and the local fibre volume concentration. The two phenomena can be separated by determining the local fibre volume concentration. First, the sample volume is determined and secondly the sample is crushed to determine the fibre content.

Manual counting is commonly composed of the following steps. A structural element made of SFRSCC is cut along a given plane of interest (Figure 5.7a). The plane is polished and the number of fibres crossing the plane is determined (Figure 5.7b,c).

5.4.2 Identification of fibre inclination

Recognition of fibre inclination is based on manual counting with the addition of fibre cross-sectional shape analysis. Similarly to manual counting, the procedure begins with cutting and polishing a given plane of interest. The plane polishing is performed to remove any fibre deformations caused by the cutting.

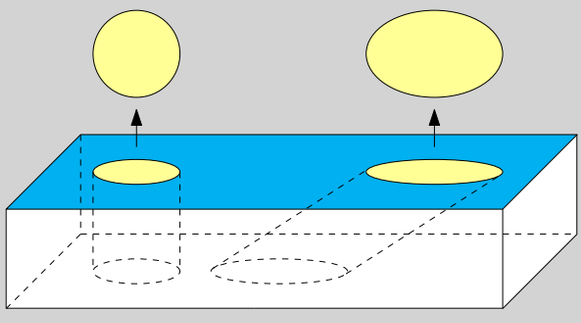

Figure 5.8: Illustration of two fibres (dashed cylinders) crossing a give plane (blue). Yellow ellipses denote fibre cross-sectional shapes at the given plane.

The number and shape of the fibres crossing the given plane is then analysed. Figure 5.8 shows an example of two fibres crossing a given plane. When the fibre is normal to the given plane, the cross-section of the fibre visible at the given plane has a circular shape (left). When the fibre crosses the given plane at a different inclination, the cross-sectional shape of the fibre becomes an ellipse (right). The inclination of the fibre relative to the given plane can be estimated based on lengths of major and minor axes of the ellipse. Note that a single ellipse can represent two different fibre inclinations.

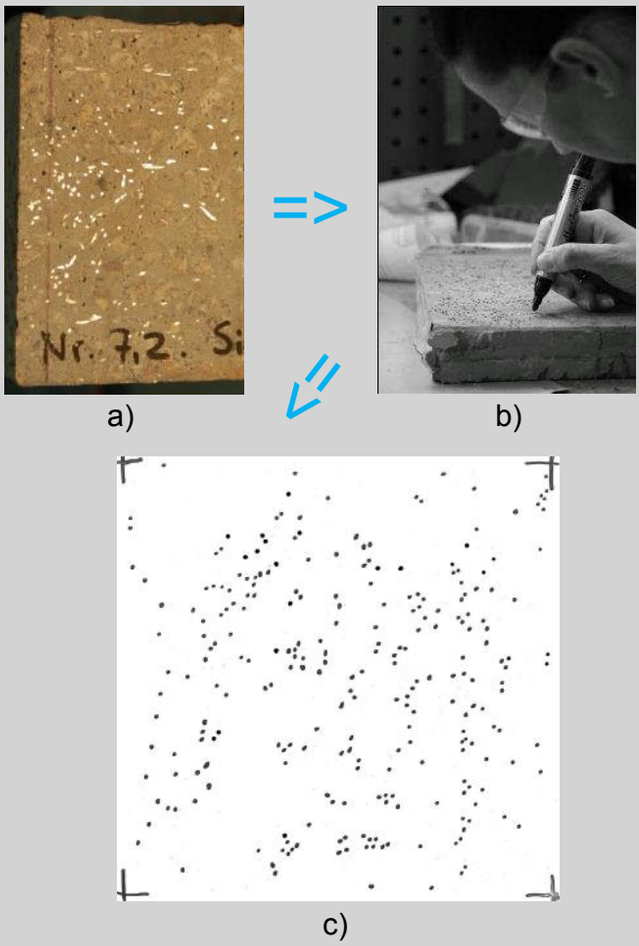

Figure 5.7: Process of manual counting. a) Cut specimen. b) Manual counting. c) Scanned result.

5.4.3 X-Ray computed tomography

X-Ray computed tomography with subsequent image analysis is an advanced experimental technique used to obtain a 3D model of the internal structure of an element. X-Ray computed tomography produces tomographic slices, i.e. images, of specific areas of the element. A set of successive tomographic slices form a 3D image which can be converted into a 3D model. X-ray computed tomography is the only experimental method capable of obtaining position and orientation of every single steel fibre.

The method is also highly efficient. As an example, a standard size beam can be scanned in less than a minute when using e.g. the medical CT scanner Siemens Somatom Sensation 4.

5.4.4 Numerical simulations

Numerical frameworks capable of predicting orientation and distribution of fibres immersed in SFRSCC can serve as an efficient alternative to the aforementioned experimental methods (Figure 5.11). Such numerical frameworks usually consist of a fluid dynamics solver and a fibre orientation and distribution solver.

Numerical simulations are relatively cheap, fast and satisfactorily accurate. It is possible to perform complicated and large parametric studies in the range of days. Therefore, numerical simulations can serve as an appropriate alternative and supplement to experiments. Different examples of numerical simulations are shown in the subsequent sections applying a new software developed within the project.

Figure 5.9: CT scanning of a cut sample.

Figure 5.10: Concrete core sample scanned by computed tomography and analyzed by image analysis [Fritz2009].

```
let getPhaseGlob (Triple(gx, gy, gz)) =
  let isInXY =
    let dist =
      let node = triple(float gx, float gy, 0.0)
      let cog = triple(inflowXY, inflowXY, 0.)
      Triple.norm (node - cog)
    dist < inflowRadius - 1.
  let isInZ =
    let isAtTopPart = gz < nodesZ - 2 && float gz >= 1.5 * beamLz
    let isAtBottomPart = float gz < beamLz
    isAtTopPart || isAtBottomPart
  if isInXY && isInZ then Fluid else Gas
```

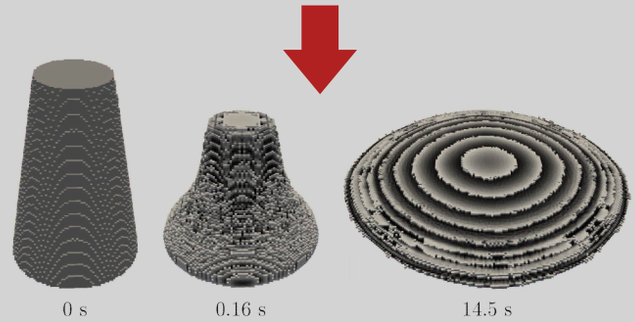

Figure 5.11: Top: Typical section of numerical code. Bottom: Result of a numerical simulation (slump flow at three different time steps).

6. Fibre orientation - recommendations

Casting of SFRSCC can lead to significant fibre orientation, which can lead to significant variations in the mechanical properties. This section presents some general recommendations followed by an overview of recommended fibre orientation factors for three different applications i.e. beams, walls and slabs. The recommendations for fibre orientation factors are based on the results obtained throughout the project and engineering judgement. For an overview of the results obtained from numerical simulations and experimental testing, see the next section "Fibre orientation - examples".

6.1 GENERAL RECOMMENDATIONS

It is recommended that fibre orientation factors are always chosen carefully with respect to the:

- structural design and safety level
- level of documentation
- level of casting process control
- level of batch control
- level of training and experience in the design and execution of SFRSCC.

Some of the keypoints to consider when using SFRSCC are listed below.

- Numerical simulations can serve as a useful tool to obtain detailed information about fibre orientation factors. Simulations can also be used to plan and optimize the casting process in such a way that the most beneficial fibre orientation is obtained in specific locations of the structure.

- Trial castings are always recommended to validate the fibre orientation factors in selected regions. Typically, it will be possible to cut sections or drill cores at specfic points of interest to perform fibre counting. Alternatively, CT scannings can be useful to obtain detailed information about the fibre orientation. Furthermore, trial castings should be used to check the concrete flow with respect to the form filling ability and stability. The flow properties are measured and the results are used to specify the acceptance range to be applied during the full-scale casting. Finally, trial castings are important in order to gain experience and knowledge about the material behaviour, in particular if the contractor has no or limited experience in using SFRSCC.

- Casting process planning: The fibre orientation factors are heavily dependent on the casting process. It is recommended to prepare a casting plan, which include a clear description of casting positions and casting rates. It is important that it is actually possible to perform the casting according to the casting plan.

- Batch control: It is recommended to perform batch control at the job site. This includes measurements of the flow properties and the fibre content (e.g. by wash-out tests). The frequency of batch control depends on the application.

- Documentation: It is recommended to document the casting process e.g. by sketches, videos and photographs. For each batch the following documentation could be included: Time of arrival, batch control results, time of casting, casting rate (truck empty time) and casting position.

- Training: Compared to traditional concrete, the use of SFRSCC and the concept of fibre orientation impose a stronger link between the design and the execution. Therefore, it is important that both the designer and the contractor are well aware of this important link. The designer should have insight into the on-site procedures and into the risk associated with SFRSCC castings. The contractor should understand how the casting procedure affects the structural performance.

- Experience is important. If possible, persons with previous experience in casting and handling of SFRSCC should be present during the execution of the structure.

6.2 FIBRE ORIENTATION FACTORS

Figure 6.1 shows recommended fibre orientation factors for SFRSCC in beams, walls and slabs (red values). The k_f^f values (red) are calculated by dividing α_o with the reference fibre orientation factor. Here, a reference fibre orientation factor of 0.60 is assumed. For comparison, the fibre orientation factors for SFRC proposed in the German DAfStB have also been shown (black values).

For walls, it is assumed that the inlet position is just below or just above the concrete surface. Thus, the values do not apply to fully submerged inlets like e.g. casting from the bottom.

Regarding shear, fibre orientation factors shall represent the strength in the direction normal to the 45 degrees inclined shear crack. The orientation of the shear crack due to a positive shear force is different from the orientation of a shear crack due to a negative shear force. The fibre orientation factors for shear cracks due to positive and negative shear force can be different and cannot be obtained by interpolation between the normal 0 and 90 degrees orientations. Therefore, for steel fibre reinforced self-compacting concrete, no general recommendation for fibre orientation factors for shear can be given. They need to be assessed individually for each case.

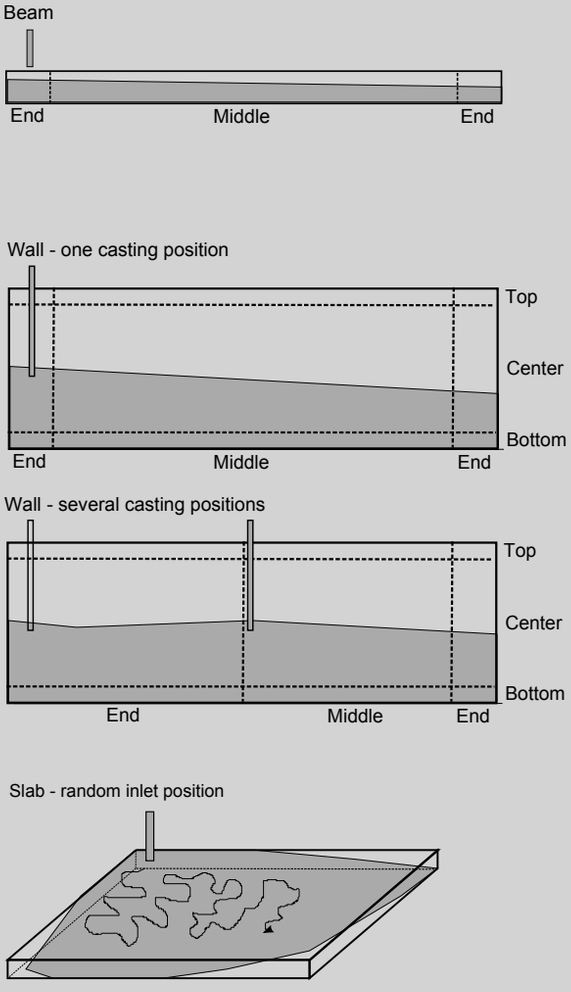

	Beam	Steel fibre reinforced self-compacting concrete				
	Middle			End		
	Longitudinal	Vertical	Transverse	Longitudinal	Vertical	Transverse
α_o	0.75	0.20	0.20	0.45	0.25	0.25
κ_f^f	1.25	0.33	0.33	0.75	0.42	0.42
κ_f^f	0.50	0.50	0.50	0.50	0.50	0.50

	Wall-Bottom	Steel fibre reinforced self-compacting concrete				
	Middle			End		
	Longitudinal	Vertical	Transverse	Longitudinal	Vertical	Transverse
α_o	0.75	0.20	0.20	0.50	0.25	0.25
κ_f^f	1.25	0.33	0.33	0.83	0.42	0.42
κ_f^f	0.50	0.50	0.50	0.50	0.50	0.50

	Wall-Center	Steel fibre reinforced self-compacting concrete				
	Middle			End		
	Longitudinal	Vertical	Transverse	Longitudinal	Vertical	Transverse
α_o	0.60	0.25	0.20	0.50	0.25	0.25
κ_f^f	1.00	0.42	0.33	0.83	0.42	0.42
κ_f^f	0.50	0.50	0.50	0.50	0.50	0.50

	Wall-Top	Steel fibre reinforced self-compacting concrete				
	Middle			End		
	Longitudinal	Vertical	Transverse	Longitudinal	Vertical	Transverse
α_o	0.50	0.25	0.15	0.40	0.30	0.30
κ_f^f	0.83	0.42	0.25	0.67	0.50	0.50
κ_f^f	0.50	0.50	0.50	0.50	0.50	0.50

	Slab	Steel fibre reinforced self-compacting concrete	
	Longitudinal	Vertical	Transverse
α_o	0.60	0.18	0.60
κ_f^f	1.00	0.30	1.00
κ_f^f	1.00	0.50	1.00

Figure 6.1. Summary of fibre orientation factors for beams, walls and slabs.

7. Fibre orientation - examples

7.1 CHANNEL FLOW - SIMULATION

This section presents simulations carried out to study the effect of rheology (yield stress and plastic viscosity) on the fibre orientation factor α_0. The fibre orientation was studied by means of channel flow (Figure 7.1). In the X direction, the flow was bounded by two vertical walls (brown) placed 20 cm apart. In the Y and Z direction, the flow was infinite. The fibre length, aspect ratio and content were 60 mm, 80, and 40 kg/m^3, respectively. The flow was driven by gravitation acting opposite to the Z direction. In the initial state, the fibres were randomly orientated. As the time evolves, more and more fibres become orientated parallel to the flow.

Figure 7.2 presents the fibre orientation factor in the Z direction as a function of time. Figure 7.2 (left) shows the fibre orientation factor for a constant yield stress = 25 Pa and for varying plastic viscosities from 20 to 120 Pa·s. Figure 7.2 (right) shows the fibre orientation factor for a constant plastic viscosity = 20 Pa·s and for varying yield stresses from 25 to 100 Pa corresponding to slump flows from 700 to 520 mm, respectively. Figure 7.2 (left) indicates that by increasing the plastic viscosity, the time needed to reach a certain fibre orientation increases, however, the resulting fibre orientation factor is the same. Figure 7.2 (right) shows that the evolution of fibre orientation is more or less independent of the yield stress.

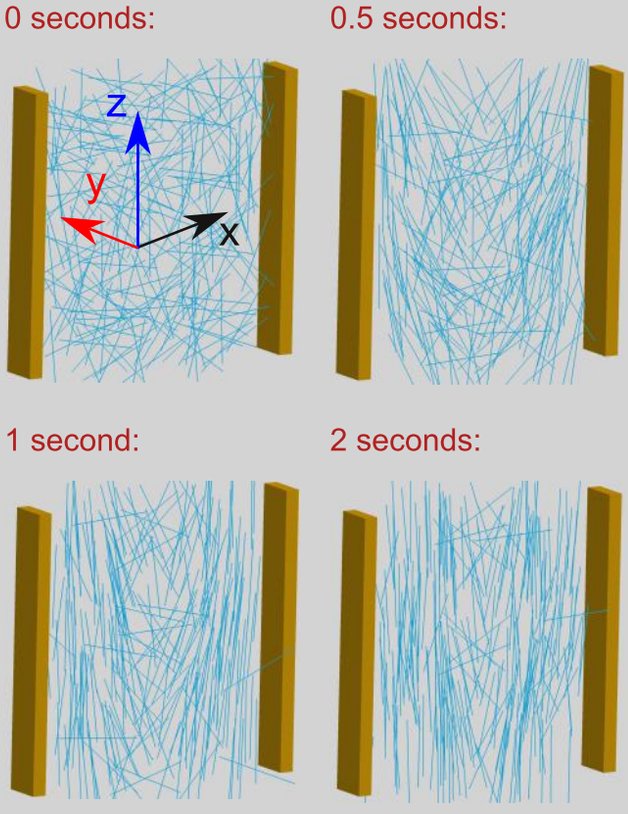

Figure 7.1: 3D view of channel flow at four different time steps. Blue lines represent steel fibres. Brown prisms represent the wall boundaries. The flow is driven by gravity pointing downwards in negative Z direction.

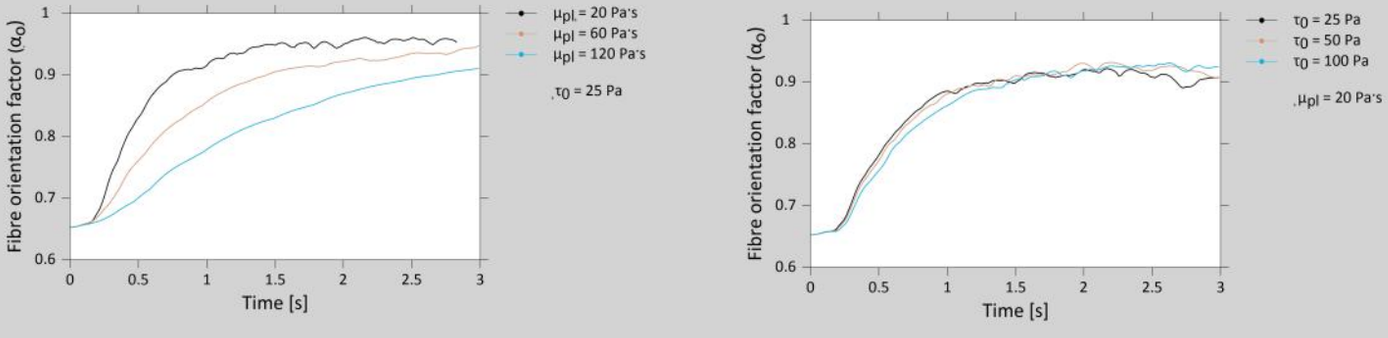

Figure 7.2: Fibre orientation factor α_0 in the Z direction as a function of time for the case of channel flow with varying plastic viscosities (μ_{pl}) and yield stresses (τ_0).

7.2 STANDARD BEAMS - SIMULATION

This section presents numerical simulations that were performed to investigate the effect of rheology, reinforcement and casting type on the fibre orientation factors (α_0 and κ_f^f) in different locations of the standard beam specimen.

7.2.1 Effect of rheology on fibre orientation

The effect of plastic viscosity and yield stress on the fibre orientation factors was investigated. The casting process simulates the proposed novel experimental casting process described in Section 4.1.2. Layout of the beam casting is shown in Figure 7.3. A continuous pouring process was simulated by continuously refilling the inlet region when it was empty (blue cylinder in Figure 7.3). The density of the SFRSCC was set to 2500 kg/m^3. The fibre length, aspect ratio and content were 60 mm, 80 and 40 kg/m^3, respectively.

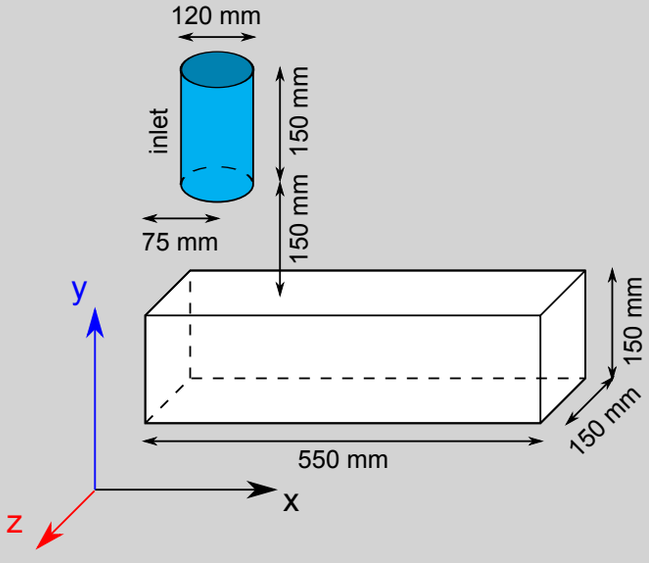

Figure 7.3: Layout of the model used to simulate the casting of a standard beam with SFRSCC.

Figure 7.4 presents 3D views of the initial and an intermediate state of the SFRSCC casting. The SCC part of the flow is presented in the left figures whereas the steel fibres are shown in the right figures. The colours of the SCC represent the flow rate (blue = low, white = high).

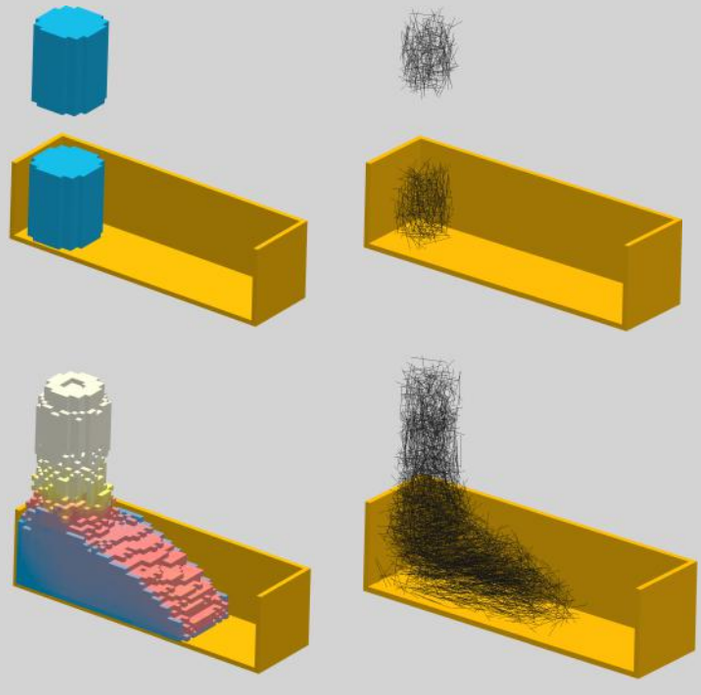

Figure 7.4: 3D views of the initial and an intermediate state of the SFRSCC casting. Left: SCC part; Right: Fibre part.

Figure 7.5 and 7.6 show side views of the SFRSCC at different time steps. Each row in the figure represents one time step (in seconds). Each column represents one set of rheological parameters. Colour represents the flow rate (blue = low, yellow = high) and the lines represent velocity directions.

Figure 7.5 shows the flow for three different plastic viscosities (20, 40, and 60 Pa·s). The individual figures show that a higher plastic viscosity results in a slower filling rate and vice versa. This is in line with observations made in Section 7.1 (Channel flow).

Figure 7.6 shows the flow for three different yield stresses (20, 40, and 60 Pa). The flow patterns are quite similar. Therefore, the figures do not indicate any pronounced effect of yield stress on the flow pattern of SFRSCC.

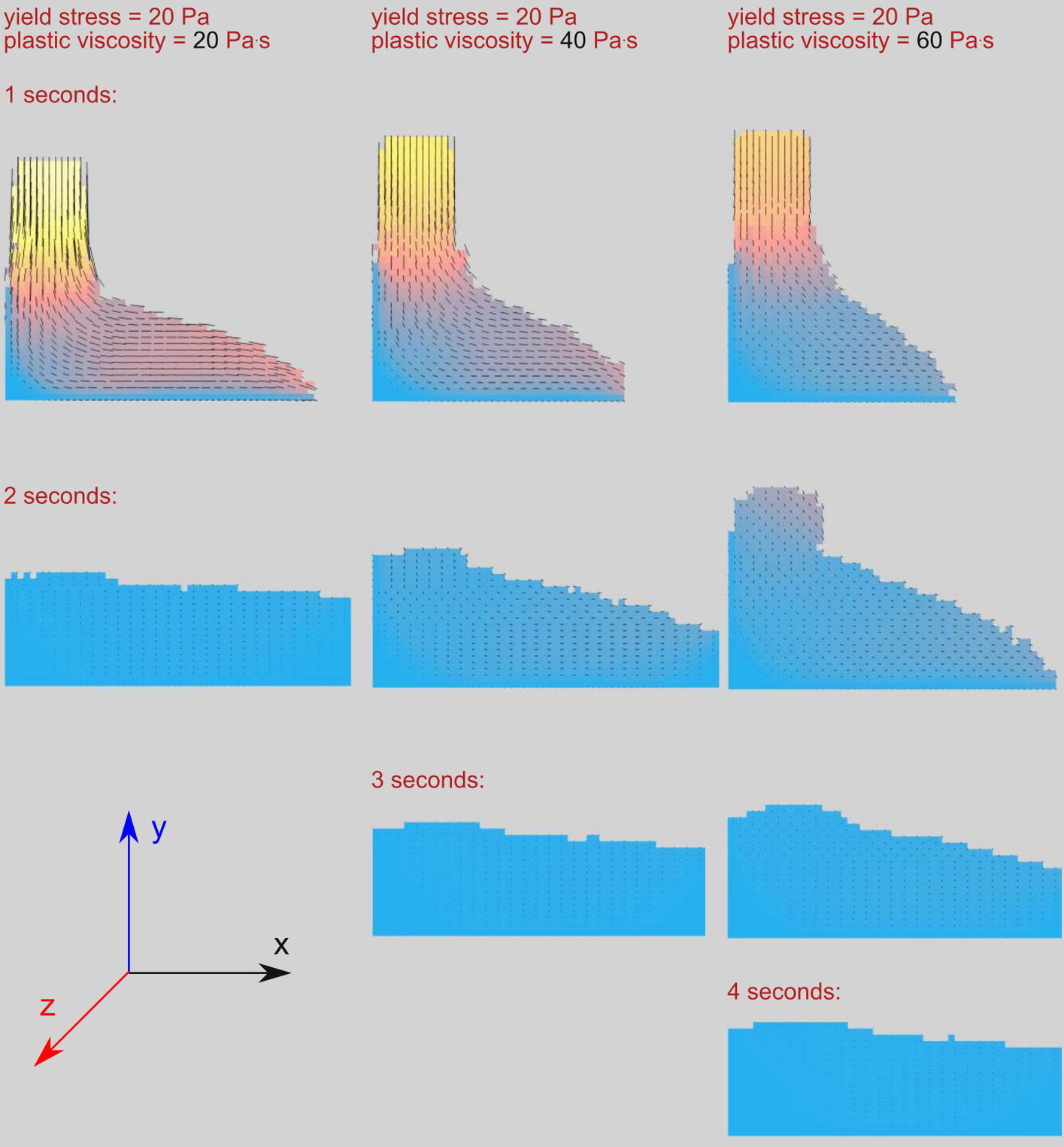

Figure 7.5: Side views of SFRSCC during casting of a standard beam. Each column represents a different plastic viscosity. Each row represents a different time step. The colour represents the flow rate of (blue = low, yellow = high). Black lines represent direction of the flow velocity.

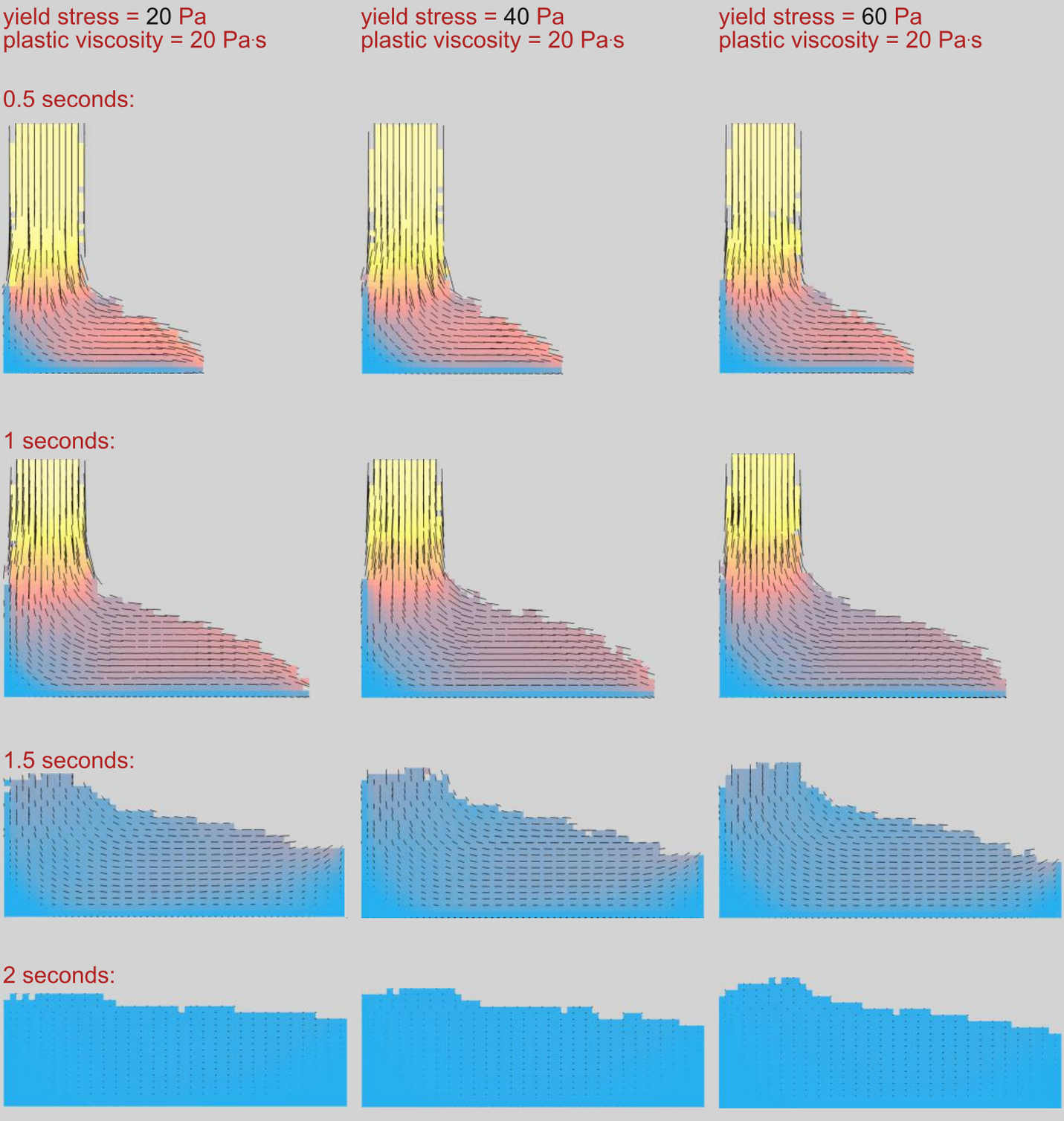

Figure 7.6: Side views of SFRSCC during casting of a standard beam. Each column represents a different yield stress. Each row represents a different time step. The colour represents the flow rate (blue = low, yellow = high). Black lines represent direction of the flow velocity.

Figure 7.7 shows the fibre orientation factors in the longitudinal (X), vertical (Y) and transverse (Z) direction as a function of the beam longitudinal position, X. The dominant fibre orientation direction is in the longitudinal direction (X). The orientation factor α_0 oscillates around the value of 0.78 in the middle part of the beam and reduces to approximately 0.50 close to the end walls. The value of 0.78 in the cracked plane is in line with experimental results.

The orientation factor α_0 in the vertical direction (Y) oscillates around the value of 0.26 in the middle part of the beam and increases to 0.41 and 0.31 at the left and right edge of the beam, respectively. The orientation factor α_0 at the left edge is higher due to the presence of inlet. The end walls hinter the concrete from flowing freely in the longitudinal direction and instead the concrete is forced in upward direction, which also force more fibres to orientate in the vertical direction.

The orientation factor α_0 in the transverse direction (Z) oscillates around the value of 0.34 in the middle part of the beam and increases to 0.52 and 0.60 at the left and right edge of the beam, respectively.

Figure 7.7 shows only small differences between the individual curves, i.e. among setups with different rheological parameters. Fibre orientation factors in the longitudinal direction slightly increase whereas fibre orientation factors in the vertical and transverse direction slightly decrease when the plastic viscosity and yield stress increase.

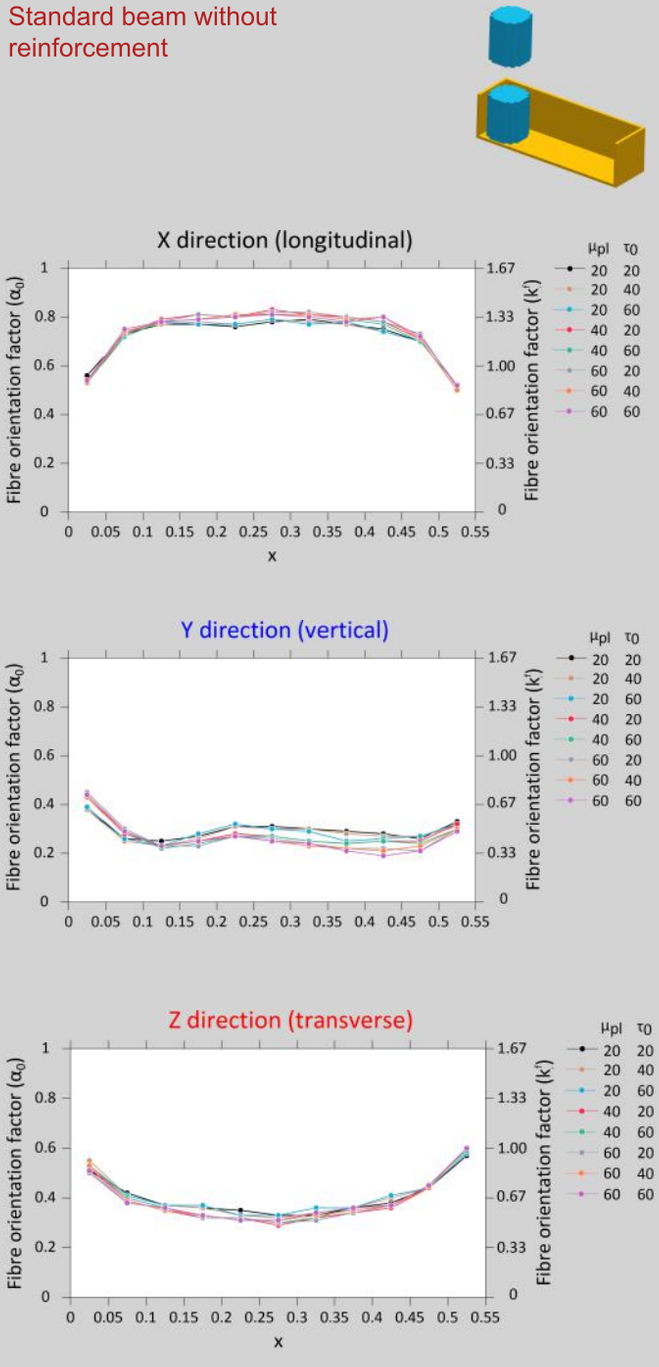

Figure 7.7: Fibre orientation factors in the X, Y and Z direction as a function of the longitudinal position, X. Standard beams cast with SFRSCC with different rheological properties.

7.2.2 Effect of reinforcement on fibre orientation

The effect of reinforcement on the fibre orientation factors was investigated. The five different setups were:

- without any reinforcement
- stirrups only
- main longitudinal reinforcement of diameter = 16 mm
- main longitudinal reinforcement of diameter = 10 mm
- main longitudinal reinforcement of diameter = 10 mm and stirrups

Layout of the beam casting is equivalent to Figure 7.3. The sectional layout in the case of the main longitudinal reinforcement and stirrups is illustrated in Figure 7.8. There are two equally spaced stirrups in the beam specimen. Figure 7.9 shows the initial state and two intermediate states of the casting process. Again, the colour represents the flow rate of the SFRSCC.

Figure 7.10 presents a set of side views of the flow at different time steps in the case of main longitudinal reinforcement (diameter = 10 mm) and stirrups. The figures indicate that the reinforcement slows down the concrete flow. In reality, filling rate would need to be reduced to avoid concrete flowing over the boundaries. In the simulation, infinitely high walls have been applied to avoid this problem.

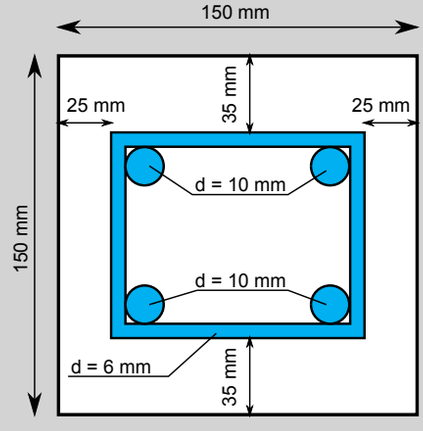

Figure 7.8: Sectional layout of the main longitudinal reinforcement and stirrups.

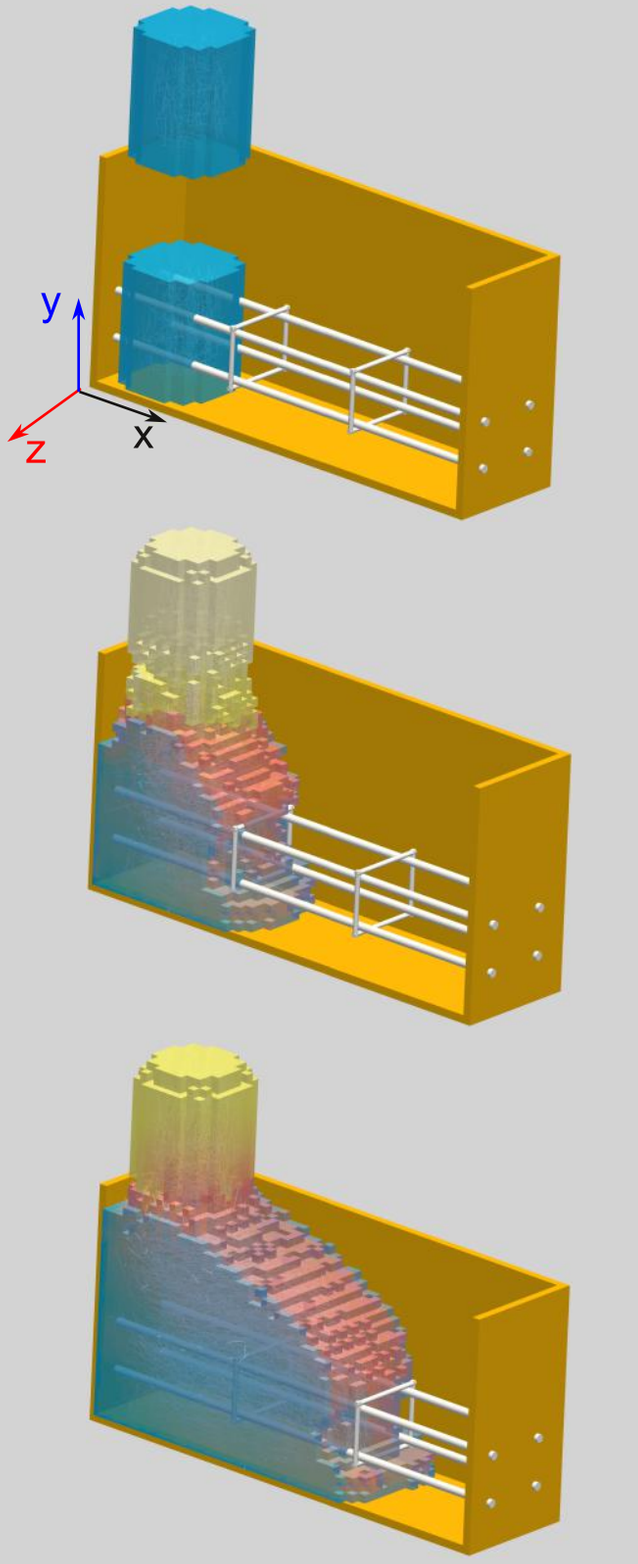

Figure 7.9: 3D view of the initial state and two intermediate states of a standard beam casting with SFRSCC. Longitudinal reinforcement and stirrups are included.

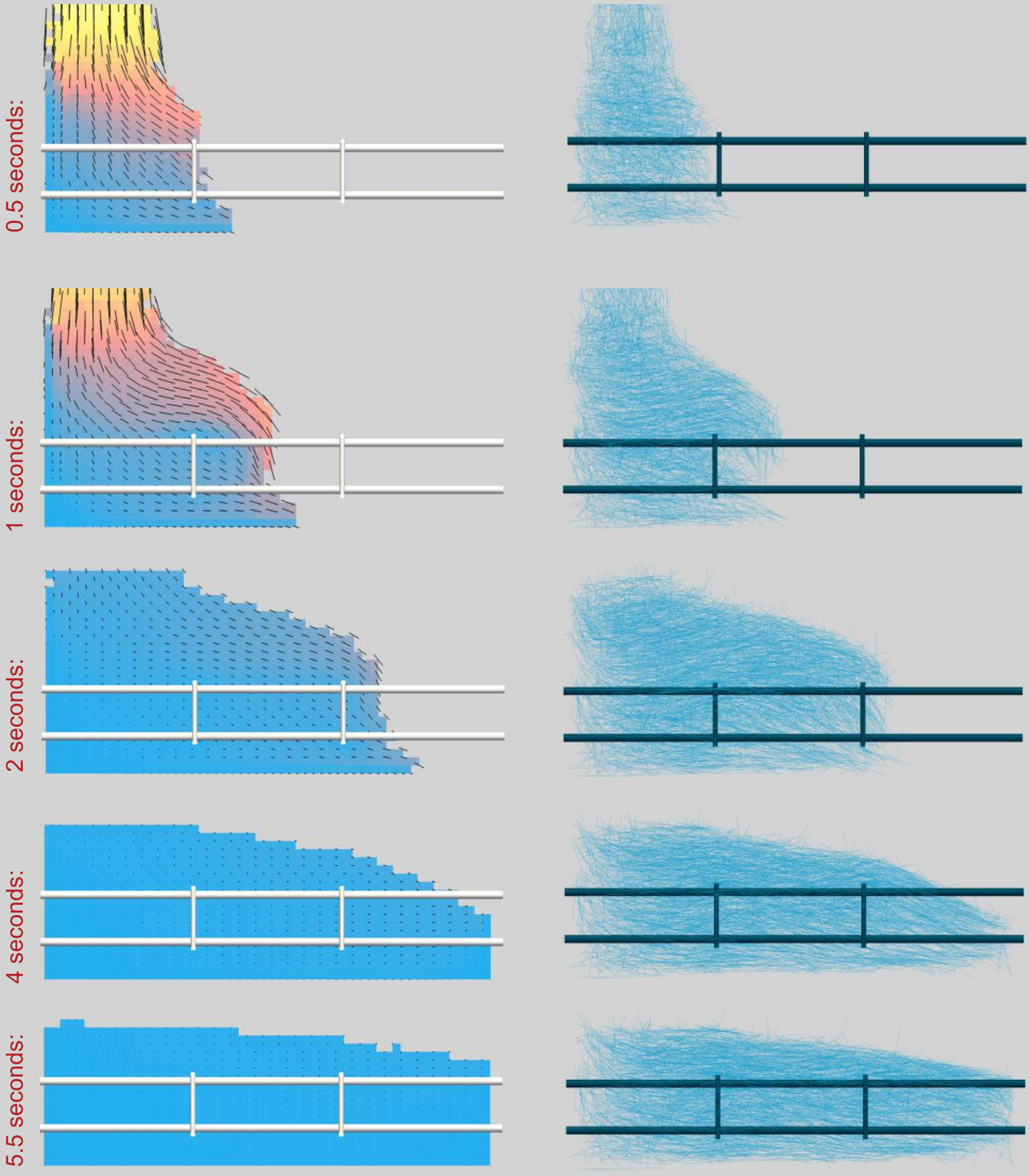

Figure 7.10: Side views of SFRSCC during casting of a standard beam containing both longitudinal reinforcement and stirrups. Individual rows represent different time steps. The left column shows the flow pattern of the SFRSCC. Colour represents the flow rate (blue = low, yellow = high). The right column shows the invidual fibres.

Figure 7.11 presents the fibre orientation factors in the longitudinal (X), vertical (Y) and transverse (Z) direction for the various setups of reinforcement as a function of the beam longitudinal direction, X.

Compared to the beam specimens without any reinforcement, the fibre orientation factors in the longitudinal direction increase due to the reinforcement.

The fibre orientation factors in the vertical and transverse direction decrease when both longitudinal reinforcement and stirrups are included.

7.2.3 Effect of casting on fibre orientation

The effect of the casting procedure on the fibre orientation factors was investigated. Three different casting procedures were applied:

- Type 1: The inlet was positioned at the left edge of the beam. After a while the inlet was repositioned to the right edge of the beam.
- Type 2: The casting was performed on an already existing layer of SFRSCC.
- Type 3: The inlet was positioned at the left edge of the beam. The casting was paused. After a short delay, the casting continued at the same position.

Figure 7.12, Figure 7.13 and Figure 7.14 shows side views of the flow pattern and the individual fibres in each case.

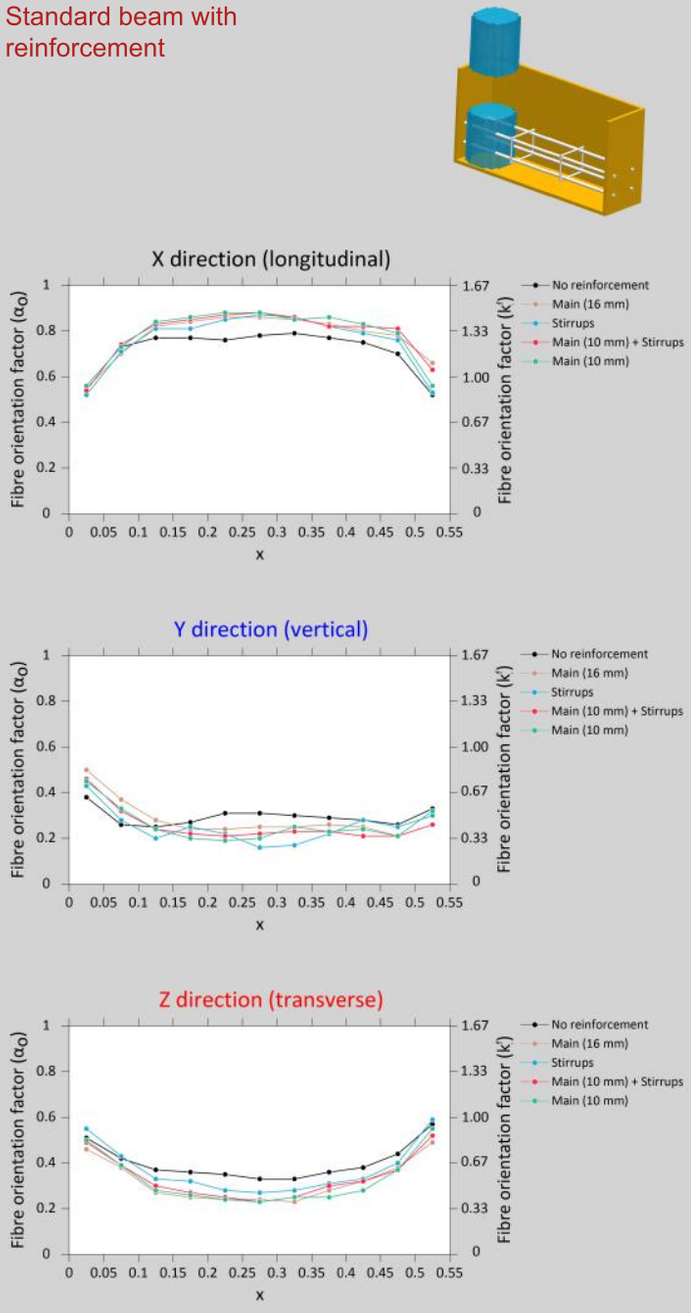

Figure 7.11: Fibre orientation factors in the X, Y and Z direction as a function of the longitudinal position, X, for the case of standard beams cast with SFRSCC. Various reinforcement setups were applied.

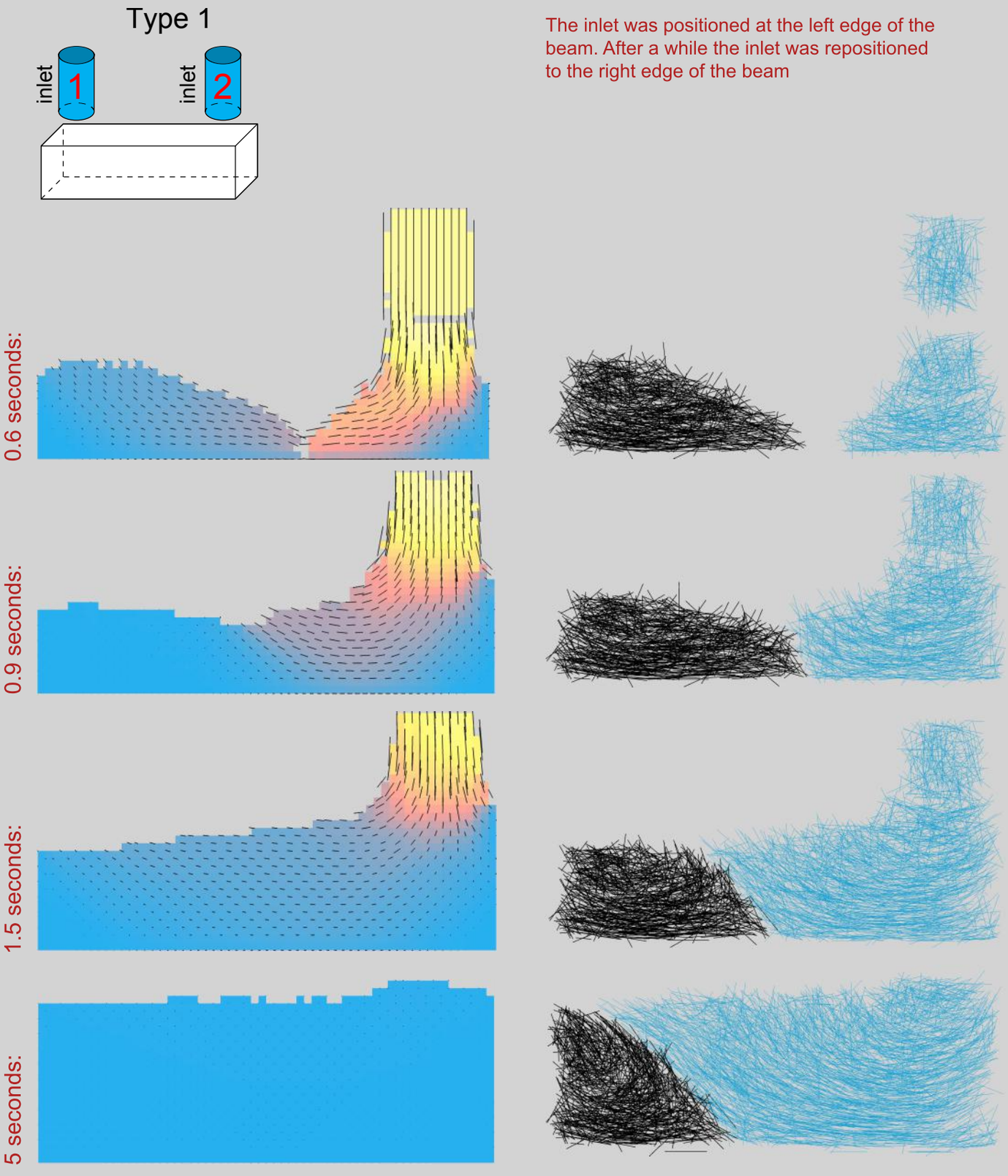

Figure 7.12: Side views of SFRSCC during casting of a standard beam applying casting type 1. Individual rows represent different time steps. The left column shows the flow pattern of the SFRSCC. Colour represents the flow rate (blue = low, yellow = high). The right column shows the invidual fibres.

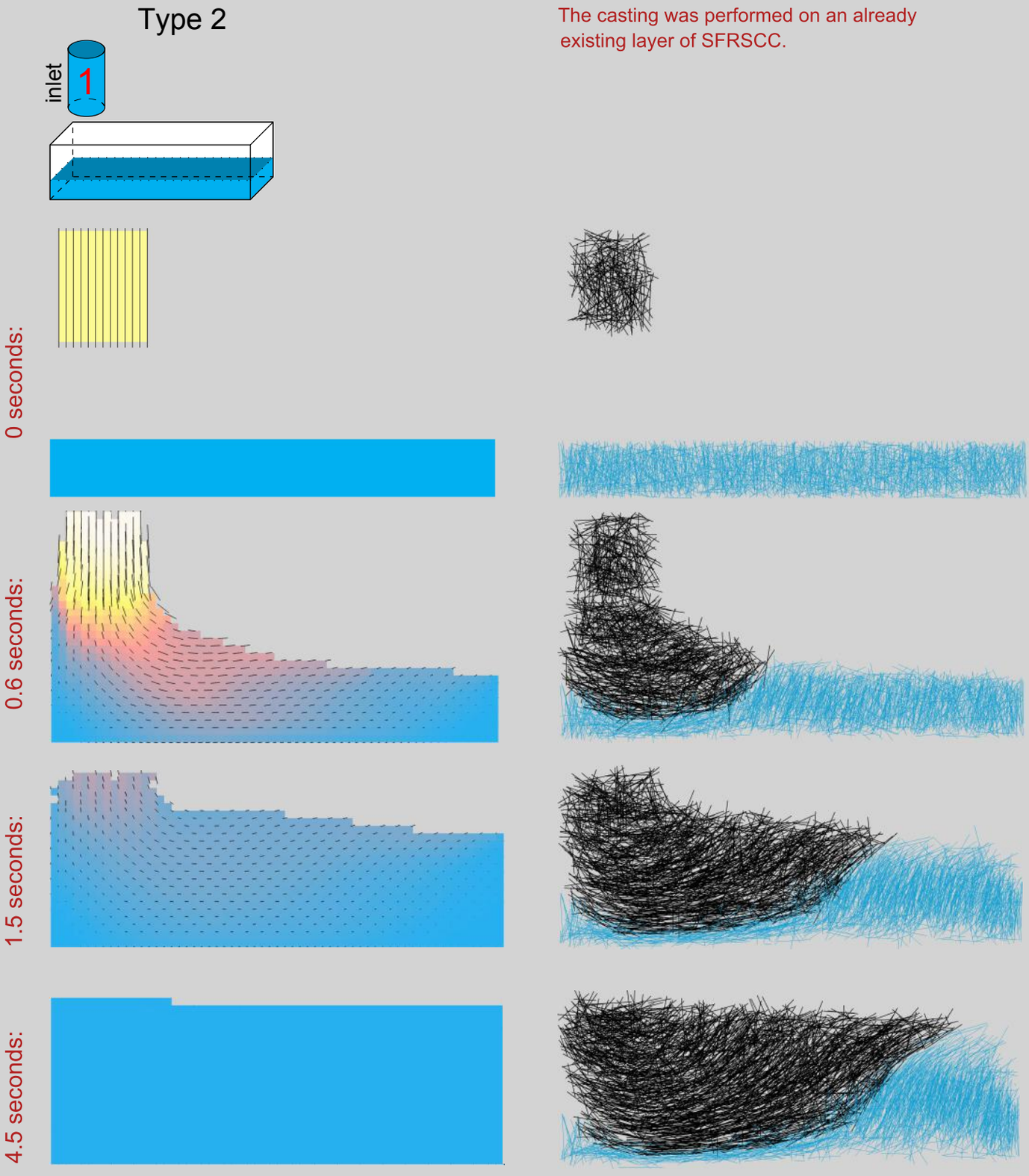

Figure 7.13: Side views of SFRSCC during casting of a standard beam applying casting type 2. Individual rows represent different time steps of the casting process. The left column shows the flow pattern of the SFRSCC. Colour represents the flow rate (blue = low, yellow = high). The right column shows the invidual fibres.

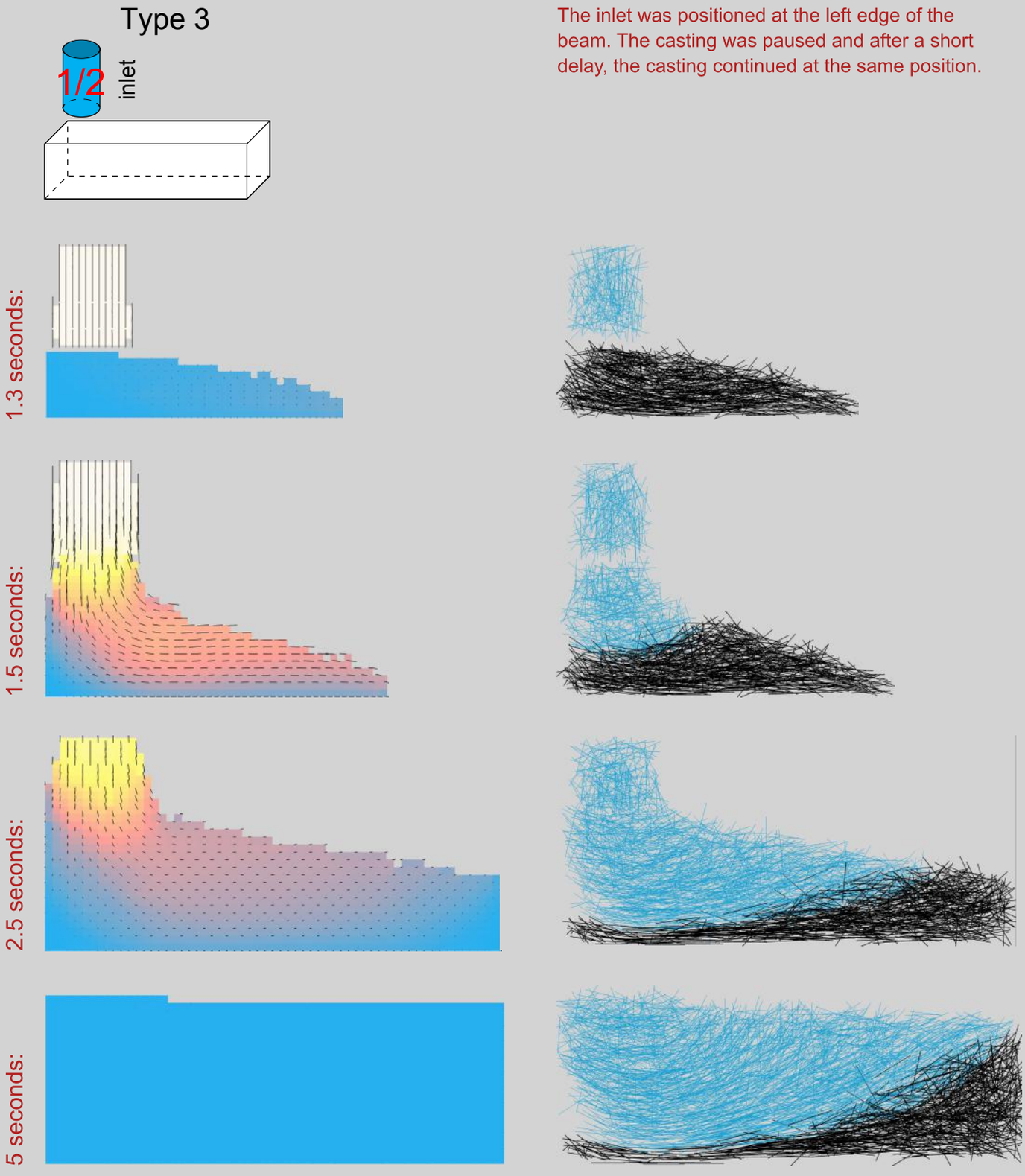

Figure 7.14: Side views of SFRSCC during casting of a standard beam applying casting type 3. Individual rows represent different time steps. The left column shows the flow pattern of the SFRSCC. Colour represents the flow rate (blue = low, yellow = high). The right column shows the invidual fibres.

Figure 7.15 presents the fibre orientation factors in the longitudinal (X), vertical (Y) and transverse (Z) direction as a function of the beam longitudinal position, X.

For all the three directions, the casting type 3 (casting with delay), resulted in fibre orientation factors similar to those obtained when using the reference casting procedure without any delay.

However, casting type 2 and 3 resulted in considerably different fibre orientation factors compared to the reference casting procedure. Thus, different casting procedures can have an influence on the fibre orientation factors and therefore on the resulting mechanical response of the beam specimens.

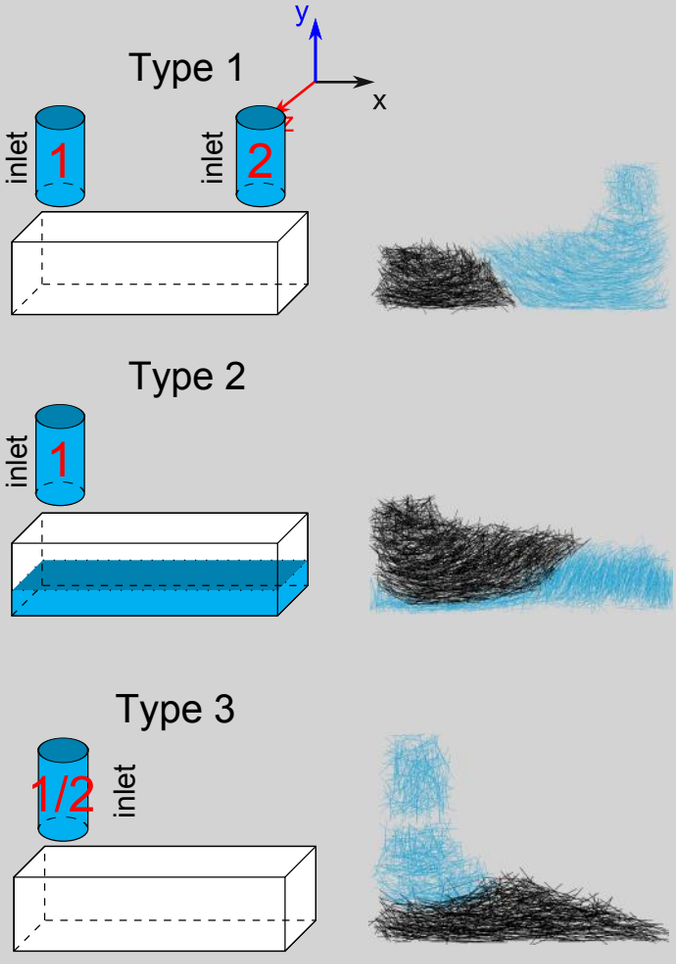

Standard beam without reinforcement
Different casting methods

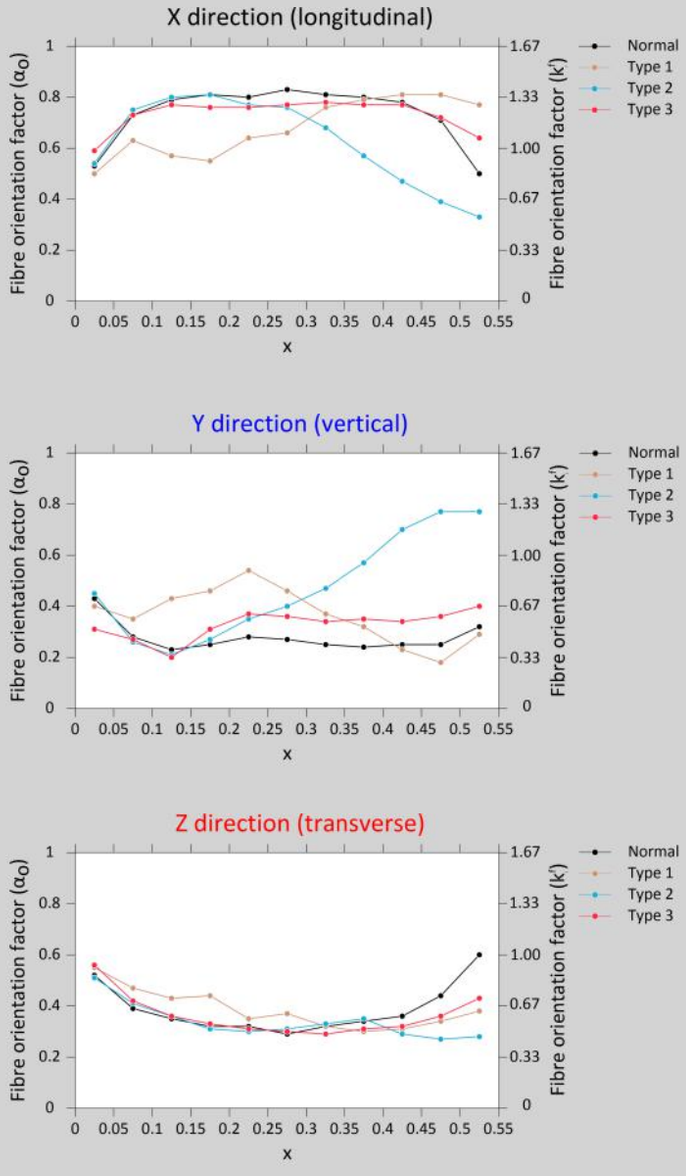

Figure 7.15: Fibre orientation factors in the X, Y and Z direction as a function of the longitudinal position, X. Different casting procedures have been applied.

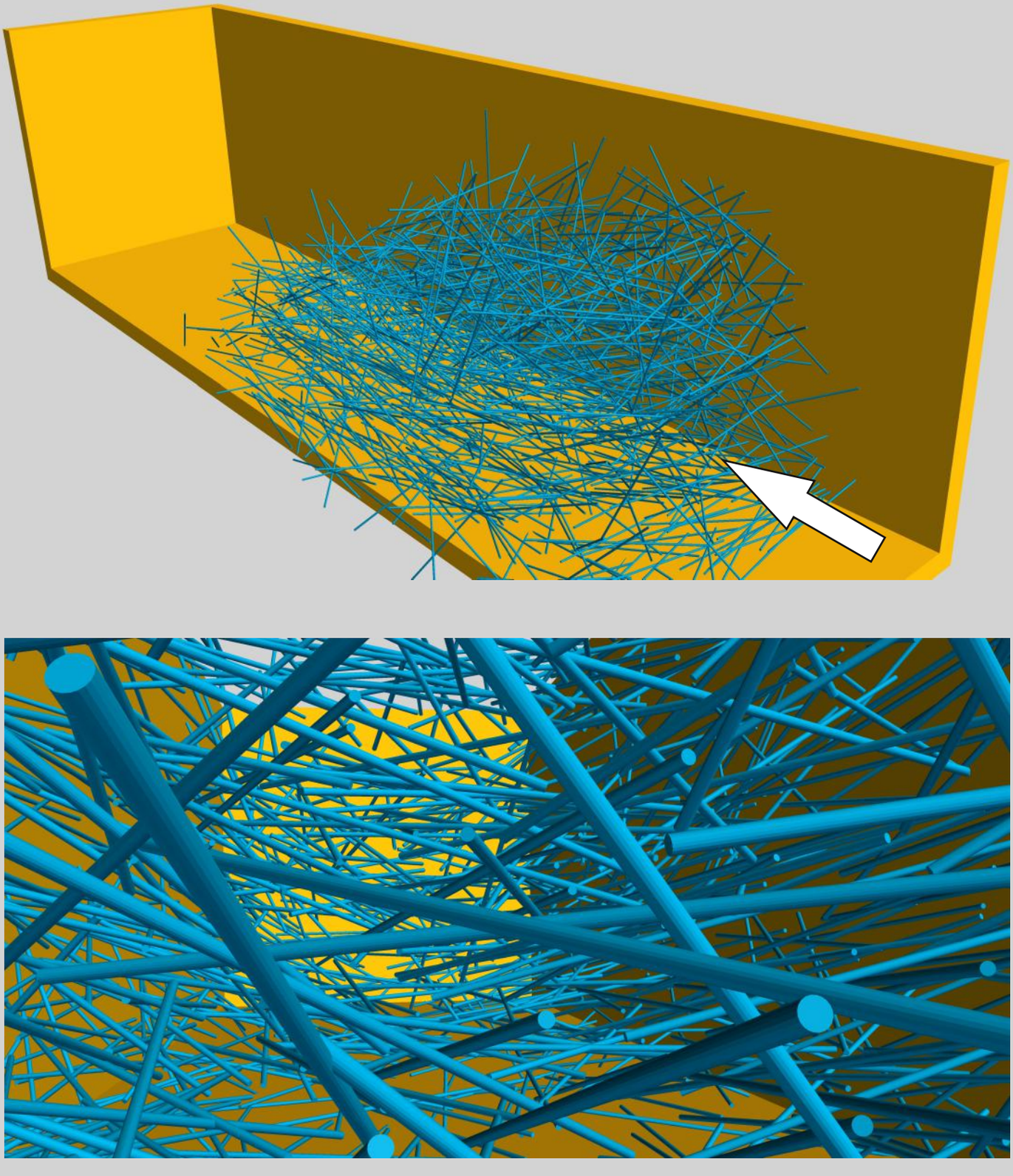

Figure 7.16: Picture to illustrate the individual fibres included in the simulation of a standard beam cast with SFRSCC.

7.3 STANDARD BEAM - EXPERIMENTAL

This section presents fibre orientation factors obtained in the cracked plane of standard beams cast with SFRSCC. The new casting procedure with a funnel placed at one end was applied. A total of 18 beams were cast and before casting the rheological properties were measured using the 4C-Rheometer. The plastic viscosity and yield stress were 90 Pa·s and 120 Pa, respectively. The slump flow was 500 mm. Fibre length, aspect ratio and content were 60 mm, 65, and 40 kg/m^3, respectively.

The beams were tested in three point bending. Afterwards, the number of fibres in the cracked plane was determined. The fibre orientation factors for each beam are shown in Figure 7.20. The mean value of the fibre orientation factor α_0 is 0.78, which corresponds to the value obtained from numerical simulations. The standard deviation of the fibre orientation factor is 0.11. The minimum and maximum value of the fibre orientation factor is 0.54 and 0.94, respectively.

Figure 7.17: Left: Sampling after pump. Right: Measurement of the rheological properties using the 4C-Rheometer.

Figure 7.18: Casting of 18 standard beams.

Figure 7.19: Three point bending test.

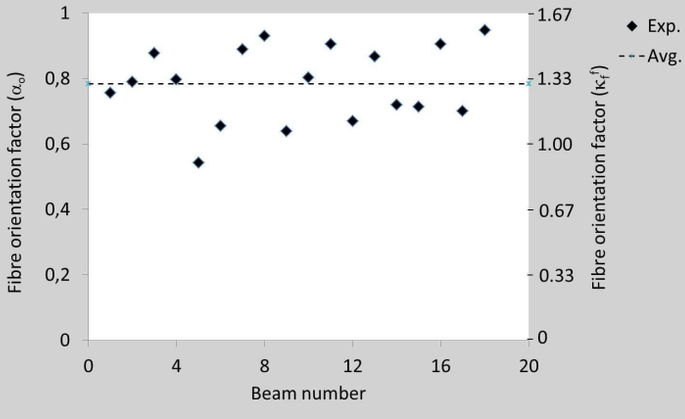

Figure 7.20: Fibre orientation factors obtained in the cracked plane of 18 standard beams cast with SFRSCC.

7.4 SHORT WALL - SIMULATION

This section presents fibre orientation factors in a vertical wall. The fibre orientation factors were obtained from a numerical simulation. Layout of the wall is shown in Figure 7.21. Four tie rods stiffening the formwork were included in the model. The concrete was cast through a pipe at a casting rate of 30 m^3/h. The pipe was pulled up in such a way that the inlet was always 10 cm above the concrete surface. The plastic viscosity and yield stress of the SCC phase were 60 Pa·s and 25 Pa, respectively. Fibre length, aspect ratio and content were 60 mm, 80, and 40 kg/m^3, respectively.

Figure 7.22 shows a 3D view of an intermediate filling state. Figure 7.23 shows a side view of all the fibres at the final filling state. Individual states of the filling process are shown in Figure 7.24 (left). The lines and their colours represent SFRSCC velocities at the given locations (yellow=high, blue=low). Figure 7.24 (right) presents the corresponding fibre orientation ellipses.

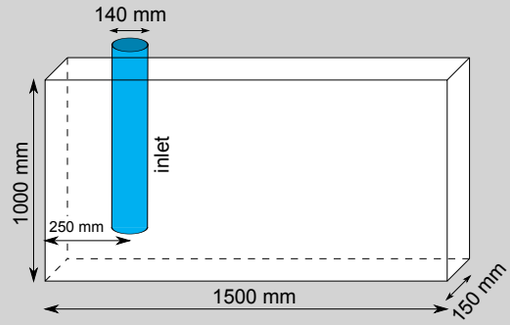

Figure 7.21: Layout of the wall casting. The inlet (blue cylinder) was always 10 cm above the concrete.

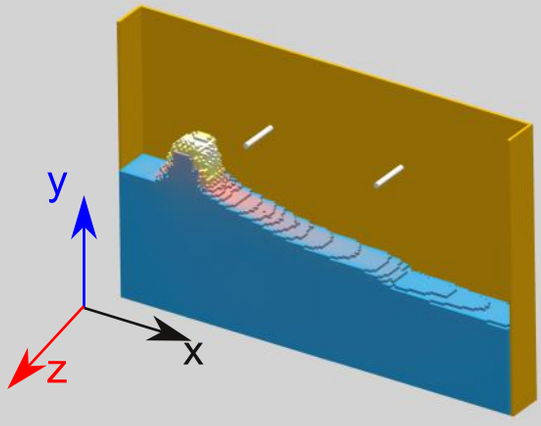

Figure 7.22: 3D view of an intermediate step of the casting process.

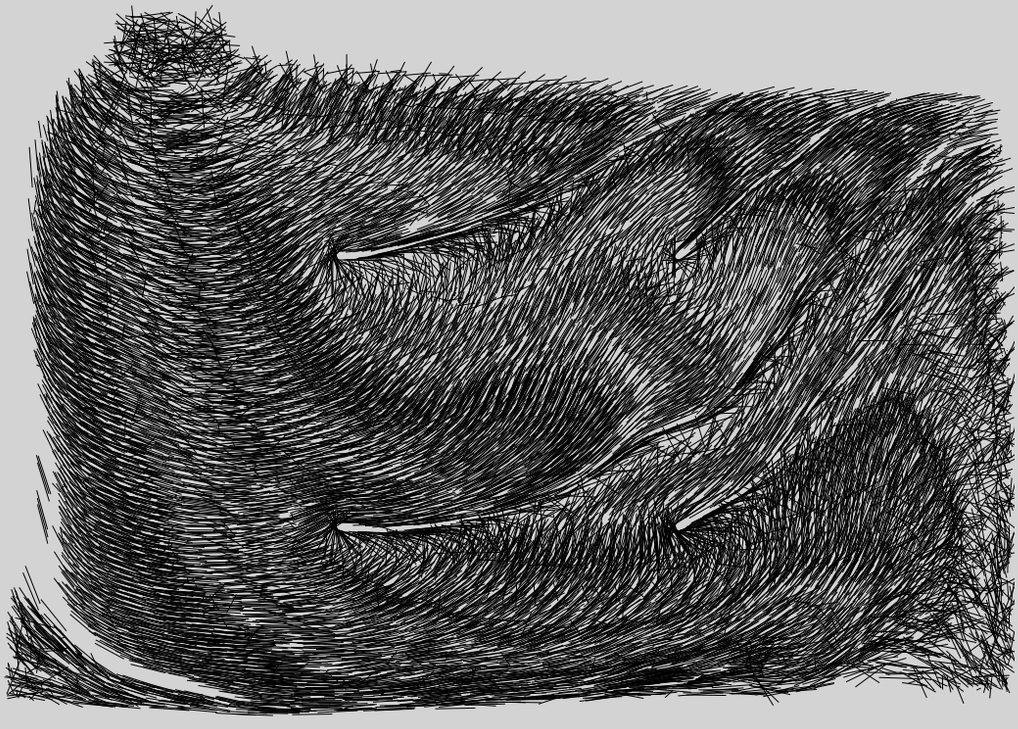

Figure 7.23: Side view of the resulting state of the immersed steel fibres.

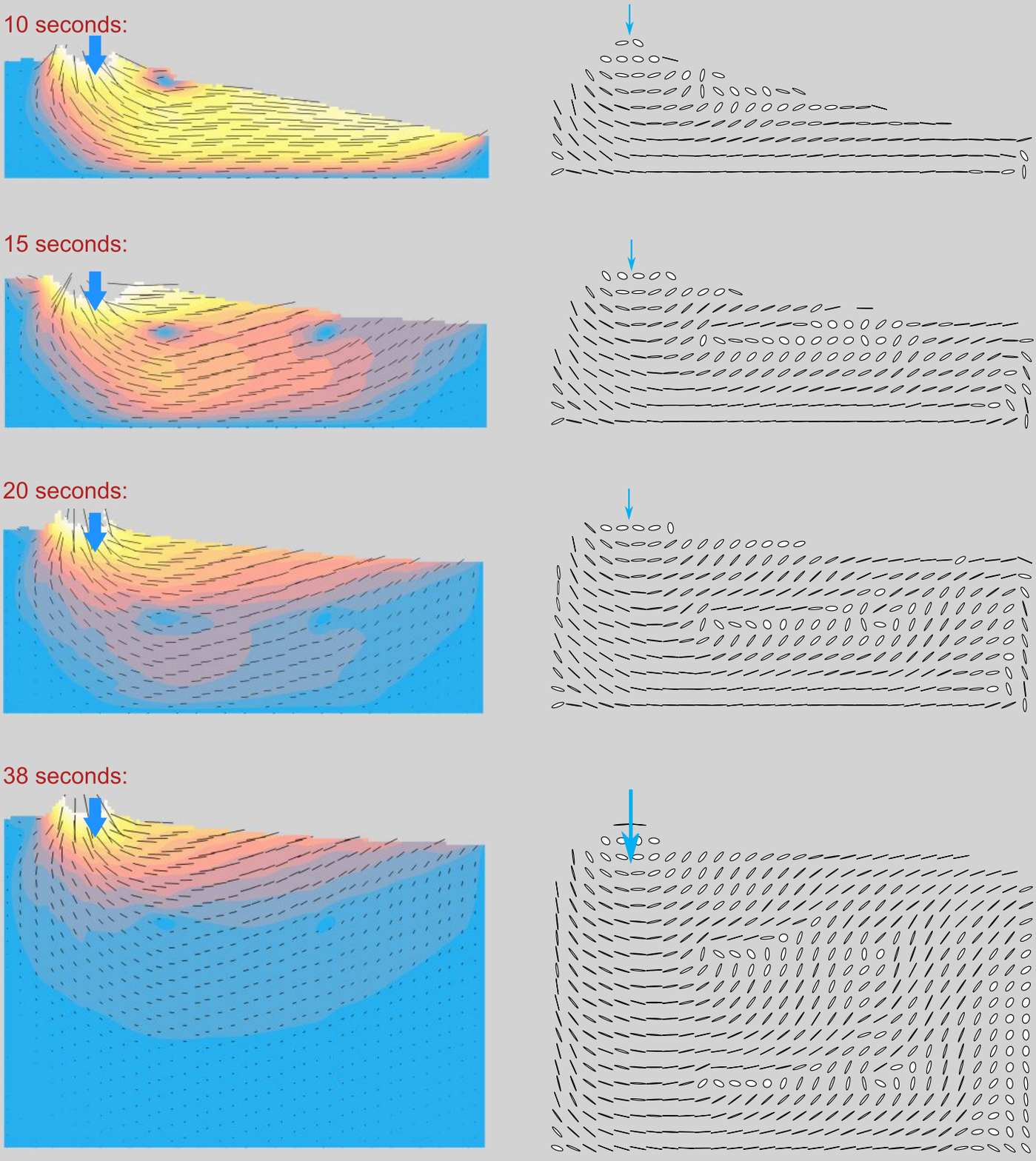

Figure 7.24: Vertical wall casting with SFRSCC. Side views of the flow pattern (left) and the fibre orientation ellipses (right) at different time steps. The colours represent the flow rate (blue = low, yellow = high).

Figure 7.25 presents fibre orientation factors in individual regions of the vertical SFRSCC wall. Dimensions of the regions are 0.25 x 0.20 x 0.15 m. At first, the fibre orientation factor is determined on several planes within each region. Hereafter, the average fibre orientation factor is calculated, which is shown in Figure 7.25. The values in rows R1 - R5 are also plotted in Figure 7.26.

The mean value of the fibre orientation factor α_o in the X, Y and Z direction is 0.72, 0.49 and 0.19, respectively. The standard deviation of the fibre orientation factor α_o in the X, Y and Z direction is 0.11, 0.15 and 0.09, respectively. The minimum and maximum value of the fibre orientation factor α_o in the X, Y and Z direction are [0.49, 0.91], [0.17, 0.77] and [0.1, 0.39], respectively.

In the XY plane, the strongest place is approximately 5.4x stronger than the weakest place (marked with ellipses in Figure 7.25). In volume, the strongest place is approximately 9.1x stronger than the weakest place (marked with rectangles in Figure 7.25).

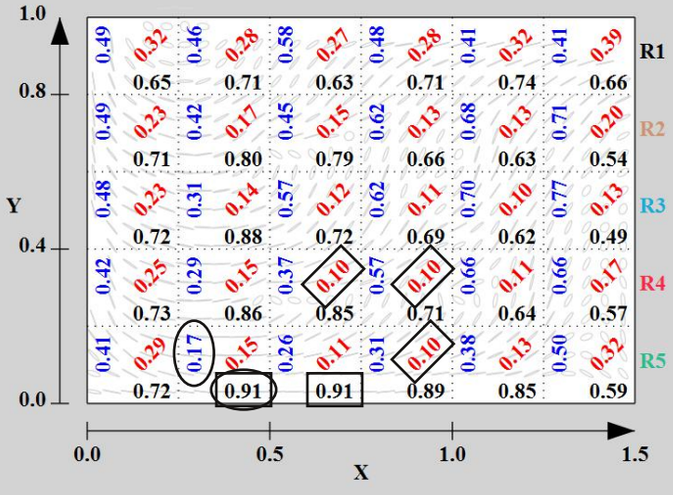

Figure 7.25: Side view of the vertical wall. Fibre orientation factors in the X, Y and Z direction in individual regions.

Vertical wall casting
Inlet 10 cm above concrete surface

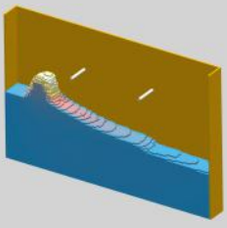

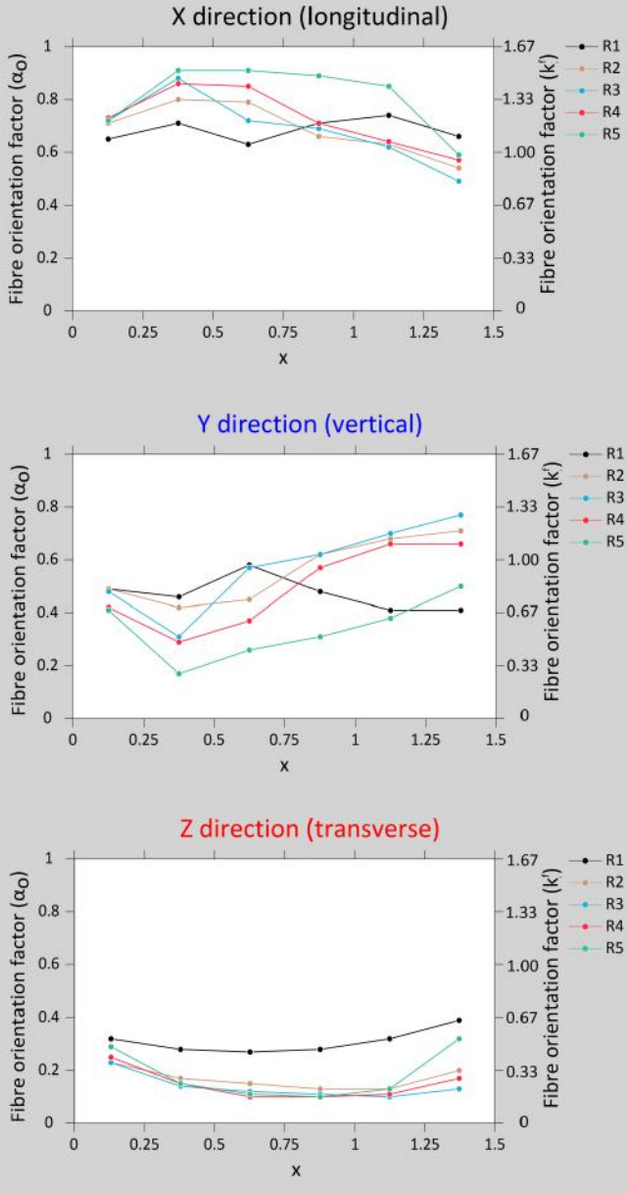

Figure 7.26: Fibre orientation factors. X-direction (black), Y-direction (blue), Z-direction (red).

7.5 LONG WALL - SIMULATION

The previous example showed a simulation of a 1.5 long wall. In most cases, walls are longer and the concrete is allowed to flow longer distances from the inlet position. In long walls, it is not uncommon that SCC is allowed to flow 5 to 10 m.

A direct simulation of a long wall has not yet been carried out. However, assuming that the middle section (from 0.5 to 1.0 m) of the 1.5 m long wall is reasonably unaffected by the inlet condition and the end boundary, the middle part may be extended to cover a wider distance as illustrated in Figure 7.27.

Long wall - simulation
Inlet just above concrete surface

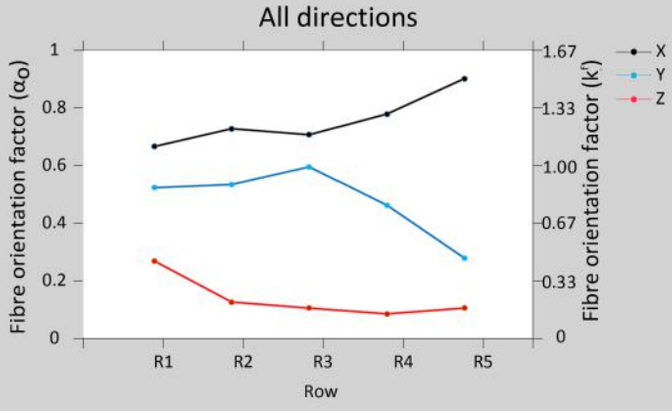

Figure 7.28: Estimated fibre orientation factors in a long wall. Longitudinal X direction (black), vertical Y direction (blue), transverse Z direction (red).

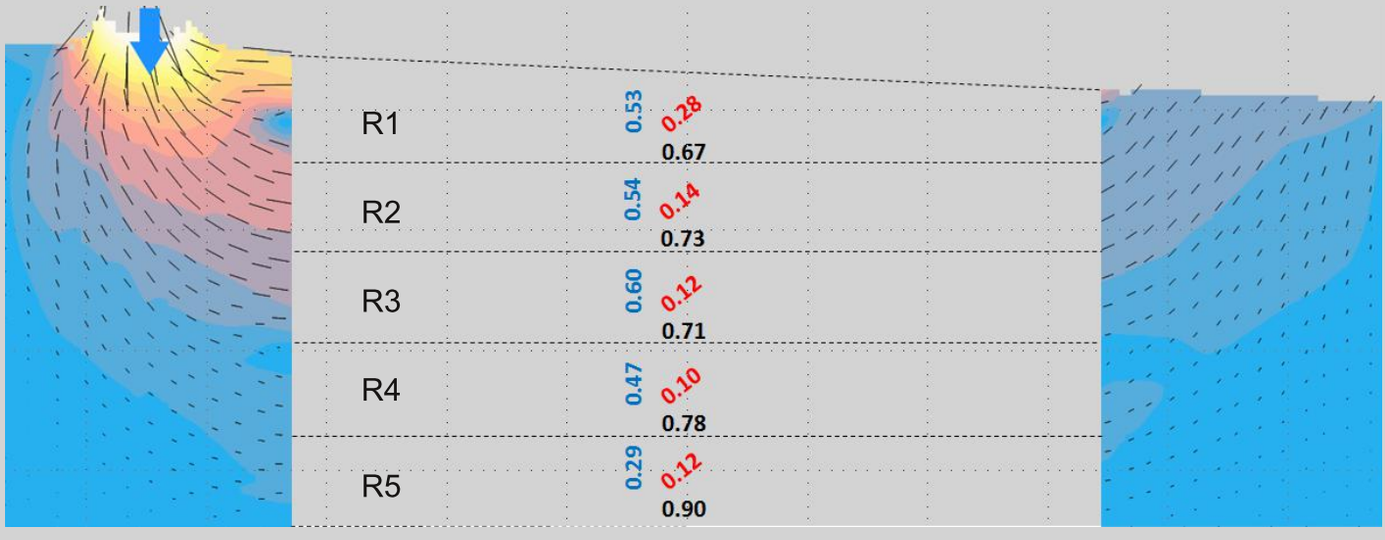

Figure 7.27. Estimated fibre orientation factors in a long wall. Longitudinal X direction (black), vertical Y direction (blue), transverse Z direction (red).

7.6 WALL WITH REINFORCEMENT - SIMULATION

A numerical simulation of an inclined wall casting was carried out. The dimensions of the wall were 2.0 x 1.5 x 0.4 m. The inclination of the wall was 30° from the vertical plane. The wall was reinforced with a reinforcement mesh placed at the upper and lower face of the wall. The cover layer was 45 mm. The reinforcement mesh was composed of steel bars with a diameter of 16 mm. Spacing of the reinforcement bars was 200 mm. The inlet diameter was 220 mm and it was placed at a distance of 200 mm from one wall edge. The inlet was positioned 250 mm above the bottom of the wall throughout the casting. Figure 7.29, Figure 7.30 and Figure 7.31 present the layout of the casting, a 3D view at an intermediate time step and a side view of the resulting state of the fibres. The plastic viscosity and yield stress of the SCC phase were 30 Pa·s and 70 Pa, respectively. Fibre length, aspect ratio and content were 60 mm, 65, and 15 kg/m^3, respectively.

Figure 7.32 shows flow velocity profiles and fibre orientation ellipses at different time steps.

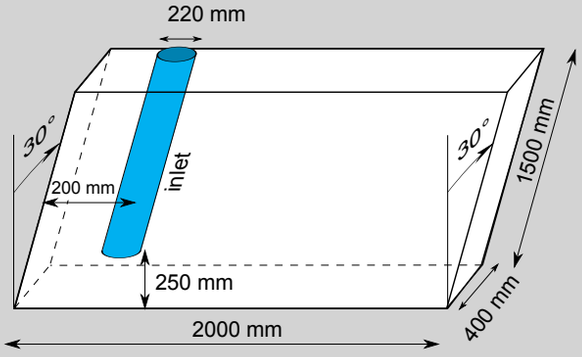

Figure 7.29: Layout of the inclined wall casting.

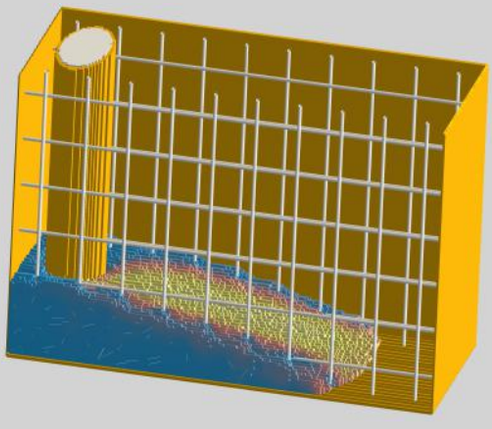

Figure 7.30: A 3D view at an intermediate time step. The colour represents the flow rate (blue = low, yellow = high).

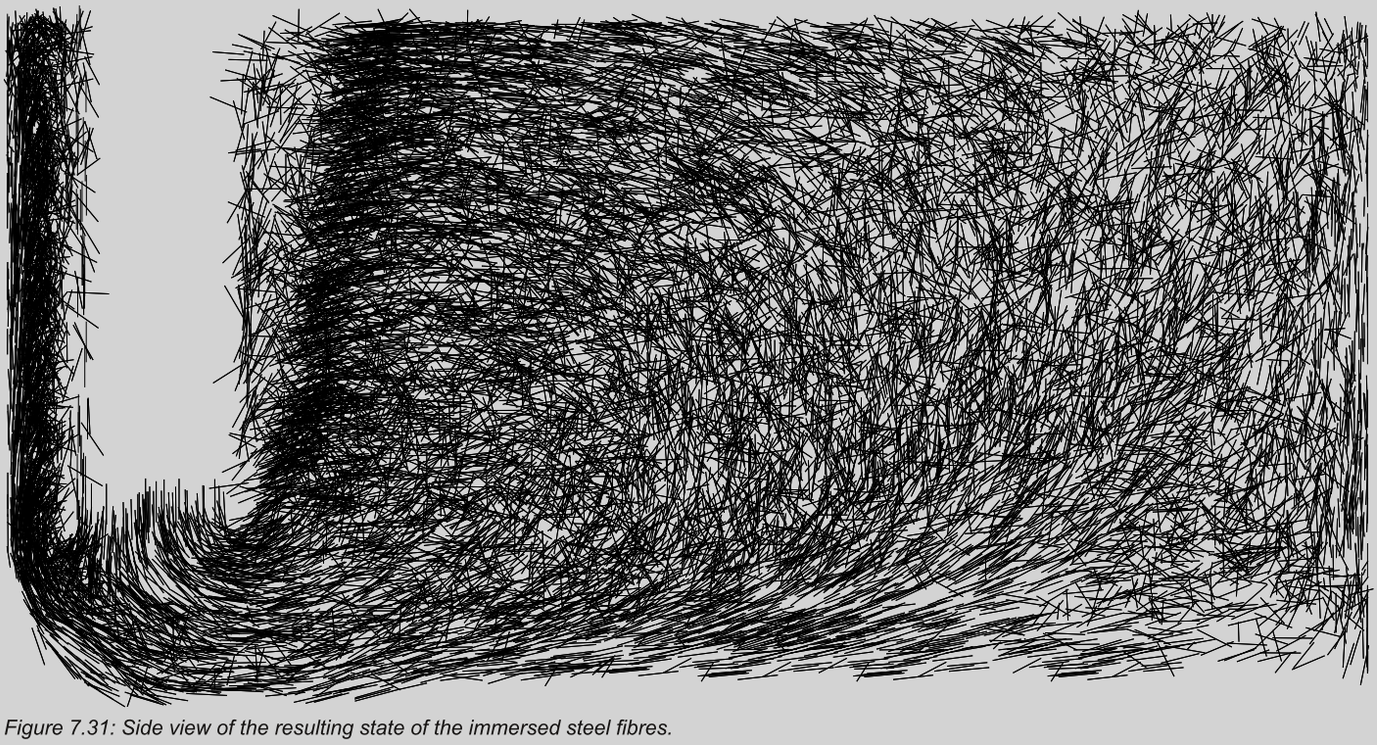

Figure 7.31: Side view of the resulting state of the immersed steel fibres.

7 seconds:

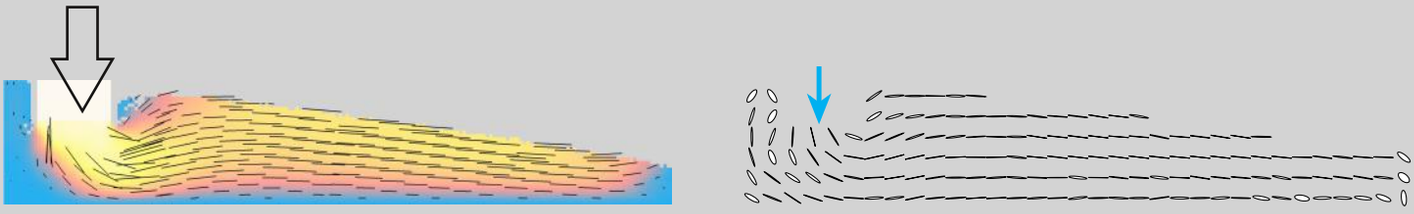

12 seconds:

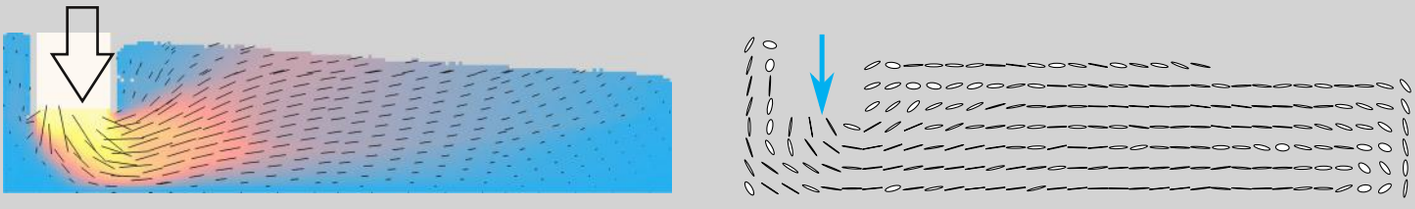

20 seconds:

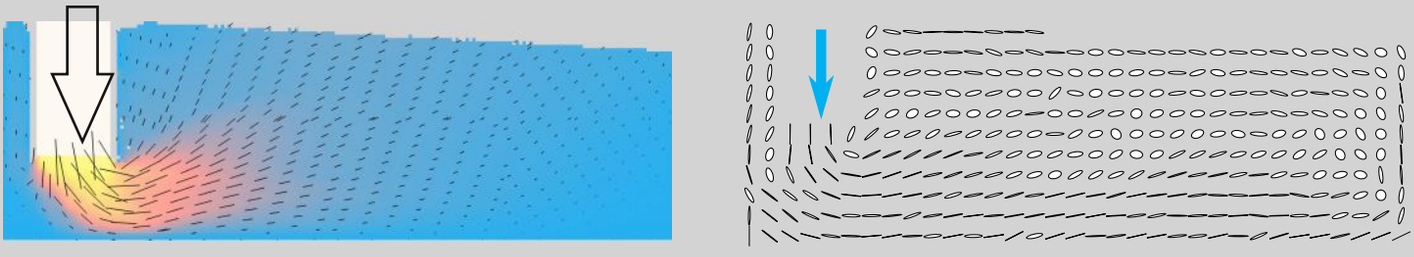

40 seconds:

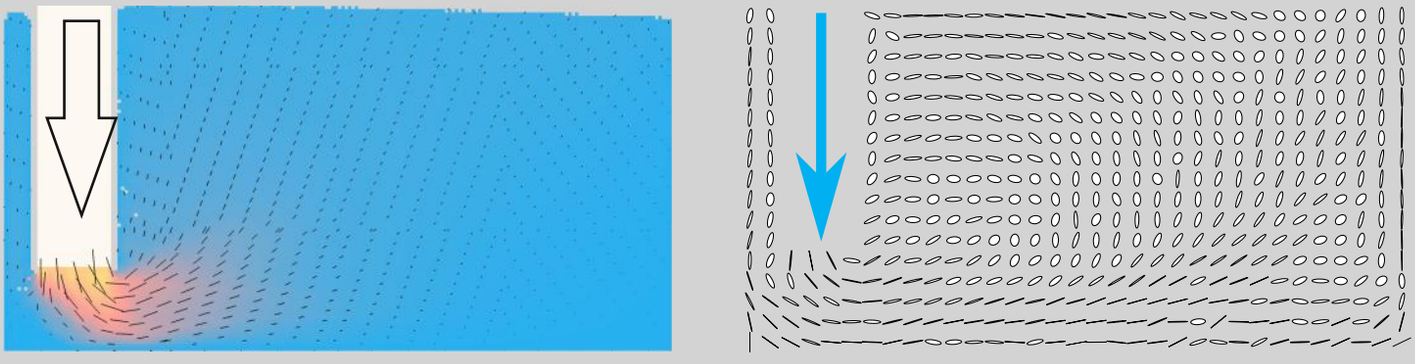

Figure 7.32: Inclined wall casting with SFRSCC. Side views of the flow pattern (left) and the fibre orientation ellipses (right) at different time steps. The colour represents the flow rate (blue = low, yellow = high).

Figure 7.33 presents fibre orientation factors in individual regions of the inclined SFRSCC wall. Values in individual rows R1 - R5 are also plotted in Figure 7.34.

The mean value of the fibre orientation factor α_o in the X, Y and Z direction is 0.56, 0.48 and 0.21, respectively. The standard deviation of the fibre orientation factor α_o in the X, Y and Z direction is 0.17, 0.17 and 0.06, respectively. The minimum and maximum value of the fibre orientation factor α_o in the X, Y and Z direction are [0.21, 0.83], [0.19, 0.74] and [0.14, 0.36], respectively.

In the XY plane, the strongest place is approximately 4.4x stronger than the weakest place (marked with ellipses in Figure 7.33). In volume, the strongest place is approximately 5.9x stronger than the weakest place (marked with rectangles in Figure 7.33).

Compared to a wall without reinforcement, the fibre orientation factors are a little different. For instance, the fibre orientation factors in the longitudinal direction are slightly lower when reinforcement is included. When the SFRSCC flows into the cover layer zone, the flow slows down significantly, which results in lower fibre orientation factors in the vincinity of the wall. Thus, the average fibre orientation factors over the full cross section are lower. Major shear takes place between the two reinforcement grids.

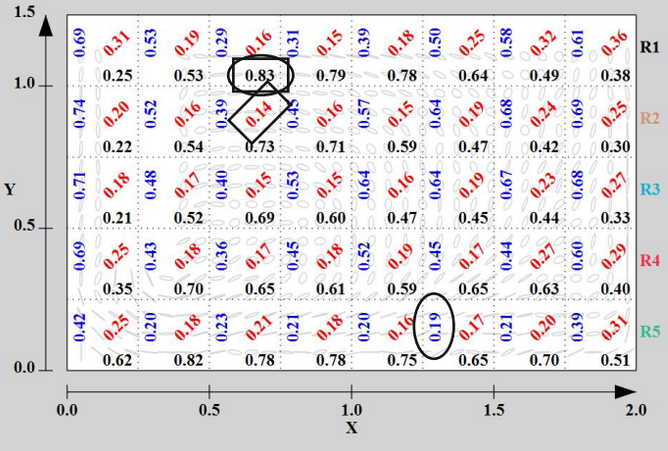

Figure 7.33: Side view of the inclined wall. Fibre orientation factors in X, Y and Z direction in individual regions.

Wall casting with reinforcement
Inlet 250 mm above formwork bottom surface

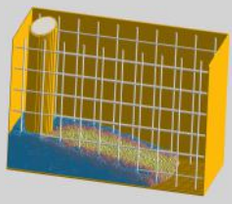

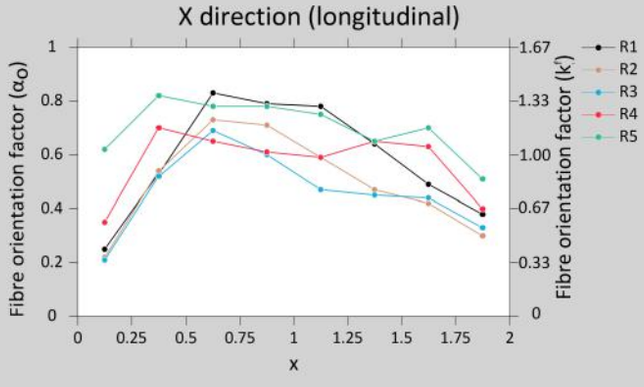

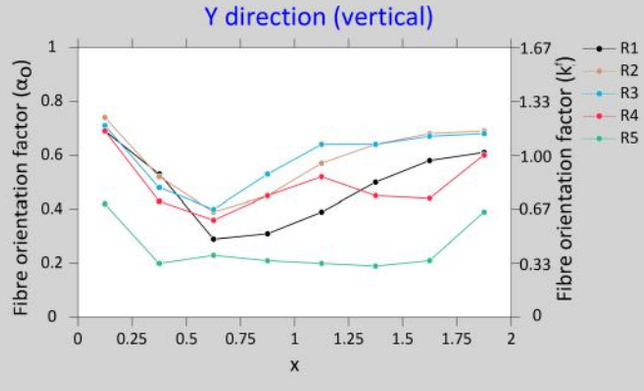

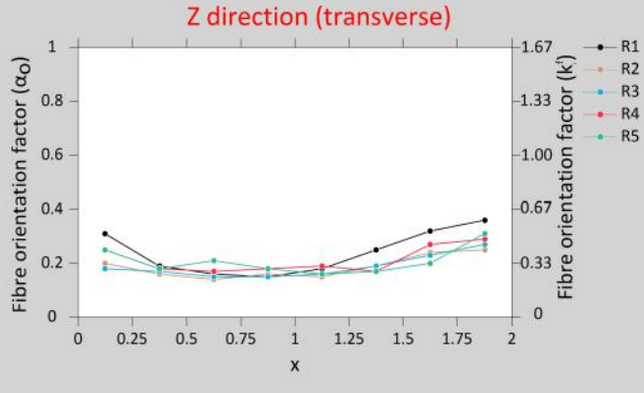

Figure 7.34: Fibre orientation factors. X-direction (black), Y-direction (blue), Z-direction (red).

7.7 WALL WITH REINFORCEMENT - EXPERIMENT

The previous sections showed examples of wall simulations. This section shows the results obtained from a real wall casting. The cross section of the wall is similar to one applied in the simulation presented in Section 7.6. However, the wall is longer and the casting procedure was different. The wall was 8 m long and the casting was carried out as shown in Figure 7.36. The casting shifted between two fixed positions. The casting started at position 1 and the concrete was allowed to flow approximately 6 m before moving the inlet to position 2. Hereafter the inlet position shifted between 1 and 2 when the concrete height was increased by approximately 0.15 m. The inlet was kept approximately 0.10 m below the concrete surface until a height of approximately 1.0 m was reached. Afterwards, the inlet was moved in a more random way back and forth to complete the casting. The fibre length, aspect ratio, and content were 60 mm, 65, and 40 kg/m^3, respectively.

To assess the fibre orientation, three columns were cut out of the wall as illustrated in Figure 7.37. These were further split into smaller sections to enable fibre counting in three directions (Figure 7.39 and 7.40). A constant fibre volume concentration was assumed for calculation of the fibre orientation factor.

Figure 7.41 and 7.42 presents the fibre orientation factors of the SFRSCC wall. The fibre orientation factors vary between the different columns. For instance, in the longitudinal direction, the highest and lowest values are found in the middle and left column, respectively. For the middle column, the concrete flows in one direction, from left to right, which tend orientate the fibres in the longitudinal direction. For the left column, the fibres may be affected by the second casting position, which force some of the concrete to flow from right to left. This seems to disturb the fibre orientation in the longitudinal direction as also shown in the simulation of the standard beam applying casting type 1 (see Section 7.2).

The mean value of the fibre orientation factors in the X, Y and Z direction is 0.63, 0.32 and 0.41, respectively. The standard deviation of the fibre

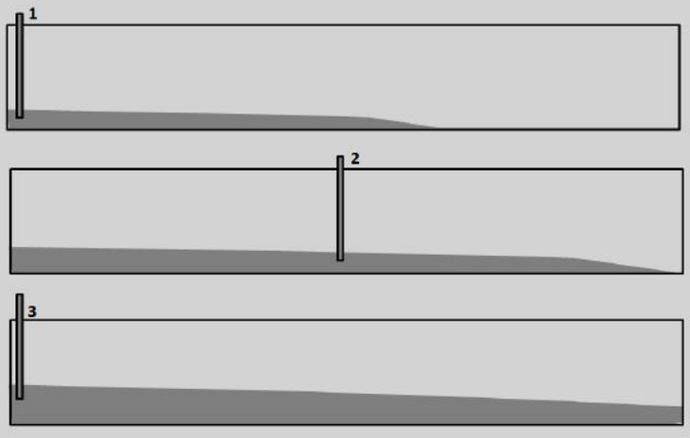

Figure 7.36: Schematic drawing of the wall casting procedure.

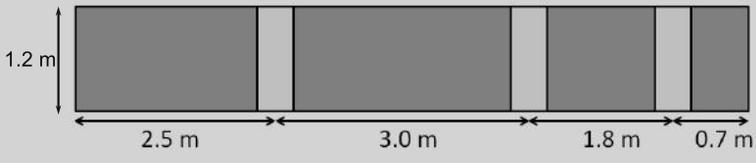

Figure 7.37: Position of cut columns.

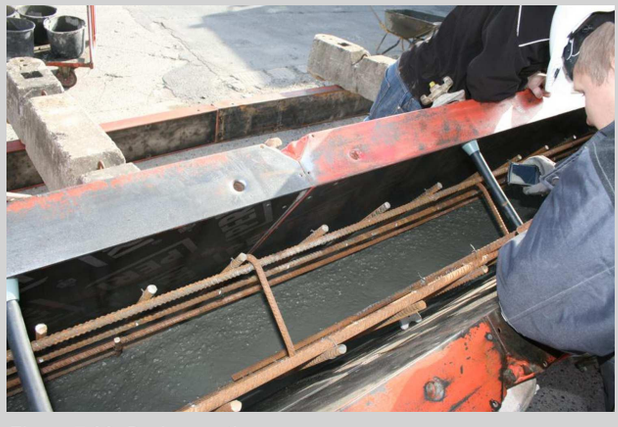

Figure 7.38: During casting.

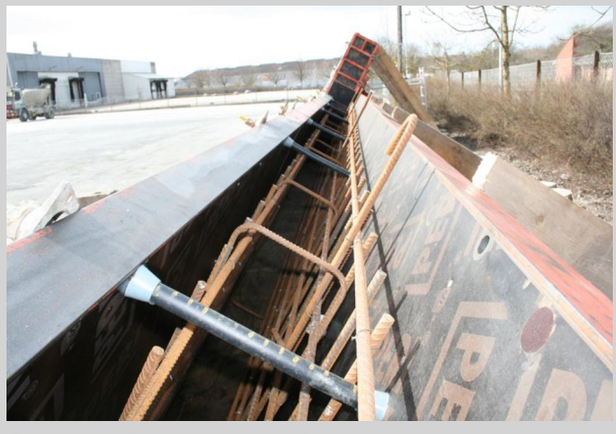

Figure 7.35: Formwork and reinforcement.

Figure 7.39: Cut columns split into smaller samples. Manual fibre counting at the right.

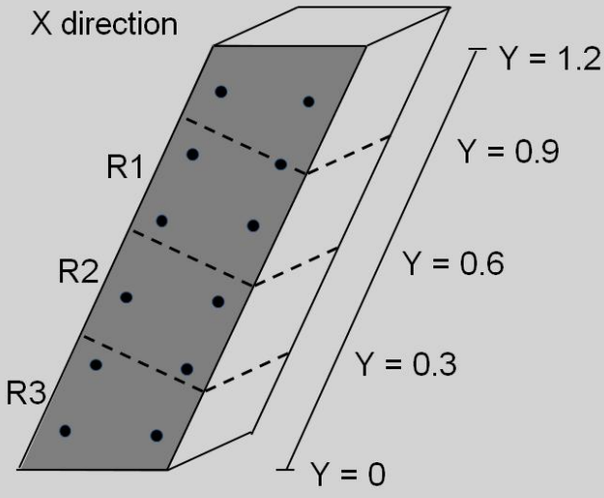

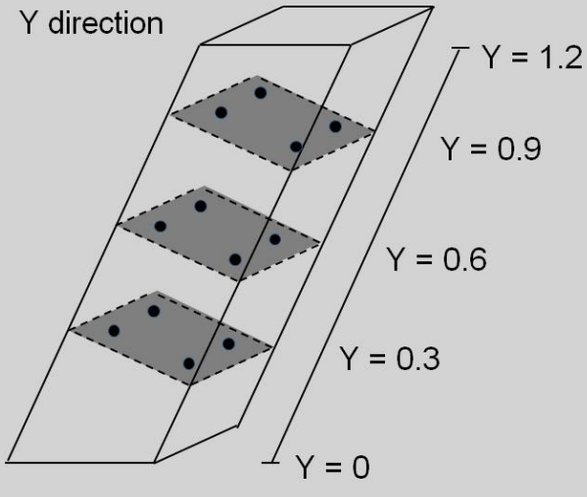

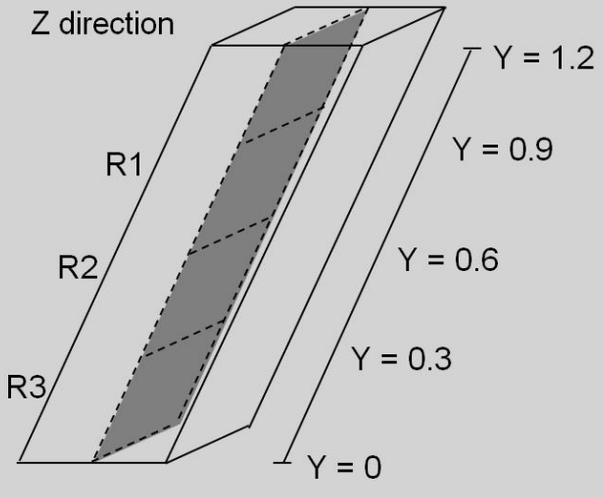

Figure 7.40: The planes on which fibre counts were determined.

orientation factors in the X, Y and Z direction is 0.11, 0.14 and 0.05, respectively. The minimum and maximum value of the fibre orientation factors in the X, Y and Z direction are [0.41, 0.78], [0.16, 0.63] and [0.33, 0.48], respectively.

A corresponding simulation of this size has not yet been carried out. Simulations of this size require a substantial amount of computer power, and future studies will look into strategies for simulating full scale castings of this size within a reasonable time. In the simulation shown in section 7.6, the casting was carried out from the bottom and the length of the wall was only 2 m. The flow pattern is significantly influenced by both factors for which reason a direct comparison of the final filling states is difficult. However, the flow pattern in the first part of the simulation (just before reaching the right end) is assumed to be somewhat similar to the flow pattern obtained in the section to the right of the second inlet in the experiment. This section includes the middle column. Overall agreement was obtained in the longitudinal and the vertical direction. For instance, in the longitudinal direction, the experiment shows the same trend as the simulation. Flow in the longitudinal direction results in almost perfectly aligned fibres in the center of the wall (α_o=1.0). In the cover layer zones fibre orientation is reduced and closer to 3D random (0.5), which results in an average fibre orientation factor in the cross section of approximately 0.75. In the transverse direction, the experimental result is approximately three time higher. An explanation for this discrepancy has not been found, and further studies will investigate it. For further information, see [Thrane LN, Svec O, Stang H, Kasper T, *Testing and simulation of fibre orientation in reinforced walls cast with SFRSCC*, Proceedings of 7th RILEM International Conference on SCC and 1st RILEM International Conference on Rheology and Processing of Construction Materials, 237-245, 2013].

Real wall casting with reinforcement
Inlet just below concrete surface

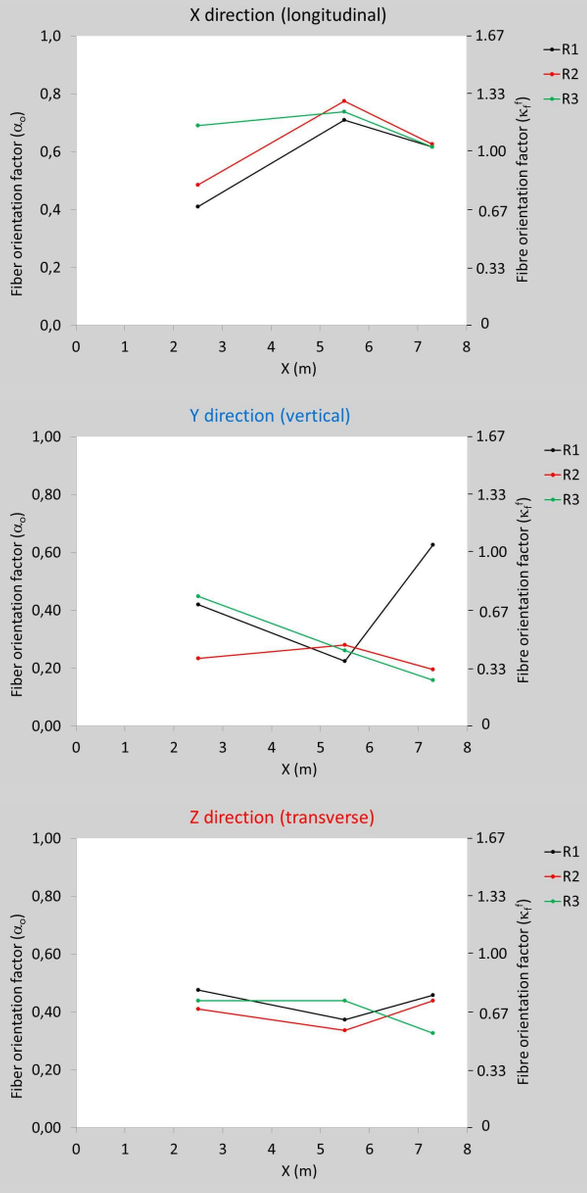

Figure 7.42: Fibre orientation factors. X-direction (black), Y-direction (blue), Z-direction (red).

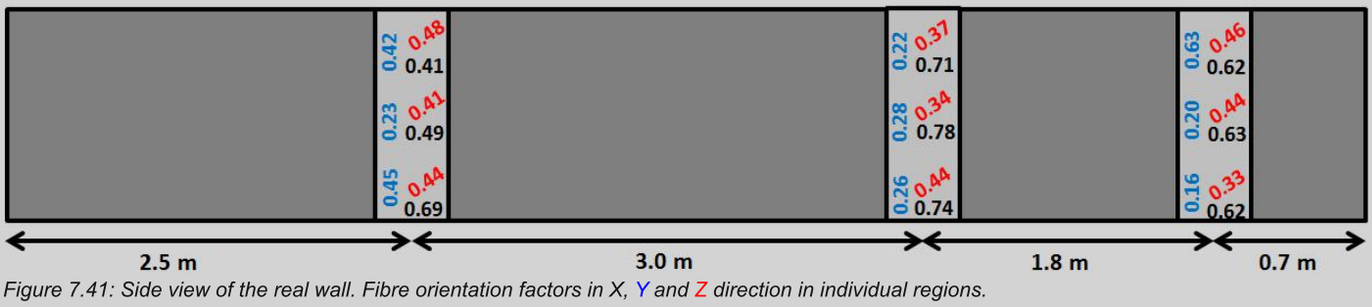

Figure 7.41: Side view of the real wall. Fibre orientation factors in X, Y and Z direction in individual regions.

7.8 SMALL SLAB - SIMULATION

A slab casting with SFRSCC is presented in this section. Layout of the slab is illustrated in Figure 7.43. Three numerical simulations were run differentiated by the type of reinforcement included in the model. The three numerical simulations were:

- with no reinforcement.
- with one-way reinforcement.
- with two-way reinforcement.

Dimensions of the slabs were 1.2 m x 1.2 m x 0.15 m. Plastic viscosity, yield stress and density of the SCC phase were set to 75 Pa·s, 22 Pa and 2318 kg/m^3, respectively. Fibre length, aspect ratio, and content were 60 mm, 80 and 40 kg/m^3, respectively. The casting was performed from a circular inlet positioned at distance of 0.25 m from one of the corners of the slab. The casting rate was approximately 30 m^3/h.

Figure 7.44, 7.45 and 7.46 show 3D views of the three numerical simulations. It is noticable how the flow pattern is influenced by the type of reinforcement.

Figure 7.47 to 7.55 show top views of the flow pattern and fibre orientation ellipses at different time steps, and the resulting fibre orientation factors.

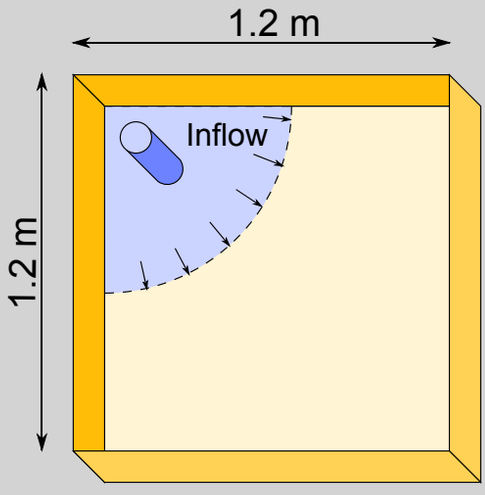

Figure 7.43: Layout of the slab casting.

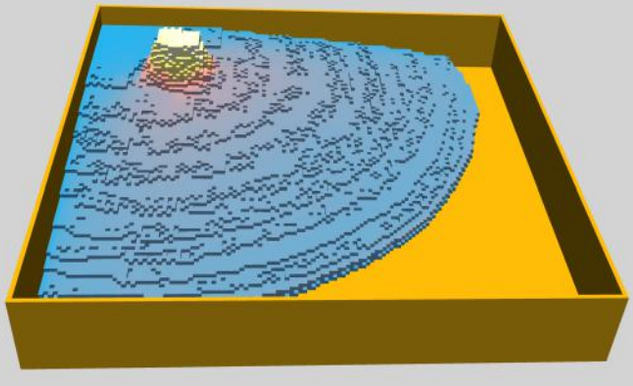

Figure 7.44: 3D view of an intermediate step of slab casting without any reinforcement.

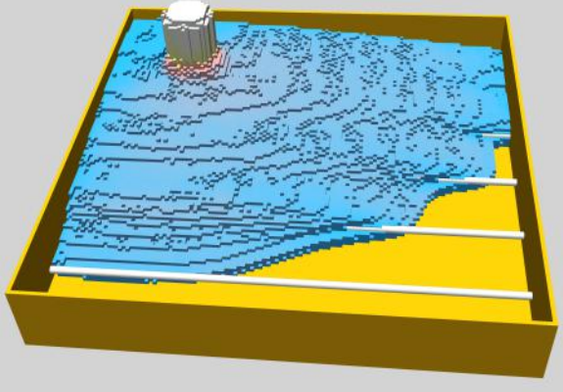

Figure 7.46: 3D view of an intermediate step of slab casting with one-way reinforcement.

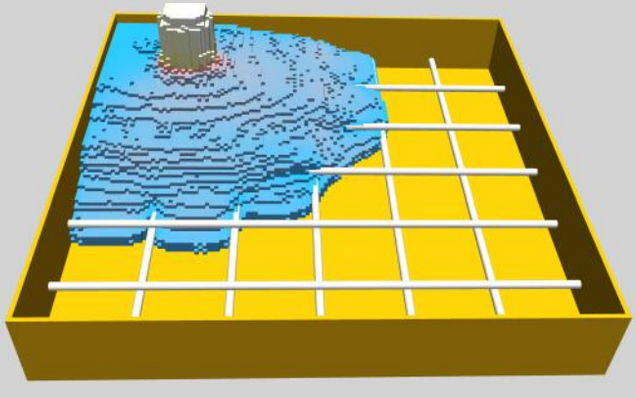

Figure 7.45: 3D view of an intermediate step of slab casting with two-way reinforcement.

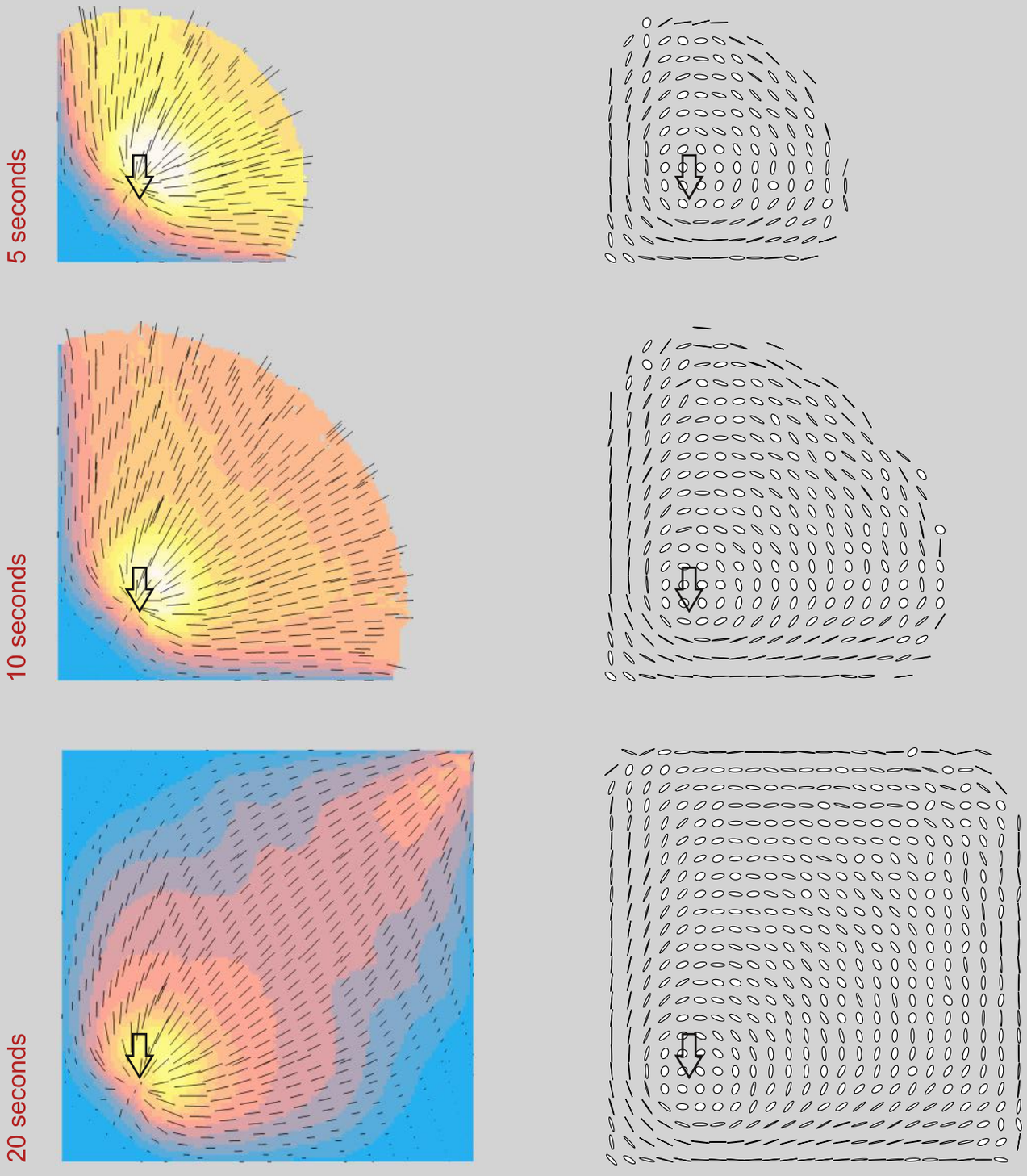

Figure 7.47: Slab casting with SFRSCC. No reinforcement. Top views of the flow pattern (left) and of the fibre orientation ellipses (right) at different time steps. The colour represents the flow rate (blue = low, yellow = high).

Figure 7.48 presents the fibre orientation factors in individual regions of the unreinforced SFRSCC slab. The values in rows R1 - R6 are also plotted in Figure 7.49.

The mean value of the fibre orientation factor α_o in the X, Y and Z direction is 0.6, 0.6 and 0.17, respectively. The standard deviation of the fibre orientation factor α_o in the X, Y and Z direction is 0.16, 0.16 and 0.06, respectively. The minimum and maximum value of the fibre orientation factor α_o in the X, Y and Z direction are [0.3, 0.83], [0.3, 0.85] and [0.09, 0.3], respectively.

In the XY plane, the strongest place is approximately 2.8x stronger than the weakest place (marked with ellipses in Figure 7.48). In volume, the strongest place is approximately 9.4x stronger than the weakest place (marked with rectangles in Figure 7.48).

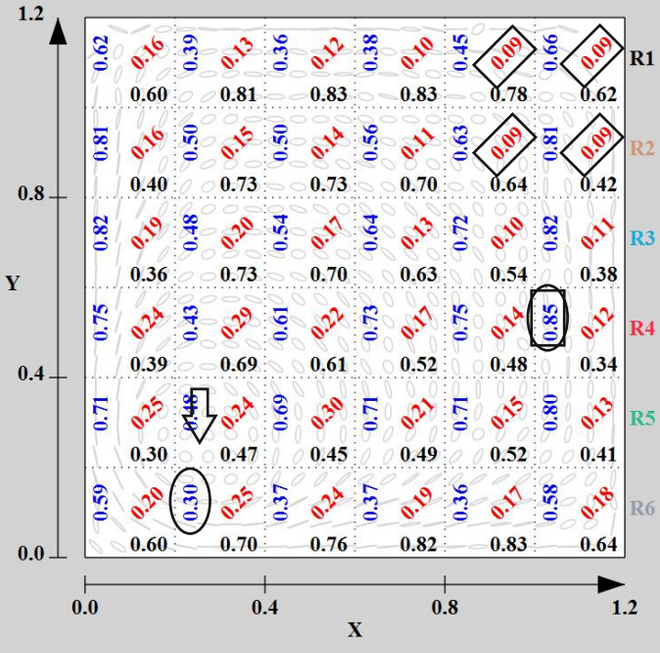

Figure 7.48: Top view of the slab. Fibre orientation factors in the X, Y and Z direction in individual regions.

Slab without reinforcement - simulation

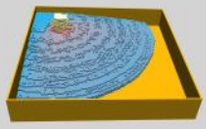

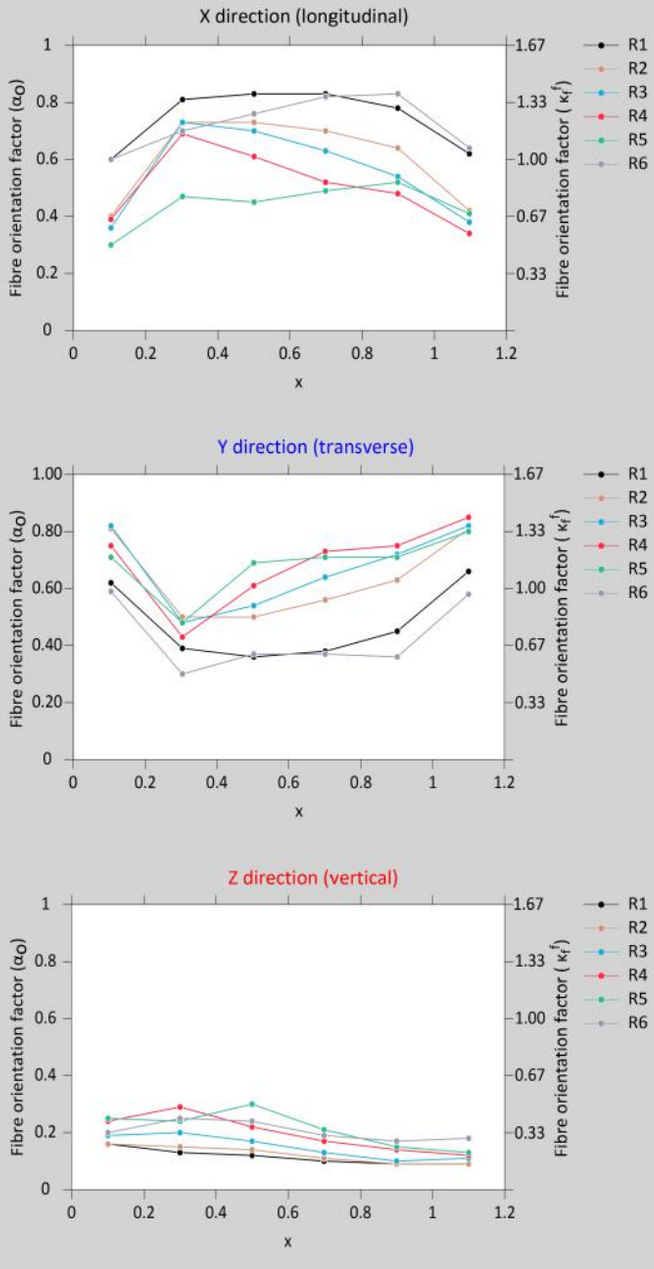

Figure 7.49: Fibre orientation factors. X-direction (black), Y-direction (blue), Z-direction (red).

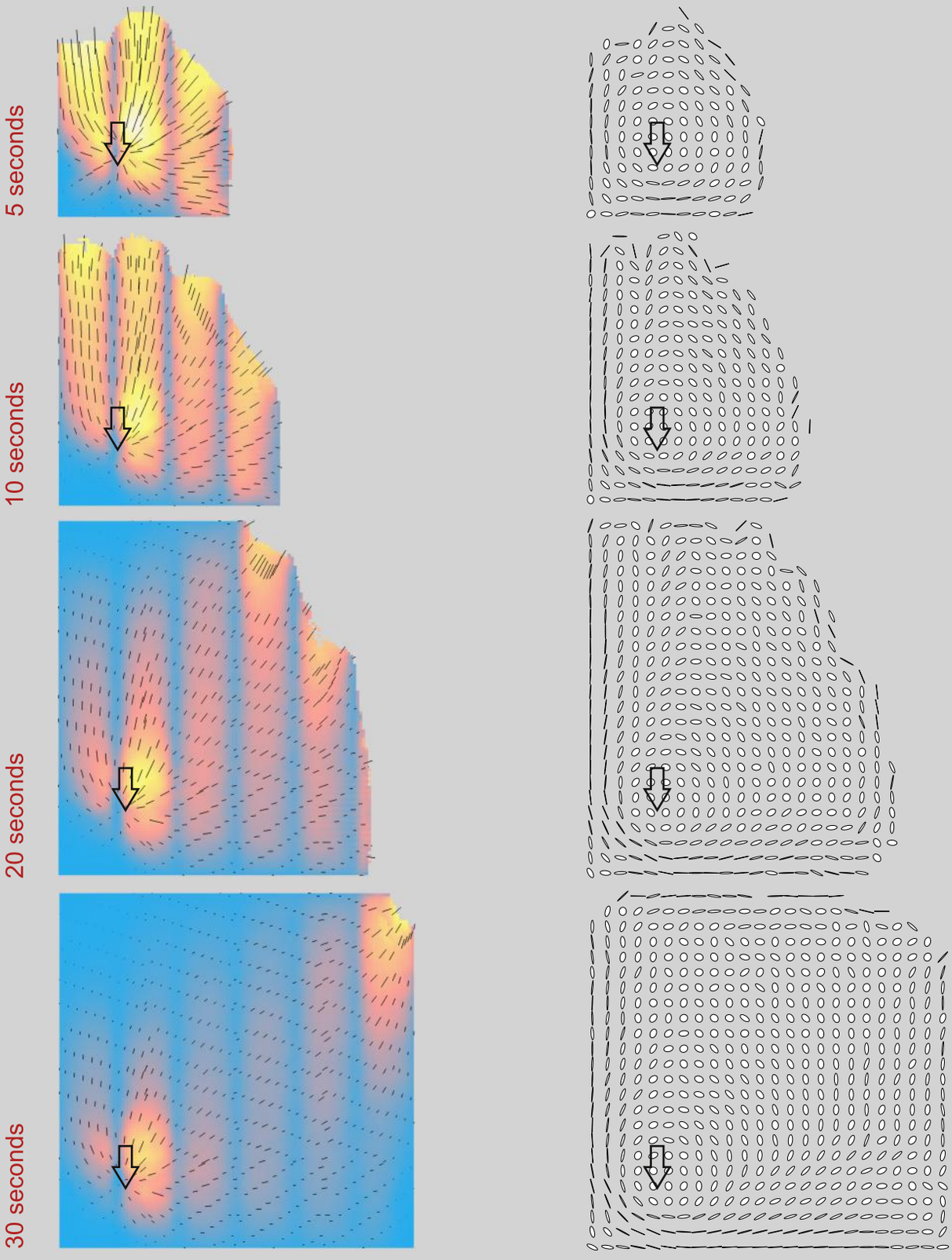

Figure 7.50: Slab casting with SFRSCC. One-way reinforcement. Top views of the flow pattern (left) and of the fibre orientation ellipses (right) at different time steps. The colour represents the flow rate (blue = low, yellow = high).

Slab with one-way reinforcement - simulation

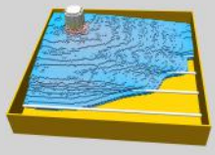

Figure 7.51 presents the fibre orientation factors in individual regions of the SFRSCC slab with one-way reinforcement. The values in rows R1 - R6 are also plotted also in Figure 7.52.

The mean values of the fibre orientation factor α_o in the X, Y and Z direction is 0.61, 0.59 and 0.18, respectively. The standard deviation of the fibre orientation factor α_o in the X, Y and Z direction is 0.12, 0.12 and 0.05, respectively. The minimum and maximum value of the fibre orientation factor α_o in the X, Y and Z direction are [0.39, 0.82], [0.33, 0.78] and [0.1, 0.31], respectively.

In XY plane, the strongest place is approximately 2.5x stronger than the weakest place (marked with ellipses in Figure 7.51). In volume, the strongest place is approximately 8.2x stronger than the weakest place (marked with rectangles in Figure 7.51).

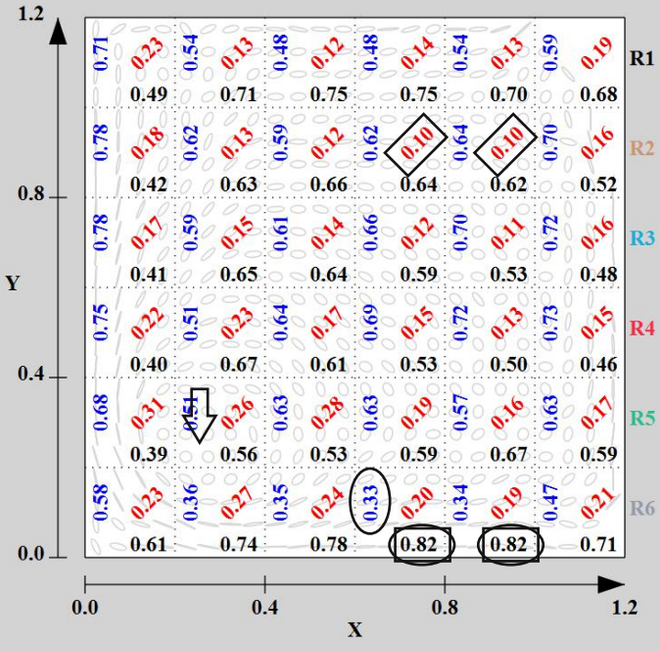

Figure 7.51: Top view of the slab. Fibre orientation factors in the X, Y and Z direction in individual regions.

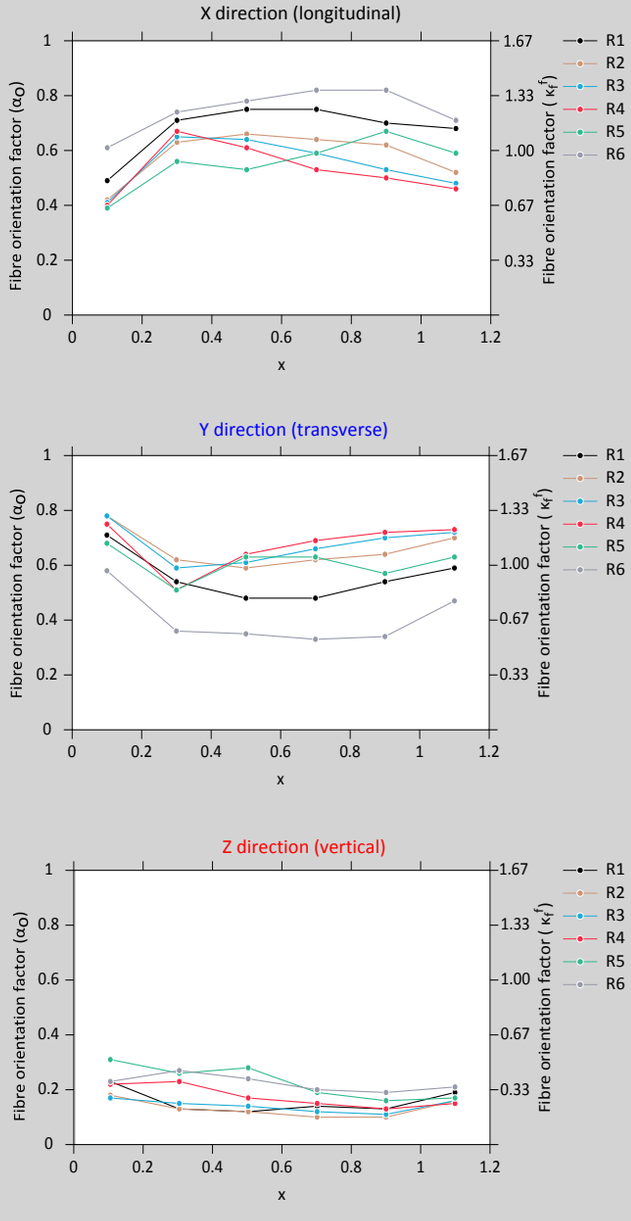

Figure 7.52: Fibre orientation factors. X-direction (black), Y-direction (blue), Z-direction (red).

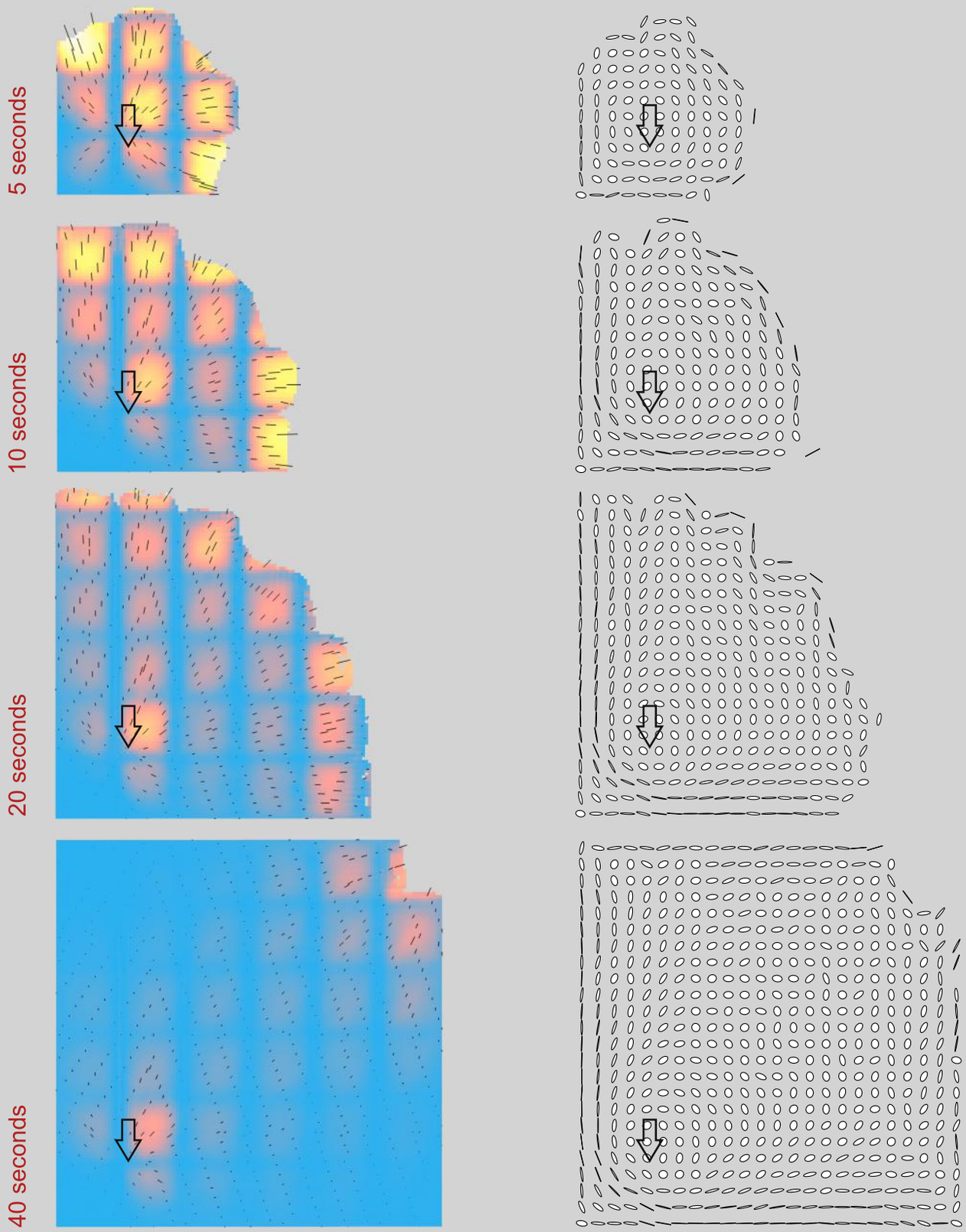

Figure 7.53: Slab casting with SFRSCC. Two-way reinforcement. Top views of the flow pattern (left) and of the fibre orientation ellipses (right) at different time steps. The colour represents the flow speed (blue = low, yellow = high).

Figure 7.54 presents the fibre orientation factors in individual regions of SFRSCC slab with two-way reinforcement. The values in rows R1 - R6 are also plottted in Figure 7.55.

The mean values of the fibre orientation factor α_o in the X, Y and Z direction is 0.62, 0.59 and 0.18, respectively. The standard deviation of the fibre orientation factor α_o in the X, Y and Z direction is 0.13, 0.13 and 0.05, respectively. The minimum and maximum value of the fibre orientation factor α_o in the X, Y and Z direction are [0.33, 0.86], [0.31, 0.81] and [0.12, 0.3], respectively.

In the XY plane, the strongest place is approximately 2.8x stronger than the weakest place (marked by ellipses in Figure 7.54). In volume, the strongest place is approximately 7.1x stronger than the weakest place (marked with rectangles in Figure 7.54).

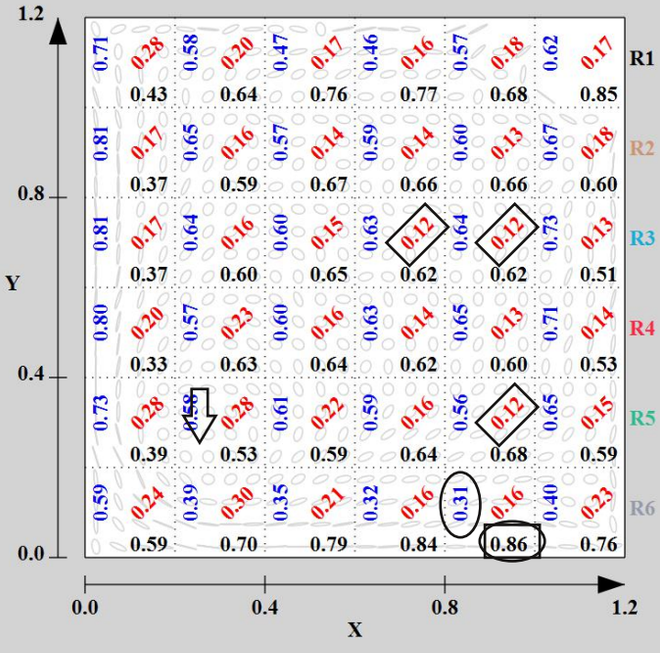

Figure 7.54: Top view of the slab. Fibre orientation factors in the X, Y and Z direction in individual regions.

Slab with two-way reinforcement - simulation

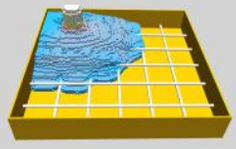

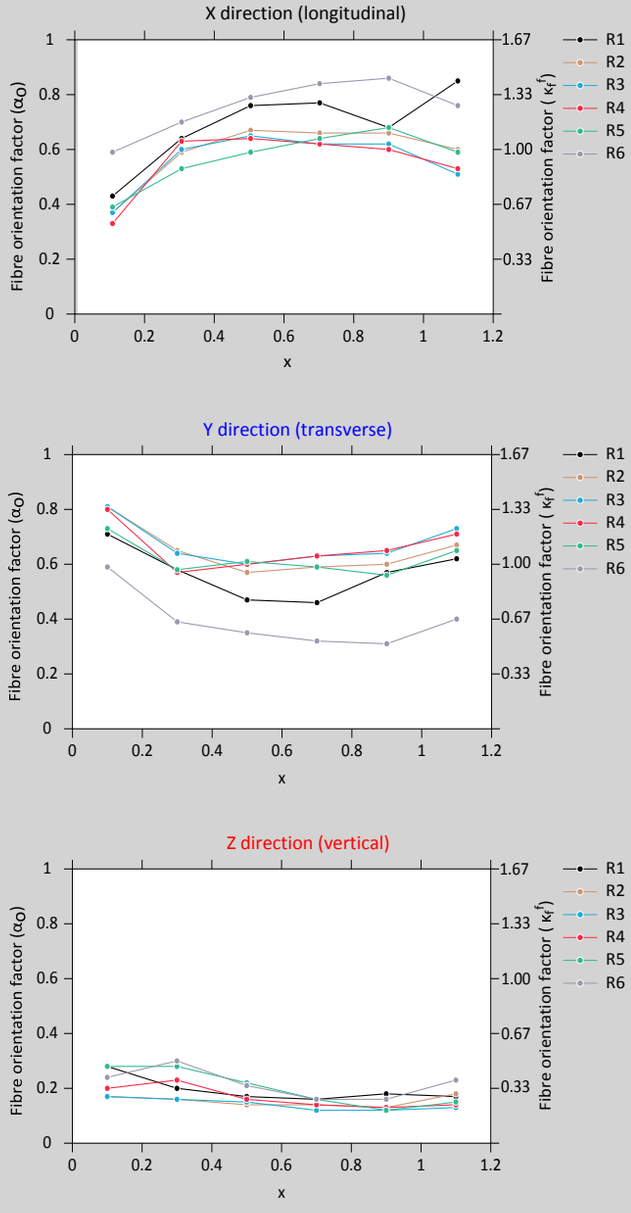

Figure 7.55: Fibre orientation factors. X-direction (black), Y-direction (blue), Z-direction (red).

7.9 SMALL SLAB - EXPERIMENTAL

This section presents the fibre orientation factors obtained from casting of a real slab with SFRSCC. The experiment is similar to the simulation without conventional reinforcement shown in the previous section.

Dimensions of the slabs were 1.60 m x 1.60 m x 0.15 m. Fibre length, aspect ratio and content were 60 mm, 80 and 40 kg/m^3, respectively. The rheological properties were measured using the 4C-Rheometer. The plastic viscosity and yield stress were 75 Pa·s and 45 Pa, respectively. The slump flow was 620 mm. The slab was cut into 24 beams, which were tested in three point bending. Subsequently, fibre counting in fracture plane was carried on 18 beams to determine the fibre orientation factor in the Y direction.

The results are shown in Figure 7.57 and Figure 7.58. The mean value of the fibre orientation factor α_o in the Y direction is 0.61. The standard deviation of the fibre orientation factor α_o is 0.18. The minimum and maximum value of fibre orientation factor is 0.33 and 0.96, respectively. The results are in line with the numerical simulation.

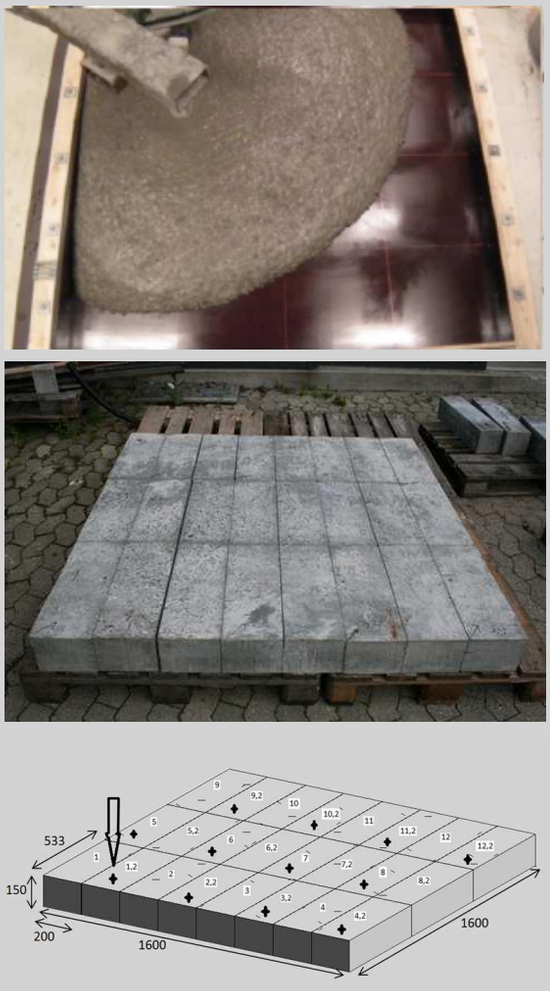

Figure 7.56: Casting and cutting of the slab.

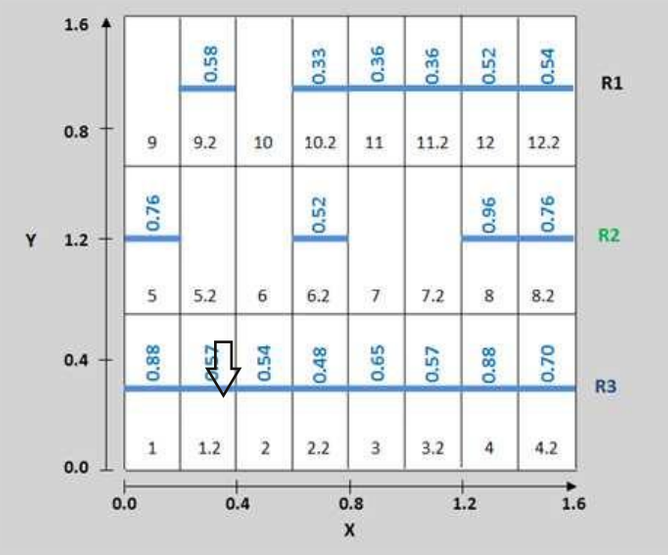

Figure 7.57: Top view of the slab. Fibre orientation factor in the Y direction.

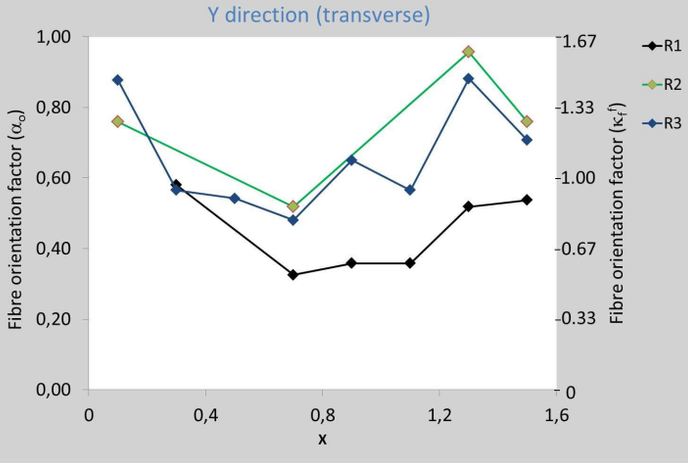

Figure 7.58: Fibre orientation factors in the Y-direction.

7.10 FULL-SCALE SLAB - EXPERIMENTAL

During the project, three full-scale demonstration projects were carried out. One of them was a foundation slab (50 m x 20 m x 0.4 m), which was cast with SFRSCC. A reinforcement mesh was placed at the top and bottom of the slab. It was composed of Y10 bars with a spacing of 100 mm in both directions. The cover layer was 35 mm. The fibre length, aspect ratio and content were 60 mm, 80 and 30 kg/m^3, respectively. Prior to the full-scale casting, a trial slab was cast (5.0 m x 5.0 m x 0.4 m).

Both slabs were cast as illustrated in Figure 7.60. The pump hose was moved from side to side. Locally, the pump hose was moved in a random way. The casting rate was approximately 30 m^3 per hour and the full-scale casting lasted for approximately 10 hours. The average yield stress, plastic viscosity and slump flow were 72 Pa, 79 Pa·s, and 532 mm, respectively.

In the following, the fibre orientation factors obtained from the trial slab and the full-scale slab are presented.

Figure 7.59: SFRSCC casting of the full-scale foundation slab (top) and trial slab (bottom).

Figure 7.60: Illustration of the casting procedure applied for casting of the foundation slab.

7.10.1 Fibre orientation

To study fibre orientation, cores were drilled from the trial slab and the full-scale slab. The core diameter was 150 mm.

Five cores were drilled from the middle part of the trial slab i.e. they represent more or less the same location. Each core was split into sections as shown in Figure 7.62. The top and bottom sections represent the cover layer zones.

The number of fibres in each plane was determined. Subsequently, the specimens were crushed and the fibre content was determined. From the number of fibres and the volume fraction, the fibre orientation factor was computed.

Figure 7.63 shows the results from the five cores. The first graph shows the fibre content from top to bottom of the slab. The top layer of the slab seems to have a higher fibre content (40 kg/m^3). The fibre content in the other sections oscillates around the value of 30 kg/m^3. The total fibre content is 30.7 kg/m^3 corresponding to the specified fibre content of 30 kg/m^3.

The second graph shows the fibre counts from top to bottom in the X, Y, and Z direction. For this specific fibre type and volume fraction, 1D fully aligned and 3D random fibre orientation correspond to fibre counts of 8646 m^{-2} and 4323 m^{-2}, respectively.

Figure 7.61: Example of a drilled core split into different sections.

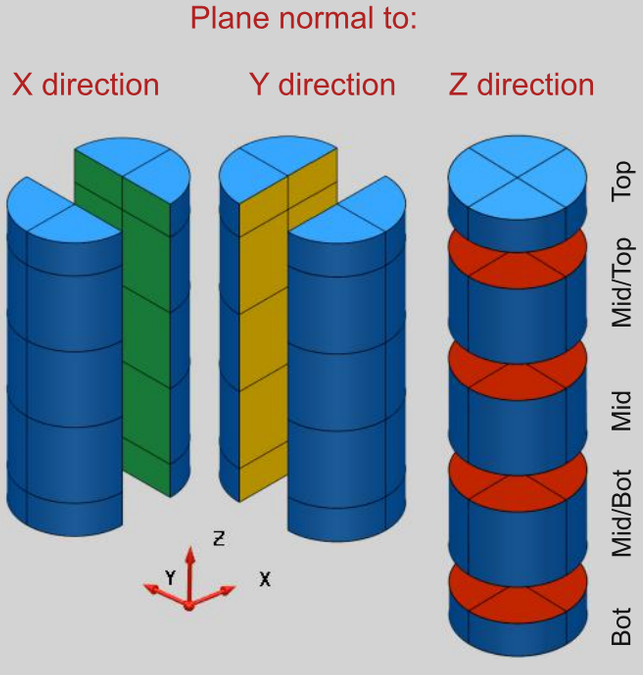

Figure 7.62 Layout of the drilled cores and the planes normal to the X, Y and Z direction.

The third graph shows the fibre orientation factors in the X (longitudinal), Y (transverse) and Z direction (vertical).

In the X and Y direction, the lowest fibre orientation factors are found in the bottom layer. The reason for this may be some of the fibres orientate normal to the reinforcement bars when the SFRSCC passes the reinforcement mesh at the bottom. This is, however, not reflected by the fibre orientation factor in the Z direction as this represent a cut plane placed approximately 60 mm from the bottom (35 mm cover layer + 2 x 10 mm rebar diameter).

The average fibre orientation factor α_o in the X, Y and Z direction is 0.48, 0.38 and 0.26, respectively. Excluding the low fibre orientation factor in the bottom layer, the average fibre orientation factor α_o of the X and Y direction is 0.47, which is close to the 3D random fibre orientation factor.

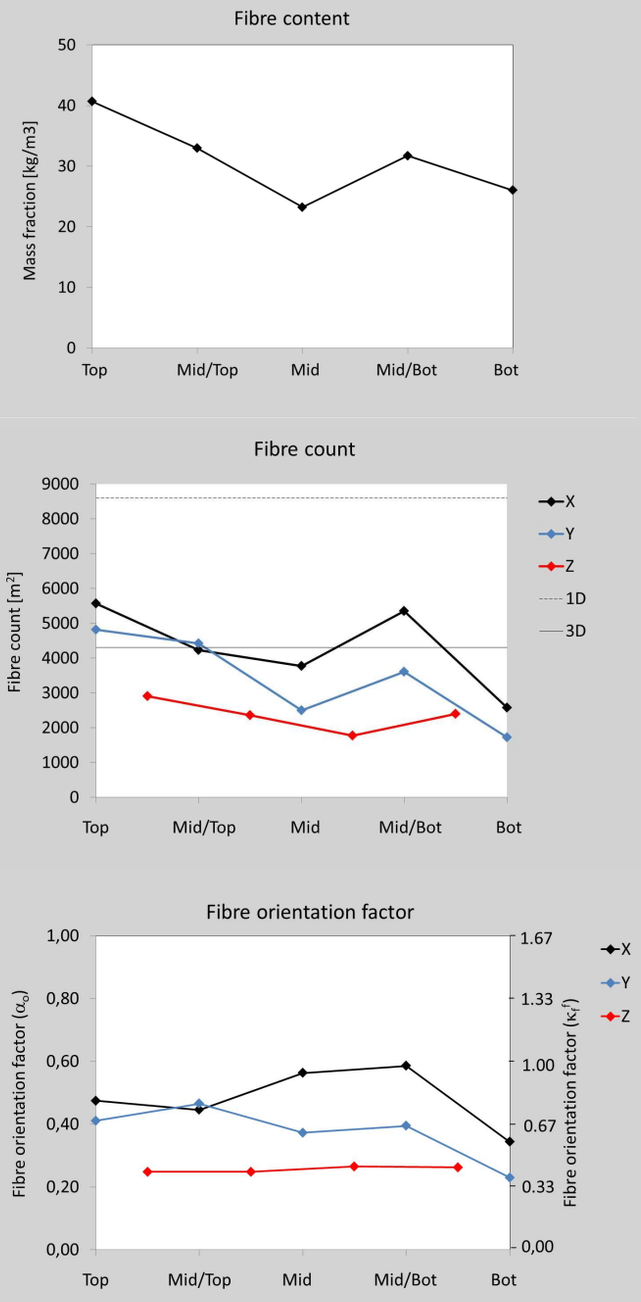

Figure 7.63: The fibre content, fibre count, and fibre orientation factor obtained from five cores drilled from the trial slab.

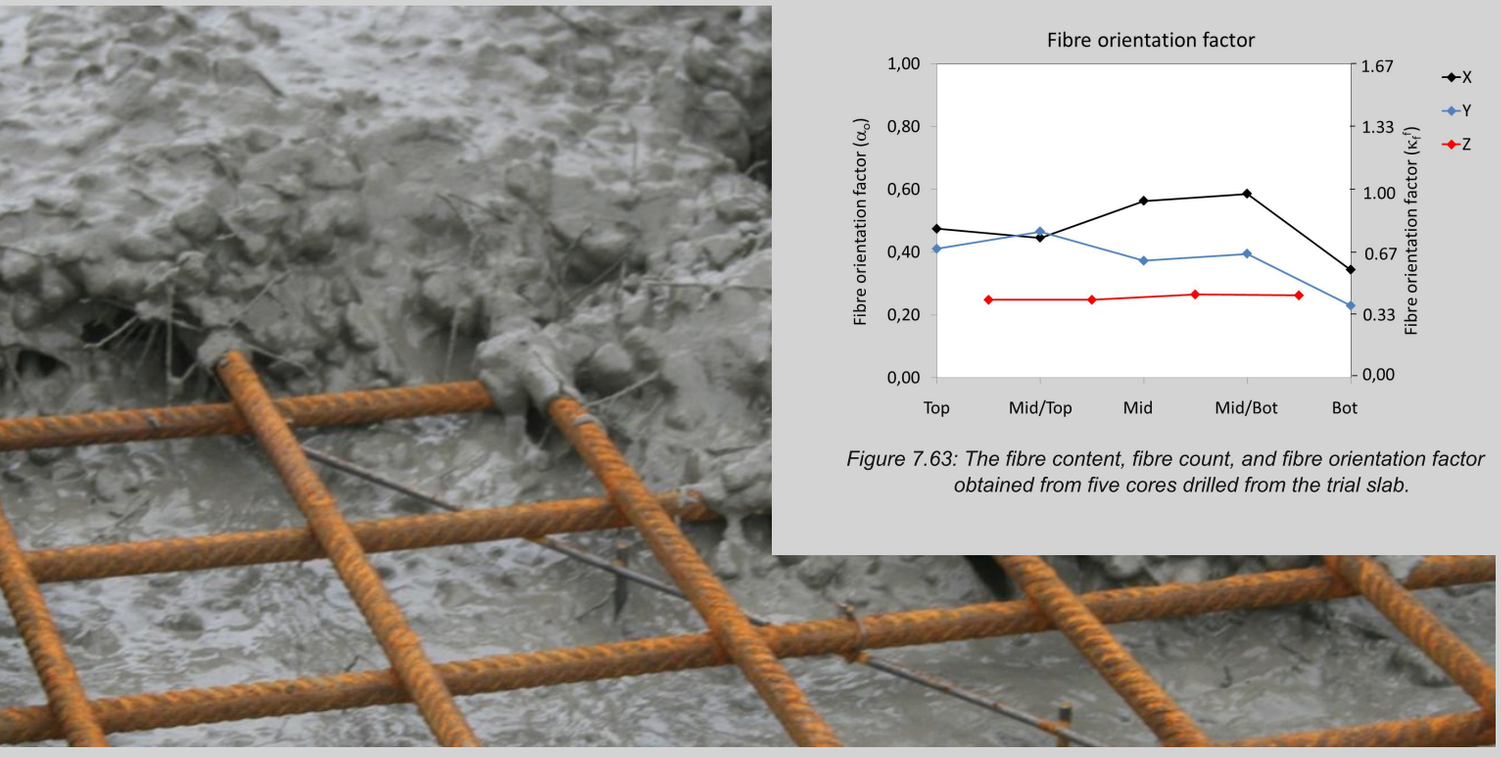

Figure 7.64. Picture of the SFRSCC close to the top reinforcement mesh.

Six cores were drilled from the full-scale slab. The cores were evenly distributed over the slab i.e. they represent different locations. Each core was split in the longitudinal direction as shown in Figure 7.65. The cut plane represent a random plane perpendicular to the xy-plane. The fibre count was determined in four different sections i.e. top, mid/top, mid/bottom, and bottom. In this case, the samples were not crushed to determine the fibre content. Thus, to compute the fibre orientation factor, a constant fibre content of 30 kg/m^3 was assumed. Figure 7.66 shows the fibre orientation factor for each sample and the overall mean value.

The fibre orientation factor α_o oscillates around the 3D random fibre orientation factor of 0.50. Compared to the trial slab, the low fibre counts in the bottom layer are not observed.

In general, the results indicate that the fibre content, fibre count and thus the fibre orientation factor varies over the height of the slab. However, it is expected that these variations level out over larger areas. Therefore, for a random type of casting process, a fibre orientation factor in the range of the 3D random value may be assumed. In Section 6.2, a fibre orientation factor α_o of 0.60 has been proposed for slabs (in general) in the longitudinal and transverse direction. This corresponds to κ_f^f of 1.0, which is also proposed by the DAfStB for conventional SFRC.

Figure 7.65: Illustration of a core drilled from the full scale slab. The cores were split in the longitudinal direction.

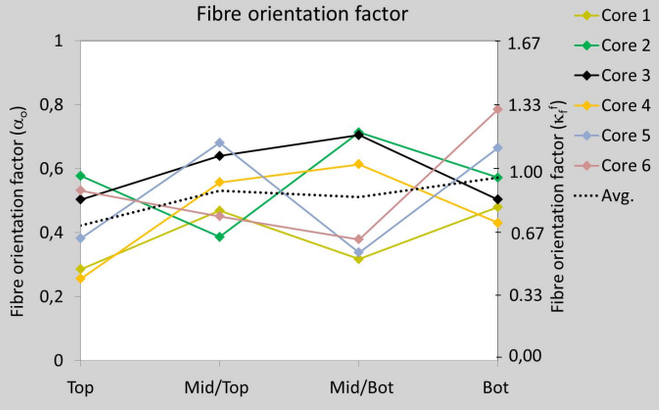

Figure 7.66: Fibre orientation factors in a random plane normal to the xy-plane in the full-scale slab.

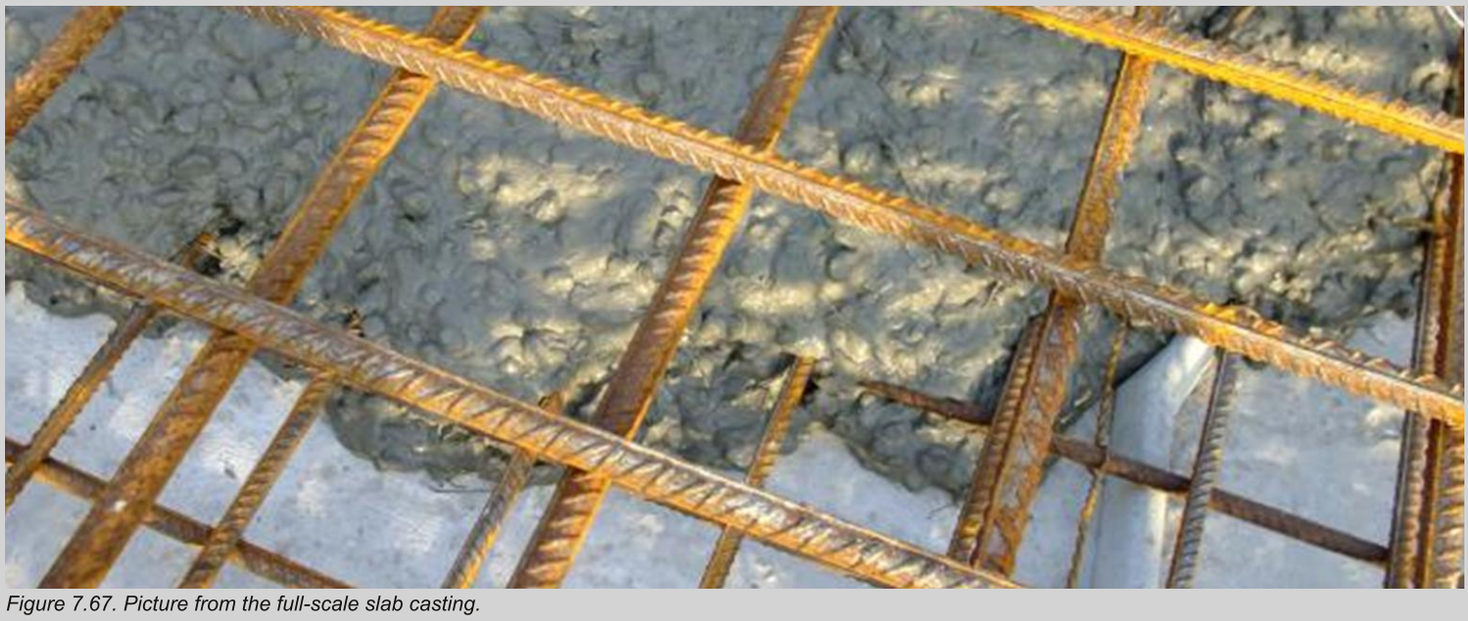

Figure 7.67. Picture from the full-scale slab casting.

7.11 STRIP FOUNDATION - EXPERIMENTAL

As part of the second demonstration project, a study was carried out to investigate the effect of the casting procedure on the fibre orientation in strip foundations. The strip foundations were part of an underpass for a new bypass around Slagelse. The underpass was designed as a frame structure and the strip foundations and the walls were cast with SFRSCC. The fibre length, aspect ratio, and content were 60 mm, 65, and 40 kg/m^3, respectively. The average yield stress, plastic viscosity, and slump flow were 46 Pa, 29 Pa·s, and 578 mm for the first foundation, and 57 Pa, 33 Pa·s and 554 mm for the second foundation. The reinforcement consisted of a reinforcement mesh at the bottom and stirrups connecting the foundations and the walls.

Two different casting procedures were applied. The first foundation was cast by placing the pump hose in

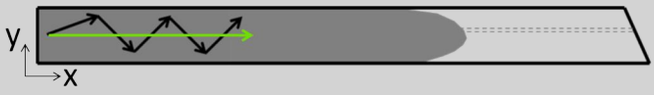

Figure 7.68. Illustration of the casting procedure applied for the first foundation (green - straight forward) and the second strip foundation (black - zig-zag movement).

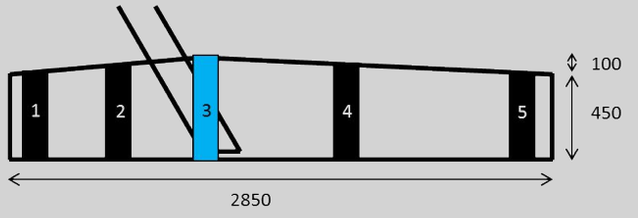

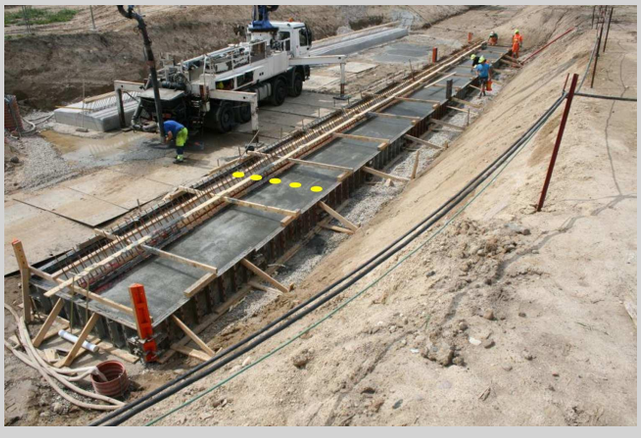

Figure 7.69. Top: Layout of the cross-section. Bottom: Position of the drilled cores.

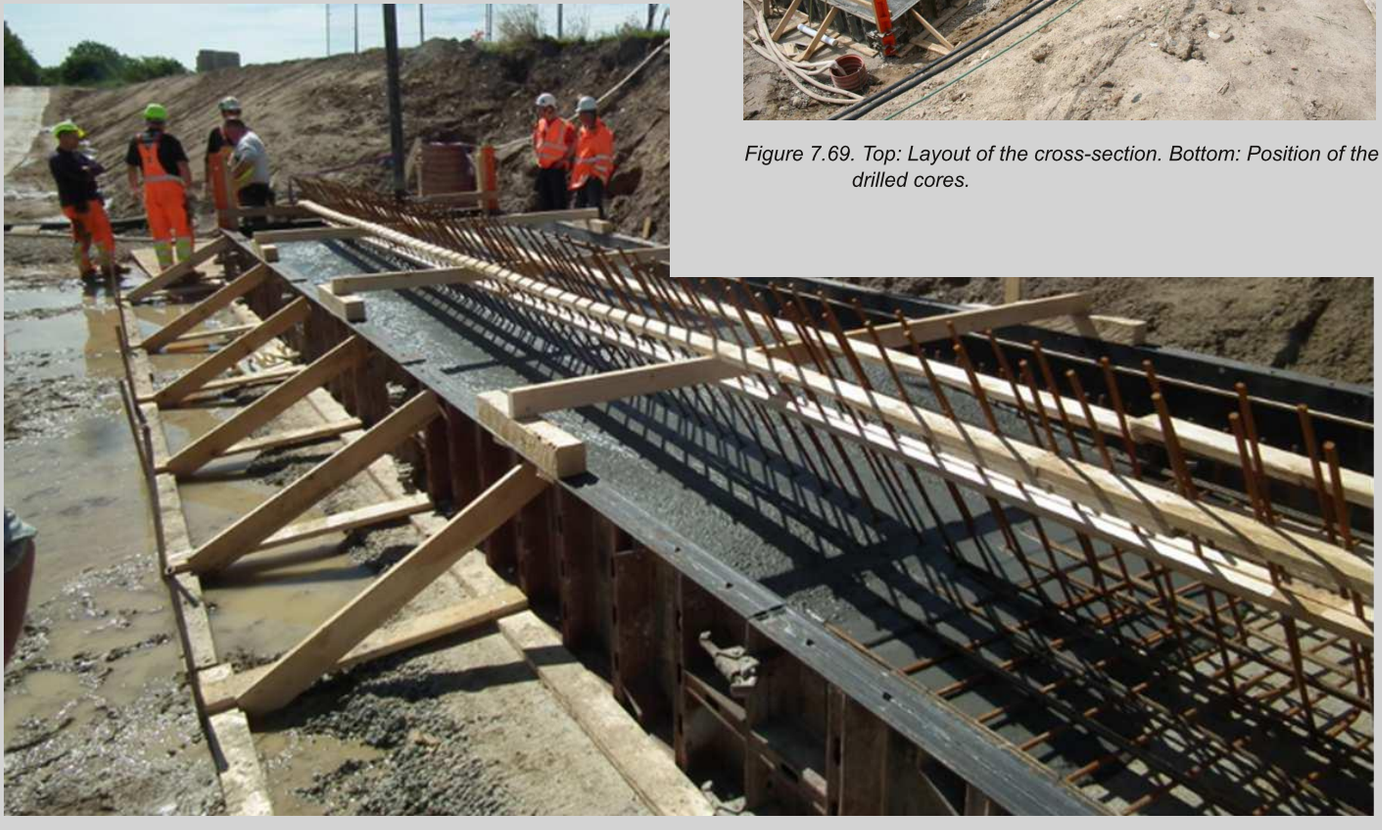

Figure 7.70. Picture from the casting of the first strip foundation.

the center at one end of the foundation. Then it was slowly moved forward in a straight line as the target height was reached. This is illustrated with a straight green line in Figure 7.68. The second foundation was cast in a similar way except the pump was moved from side to side instead of moving it in a straight line. This is illustrated with a black zig-zag curve in Figure 7.68.

Five cores were drilled from each foundation. The positions are shown in Figure 7.69. Fibre counts were determined in three sections (bottom, middle and top). The samples were not crushed so to compute the fibre orientation factor, a constant fibre content of 40 kg/m^3 was assumed. Figure 7.71 shows the fibre orientation factors in the X, Y, and Z direction. It shows the average fibre orientation factors of core 1, 2, 4, and 5, which were drilled outside the stirrups. A seperate graph is shown for core number 3, which was drilled in the zone with the stirrups.

The results show that the zig-zag casting procedure results in the most even fibre orientation in the three directions. The straight casting procedure results in a stronger fibre orientation in the longitudinal direction, however, not in the reinforcement zone (core 3), where the highest value is found in the transverse direction. The reason is that the concrete flows into the reinforcement zone where it slows down significantly. Therefore, the flow in the longitudinal direction is no longer dominant.

The mean value of the fibre orientation factor α_o in the X, Y and Z direction is:

- Straight without core 3 [0.68, 0.39, 0.28]
- Straight core 3 [0.38, 0.50, 0.39]
- Zig-zag without core 3 [0.52, 0.46, 0.44]
- Zig-zag core 3 [0.43, 0.47, 0.29]

The standard deviation of the fibre orientation factor α_o in the X, Y and Z direction is:

- Straight without core 3 [0.03, 0.07, 0.09]
- Straight core 3 [0.07, 0.09, 0.09]
- Zig-zag without core 3 [0.04, 0.03, 0.06]
- Zig-zag core 3 [0.02, 0.11, 0.14].

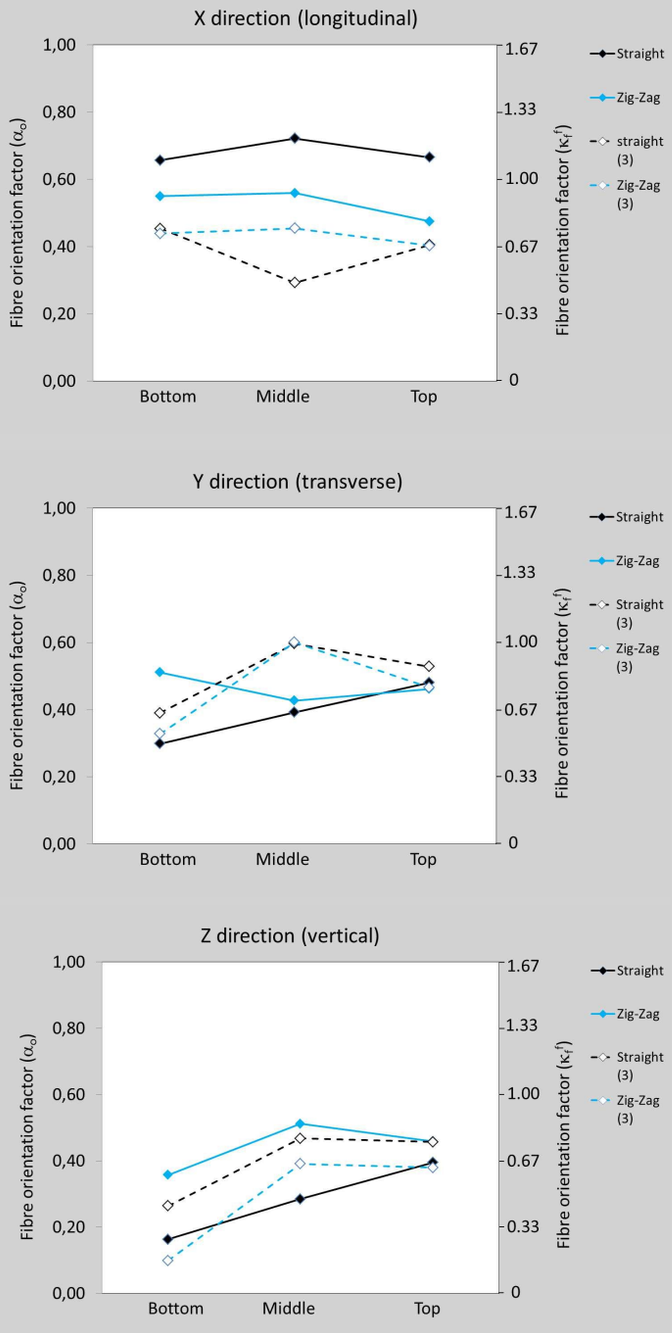

Figure 7.71. Fibre orientation factors in two strip foundations cast with SFRSCC. Two different casting procedures were applied referred to as straight and zig-zag.

8. Practical observations and recommendations

This section describes some of the practical observations made during the full-scale projects carried out in the project. Based on these observations, some recommendations are given for the use of SFRSCC.

The first project was carried out in Aalborg. Here, a foundation slab was cast with SFRSCC. The fibre length, aspect ratio and content were 60 mm, 80, and 30 kg/m^3, respectively.

The second project was carried out in Slagelse. Here, an underpass was executed, where the strip foundations and the walls were cast with SFRSCC. The bridge deck was cast with SFRC. The steel fibre length, aspect ratio, and content were 60 mm, 65, and 40 kg/m^3, respectively.

The third project was carried out in Herning. Here, a precast concrete bridge was executed. The bridge consists of six concrete elements. SFRSCC was applied in one of the two edge beams. The fibre length, aspect ratio, and content were 60 mm, 65, and 40 kg/m^3, respectively. Otherwise, the reinforcement of the edge beams was identical. The aim was to provide the opportunity to study long term durability aspects of SFRSCC in full-scale. Furthermore, the project focused on the joints between the concrete elements. In two of the joints, an alternative solution was investigated using steel fibre reinforced high strength concrete. Due to a very high bond strength, it is possible to reduce the anchor length of the reinforcement bars. Thus, it is possible to reduce and simplify the reinforcement configuration in the joint. Compared to normal strength concrete, the concrete composition of high strength steel fibre reinforcement is significantly different. Coarse aggregates are not included and the steel fibre content is significantly higher - in this case 363 kg/m^3. The fibre length and aspect ratio were 12.5 mm, and 41.7, respectively.

Figure 8.1: Pictures from the three full-scale projects carried out during the project.

8.1 SLABS

8.1.1 Orientation of spacers

Orientation of the spacers separating the top and bottom reinforcement mesh affects the control of the casting process. In the full-scale slab, the spacers were placed in the transverse Y direction. The spacer positions are indicated by the red rectangles in Figure 8.2. The pump hose was moved as illustrated by the white curve in Figure 8.2. The main flow direction was in the X direction i.e. perpendicular to the spacers. If possible, it is recommended to cast the concrete so the main flow direction is parallel to the spacers. This gives a slightly better control of the casting process. In this case, the pump hose would have had to be moved as illustrated by the yellow curve.

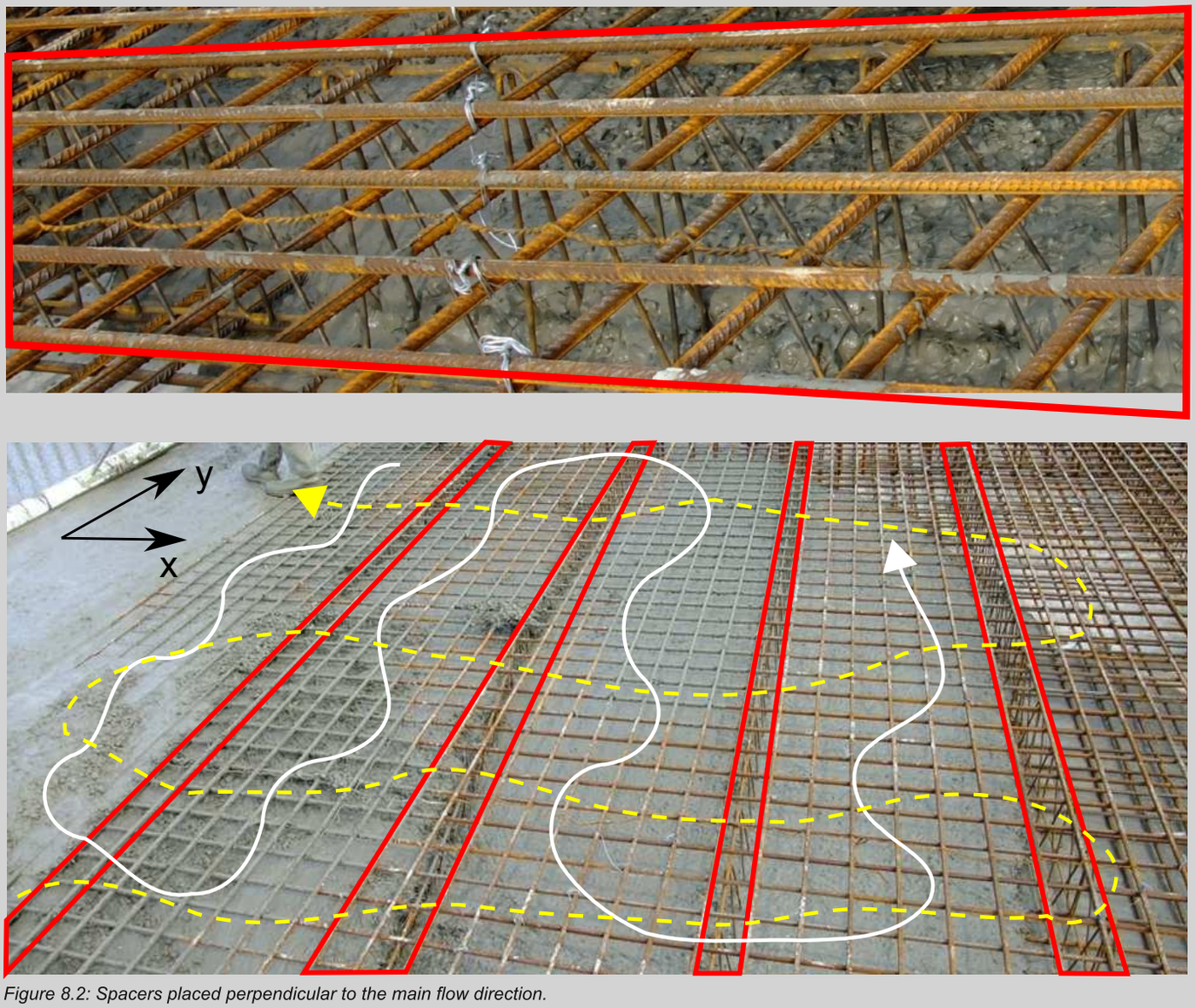

Figure 8.2: Spacers placed perpendicular to the main flow direction.

8.1.2 Type of spacer

The type of spacer separating the top and bottom reinforcement mesh is important to consider with respect to blocking. Two different types of spacer have been tested. The rectangular spacers shown at the top of Figure 8.3 allowed the concrete to flow freely. However, the triangular shaped spacers shown at the bottom of Figure 8.3 did cause fibre blocking in some places. The clear spacing varies due to the triangular shape. The risk of fibre blocking increases when the clear spacing is below approximately 100 mm as illustrated by the red circles in Figure 8.3. This corresponds to a clear spacing over fibre length of 1.7, which is also below the value of 2.0, which was described in section 2.3 as a general rule of thumb. In this case, to avoid blocking and to ensure the integrity of the structure, the pump hose was carefully moved from side to side over the spacers.

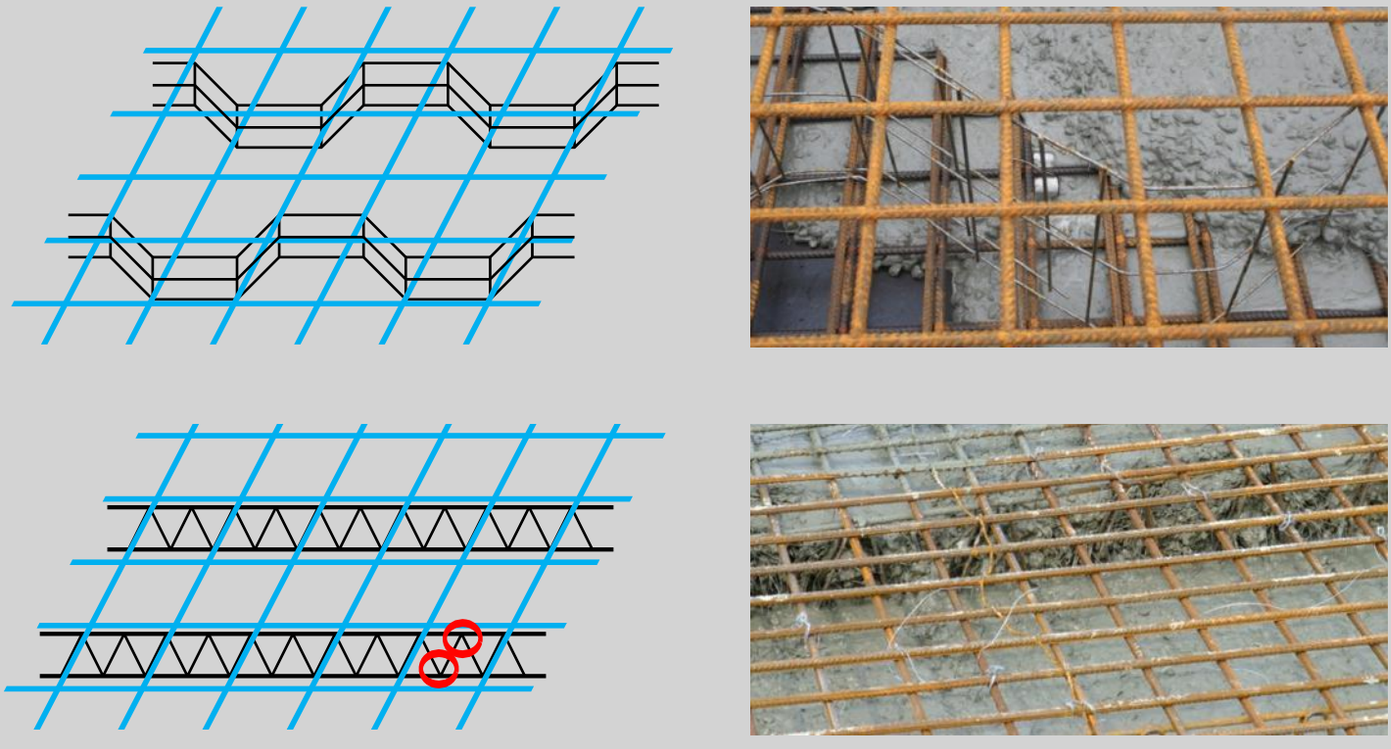

Figure 8.3: The spacer type is important to consider with respect to the risk of blocking. No blocking was observed using the spacer with a rectangular grid (top). Blocking was observed in critical areas when using a spacer type with a triangular grid (bottom).

8.1.3 Casting procedure

As previously described, the top and bottom reinforcement mesh were composed of Y10 bars with a spacing of 100 mm in both directions. It was observed that the fibres had a tendency to accumulate on the top reinforcement mesh when the inlet was kept for too long in the same position as shown in Figure 8.4 (top). Instead, if the pump hose was continously moved from side to side, the fibres did not accumulate to cause fibre blocking. Based on these observations, the following recommendations are proposed with respect to the ratio of clear spacing over fibre length:

> 2.0 is ok with a constant pump hose position
~ 1.5 is ok if the pump hose is moving
<< 1.5 is not ok.

Figure 8.4: Fibre accumulates on the top reinforcement mesh when the pump hose is not moving (top). Fibres do not accumulate on the top reinforcement when the pump hose is moving (bottom).

8.1.4 Rheology

Different observations were made during the full-scale casting with respect to the rheological properties. Figure 8.5 shows the average yield stress, plastic viscosity, slump flow and t_{500} value obtained using the 4C-Rheometer. The manual measurements of the slump flow and t_{500} value are also shown. A total of 55 truckloads were delivered at the job site amounting to a total of 385 m^3 of concrete. Samples were taken from 18 of these trucks and the rheological properties were measured before and after pumping.

It was observed that when the SFRSCC was too fluid, it was more difficult to control the front of the concrete and it would flow too far away from the position of the pump hose. However, if the SFRSCC became too stiff it was more difficult to penetrate the reinforcement mesh.

With respect to the plastic viscosity, the Danish guideline on execution of SCC recommends to apply SCC with a low plastic viscosity for slabs (< 40 Pa·s). However, for SFRSCC, it is recommended to apply a medium range plastic viscosity to maintain a good stability (40-100 Pa·s).

Thus, for slabs it is recommended to apply:

- Yield stress (4C-Rheometer): 70-100 Pa
- Plastic viscosity (4C-Rheometer): 40-100 Pa·s
- Slump flow (4C-Rheometer): 500-550 mm
- Slump flow (manual): 550-600 mm

The 4C-Rheometer applies a dry base plate compared to a moist base plate in the standard slump flow test. Therefore, the recommended slump flow is lower.

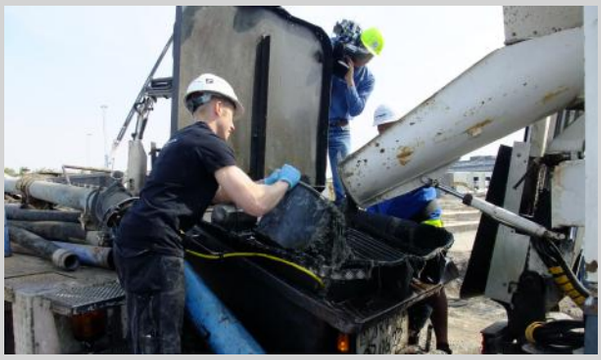

	4C Rheometer		Manual testing	
	Before pump	After pump	Before pump	After pump
Slump flow [mm]				
Average	532	521	546	575
Standard deviation	34	38	41	40
t_{500} [sec]				
Average	4.5	4.6	5.3	2.6
Standard deviation	1.0	1.8	2.1	0.9
Plastic viscosity [Pa·s]				
Average	79	68		
Standard deviation	16	30		
Yield stress [Pa]				
Average	72	80		
Standard deviation	27	29		

Figure 8.5: Top: Sampling before and after pump. Middle: 4C-Rheometer measurement. Bottom. Measured flow properties.

8.1.5 Surface finish

Figure 8.6 shows a typical concrete surface just after casting of SFRSCC i.e. before any surface finish procedures have been applied. Both aggregates and steel fibres are observed at the surface. Some fibres are sticking out of the surface. To submerge the fibres and aggregates, the methods recommended for SCC do also apply for SFRSCC. The following figures show some examples of these different surface finishing procedures.

Figure 8.6: Typical surface of SFRSCC just after casting and before any surface finish procedure has been applied.

The cylinder shaped pipe shown in Figure 8.7 and Figure 8.8 is often used to finish SCC surfaces. It also works well with SFRSCC. Careful finishing will ensure that the fibres get submerged below the surface.

Figure 8.7. Surface finishing of SFRSCC using a cylinder shaped pipe.

Figure 8.8. Surface finishing of SFRSCC using a cylinder shaped pipe.

Other tools, such as a screed bar shown in Figure 8.9 does also work well. The final surface appearence will be very similar to the surface obtained using the cylinder shaped pipe tool.

Figure 8.9. Surface finishing of SFRSCC using a screed bar.

Figure 8.10 shows manual trowelling of the surface. If no other surface finishing procedures have been applied beforehand, it can be difficult to obtain a smooth surface where all the steel fibres are submerged below the surface (see Figure 8.11).

Figure 8.10. Surface finishing by manuel trowelling.

Figure 8.11. The surface appeareance of SFRSCC after manuel trowelling. No other surface finishing procedures have been applied. Difficult to submerge all the fibres.

For comparison, Figure 8.12 and Figure 8.13 show the surface of conventional SFRC. The pictures are from the casting of the underpass bridge deck. The concrete surface was finished using a beam vibrator. Some fibres were fully submerged below the surface whereas others could be observed at the surface. Fibres sticking out were cut off before epoxy was applied on top of the concrete. The deck was finished with a water proofing membrane and asphalt.

Figure 8.12. The underpass bridge deck was cast with conventional SFRC.

Figure 8.13. The surface appearence after applying a beam vibrator on top of conventional SFRC.

8.2 WALLS

8.2.1 Rheology and casting procedure

To ensure complete form filling, it is important to consider both the rheological properties and the casting procedure. How far the concrete is able to flow is balance between the yield stress, the dimensions of the walls and the reinforcement configuration. In the case of the underpass bridge walls, the most challenging part was filling the wing walls. The wall was 35 cm thick and reinforcement was applied on both sides with a rebar spacing of 150-175 mm in both directions and a cover layer of 45 mm. It was found that a yield stress in the range of 50 Pa would be sufficiently low to obtain complete form filling. This corresponds to a slump flow of approximately 560 mm. To avoid dynamic segregation, it is normally recommended to avoid too long flow distances. Therefore, the walls were cast from four inlet positions (Figure 8.14). Slides were prepared in order to avoid high drop heights. Furthermore, it is recommended to apply a medium (40-100 Pa·s) or high plastic viscosity (> 100 Pa·s) according to the definitions given in the Danish guideline on execution of SCC. In this case, the average plastic viscosity was approximately 60 Pa·s. The meaurements of yield stress, plastic viscosity, slump flow and t_{500} using the 4C-Rheometer are shown in Figure 8.15. Every batch was measured.

In general, the results of the walls were acceptable. The concrete was able to fill the wing walls and dynamic segregation was avoided. However, local segregation did occur as explained in the next section.

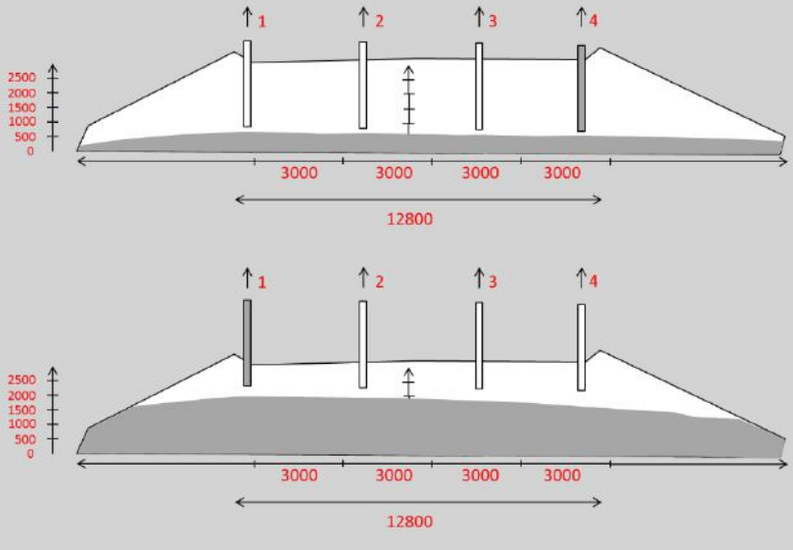

Figure 8.14: The casting procedure applied for the underpass bridge walls.

	4C Rheometer	
	Before pump	After pump
Slump flow [mm]		
Average	530	560
Standard deviation	20	28
t_{500} [sec]		
Average	5.1	4.1
Standard deviation	1.0	2.2
Plastic viscosity [Pa·s]		
Average	59	58
Standard deviation	22	31
Yield stress [Pa]		
Average	72	54
Standard deviation	12	13

Figure 8.15: Rheological properties of the SFRSCC applied for casting of the underpass bridge walls. 4C-Rheometer measurements before and after pumping.

Figure 8.16: Pictures from the SFRSCC casting of the underpass bridge walls.

Figure 8.17: Pictures of the underpass bridge walls.

8.2.2 Segregation

Substantial honeycombing was observed very locally below all the inlet positions at a height of approximately 1-1.5 m above the bottom. To control the temperature in the wall, cooling pipes were applied (yellow line) for which reason it was only possible to lower the slides down to a position just above these pipes. Unfortunately, casting from this position caused severe segregation of the fibres and aggregates as the concrete hit the cooling pipes. In this case, it is likely that segregation could have been avoided if the filling process was initiated from the bottom. Then the cooling pipes would have been submerged before continuing the casting process from the top.

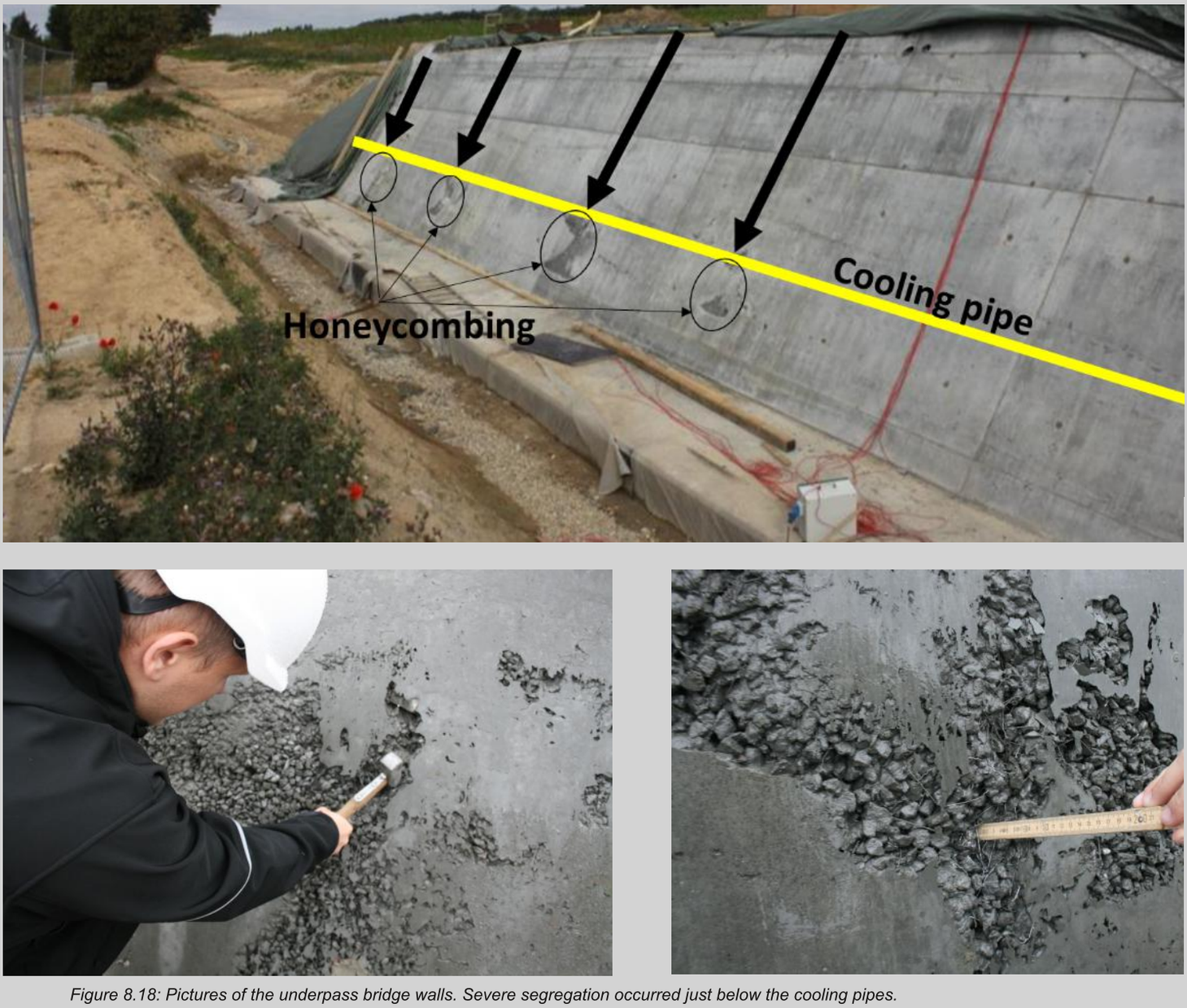

Figure 8.18: Pictures of the underpass bridge walls. Severe segregation occurred just below the cooling pipes.

8.2.3 Surfaces

Figure 8.19 to 8.25 show pictures of the surfaces of the underpass bridge walls. The formwork consisted of rough wood boards on the inside and smooth plywood on the outside. The pictures from the inside are taken one year after execution. The pictures from the outside are taken a week after demoulding. In general, relatively few fibres and rust spots are observed at the surfaces. At a viewing distance of a few metres, it is difficult to distinguish this structure from one without steel fibres. It seems the visible steel fibres appear locally, in particular in places where challenges occured during the casting e.g. in the transition from the SFRSCC in the walls to the conventional SFRC in the deck.

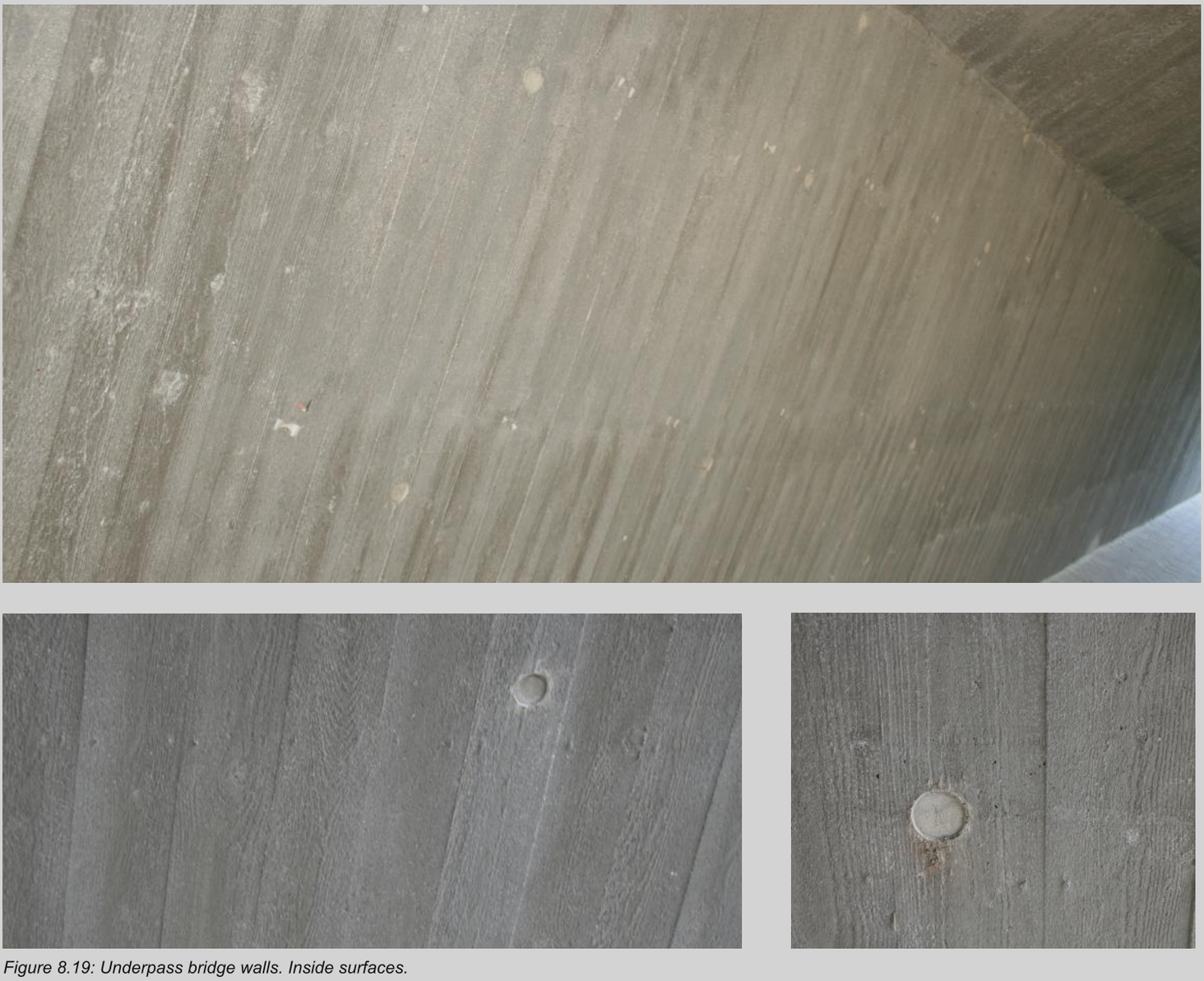

Figure 8.19: Underpass bridge walls. Inside surfaces.

Figure 8.20: Underpass bridge. Wing wall.

Figure 8.21: Underpass bridge. Edge beam from below.

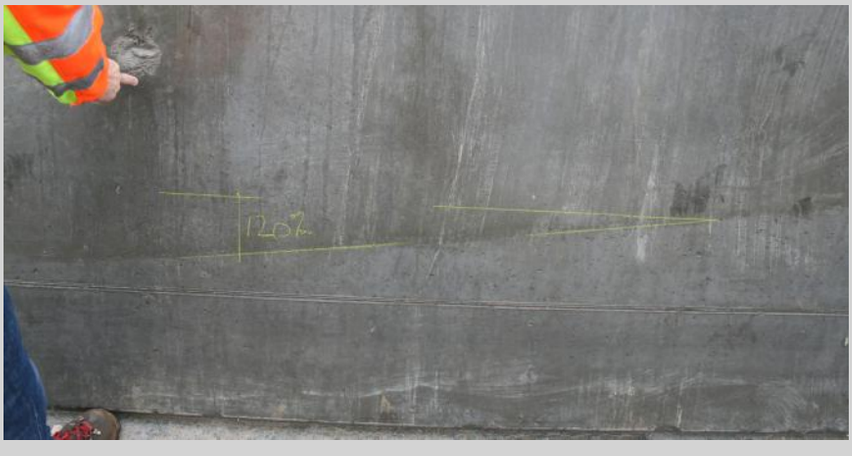

Figure 8.22: Underpass bridge. Outside surfaces.

Figure 8.23: Underpass bridge. Deck from below.

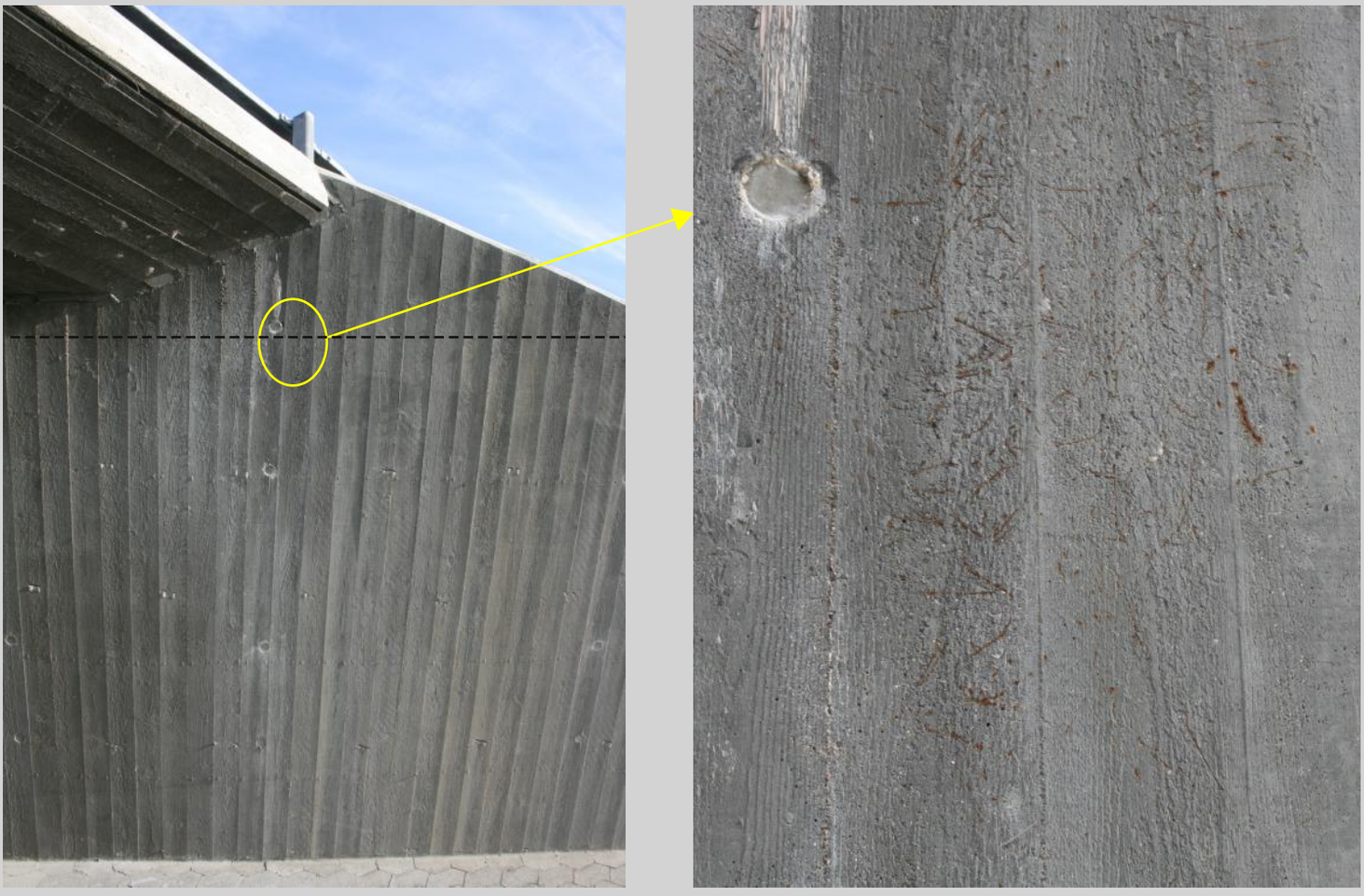

Figure 8.24: Transition zone from SFRSCC in the walls to SFRC in the deck (black dotted line). Visible fibres within the yellow ellipse.

Figure 8.25: Visible fibres and rust spots on the inside walls. To the right, a fibre is sticking out.

8.3 HIGH STRENGTH STEEL FIBRE REINFORCED CONCRETE

For the precast bridge in Herning, high strength steel fibre reinforced concrete was applied in two of the joints between the concrete elements. Specifically, the product JointCast from Hi-Con was applied. Faster strength development and the option of a more simple reinforcement configuration in the joint are the main motivations for applying such solution. For instance, parallel to the full-scale activities, a lab-scale study was carried out to compare the mechanical properties of the JointCast solution and a traditional joint solution. The results showed that the JointCast solution gave similar or higher performance. Figure 8.26 shows the reinforcement configuration applied in the tests.

Figure 8.27, 8.28 and 8.29 shows pictures from the full-scale execution. The reinforcement configuration was somewhat different from the lab-scale trials. The JointCast was mixed on site and cast from a wheel barrow. From a casting point of view, the JointCast is a very viscous material that needs to be vibrated. The slump is in the range of 150-200 mm. Due to a very high viscosity, more work must be expected when casting the JointCast compared to casting and vibrating traditional ready-mixed concrete, which is delivered on site and cast from a conveyor belt.

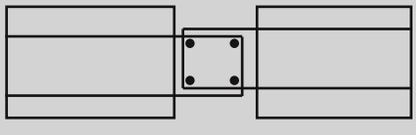

2 stirrups (Y10)
4 rebars in longitudinal direction (Y10)

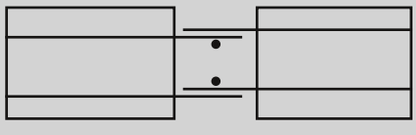

4 rebars (Y10)
2 rebars in longitudinal direction (Y10)

Figure 8.26: Reinforcement configurations applied for testing the mechanical performance of joints between precast concrete elements. Top: Traditional solution. Bottom: Alternative solution using high strength steel fibre reinforced concrete (JointCast).

Traditional

JointCast solution

JointCast mixing on site

JointCast

JointCast

JointCast

JointCast

Figure 8.27: Pictures from the casting of the joints between the precast concrete elements.

Figure 8.28: Close up picture of the high strength steel fibre reinforced concrete (JointCast).

Traditional

JointCast

Figure 8.29: Top: Vibration of the traditional concrete and the high strength steel fibre reinforced concrete. Bottom: Picture after casting and finishing of the joints.

DANISH
TECHNOLOGICAL
INSTITUTE

SFRC-Consortium